A Rationally Designed Metal-Binding Helical Peptoid for Selective Recognition Processes

Maria Baskin and Galia Maayan

Schulich Faculty of Chemistry, Technion- Israel Institute of Technology, Haifa, Israel, 32000

Supporting Information

Table of Contents

Instrumentation:

Peptoid oligomers were analyzed by reversed-phase HPLC (analytical C18(2) column, Phenomenex, Luna 5μm, 100 Å, 2.0x50 mm) on a Jasco UV-2075 PLUS detector. A linear gradient of 5–95% ACN in water (0.1% TFA) over 10 min was used at a flow rate of 700 μL/min. Preparative HPLC was performed using a AXIA Packed C18(2) column (Phenomenex, Luna 15μm, 100 Å, 21.20x100mm). Peaks were eluted with a linear gradient of 5–95% ACN in water (0.1% TFA) over 50 min at a flow rate of 5 mL/min. Mass spectrometry of peptoid oligomers and their metal complexes was performed on a Advion expression CMS mass spectrometer under electrospray ionization (ESI), direct probe ACN:H_2O (95:5), flow rate 0.2 ml/min and on a Waters LCT Premier mass spectrometer under electrospray ionization (ESI), direct probe ACN:H_2O (70:30), flow rate 0.3 ml/min. UV measurements were performed using an Agilent Cary 60 UV-Vis spectrophotometer, a double beam, Czerny-Turner monochromator. CD measurements were performed using a circular dichroism spectrometer Model Jasco 810 Spectropolarimeter and AppliedPhotophysics Chirascan. ICP measurements were performed using Thermo Scientific iCAP 6000 ICP-OES analyzer. EPR spectra were recorded on a Bruker EMX-10/12 X-band (ν=9.4 GHz) digital EPR Spectrometer. Spectra processing and simulation were performed with Bruker WIN-EPR and SimFonia Software. Data processing was done with the softwares Excel and KaleidaGraph.

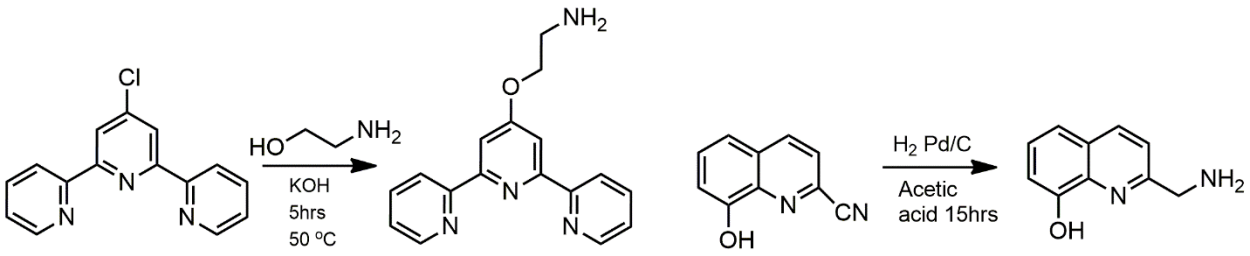

Scheme 1: Synthetic routs to the primary amines *N*terpy and *N*hq.

HPLC

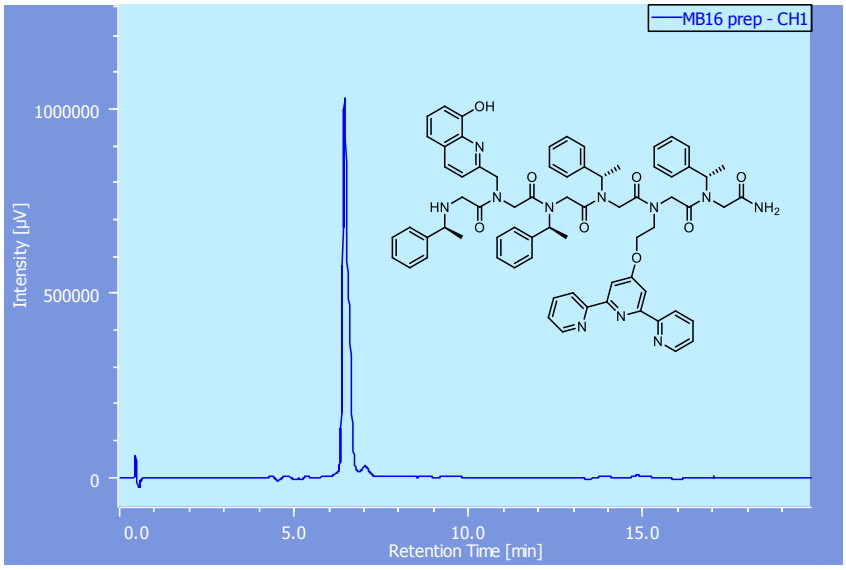

Figure S1. HPLC traces of purified peptoid oligomer **Helix HQT i+3** at 214nm.

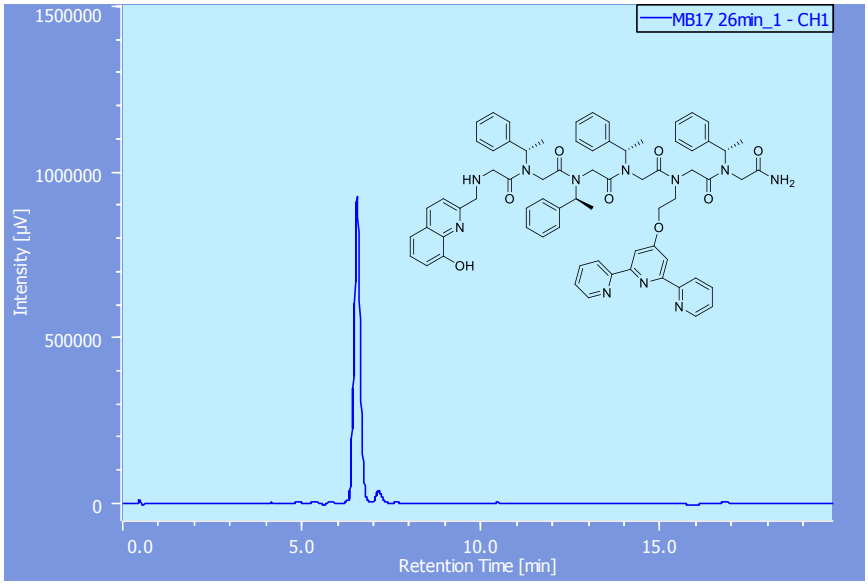

Figure S2. HPLC traces of purified peptoid oligomer **Helix HQT i+4** at 214nm.

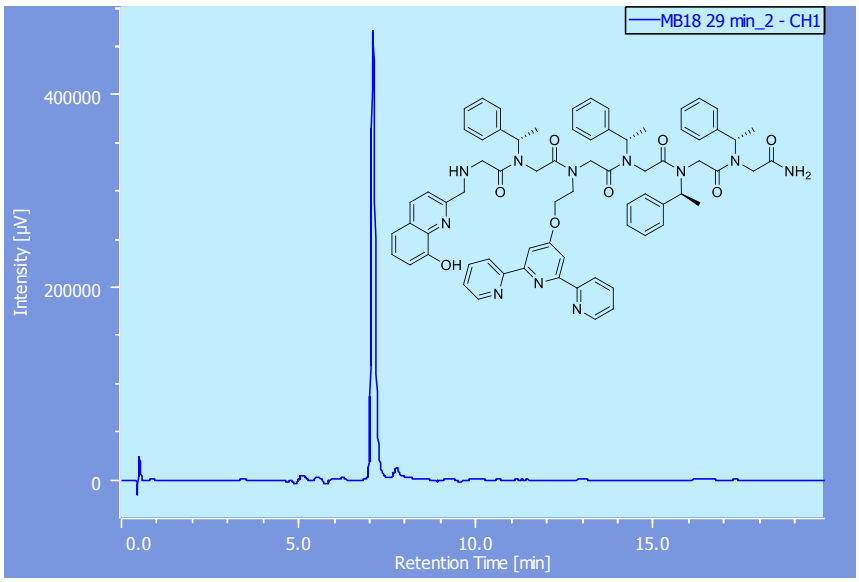

Figure S3. HPLC traces of purified peptoid oligomer **Helix HQT i+2** at 214nm.

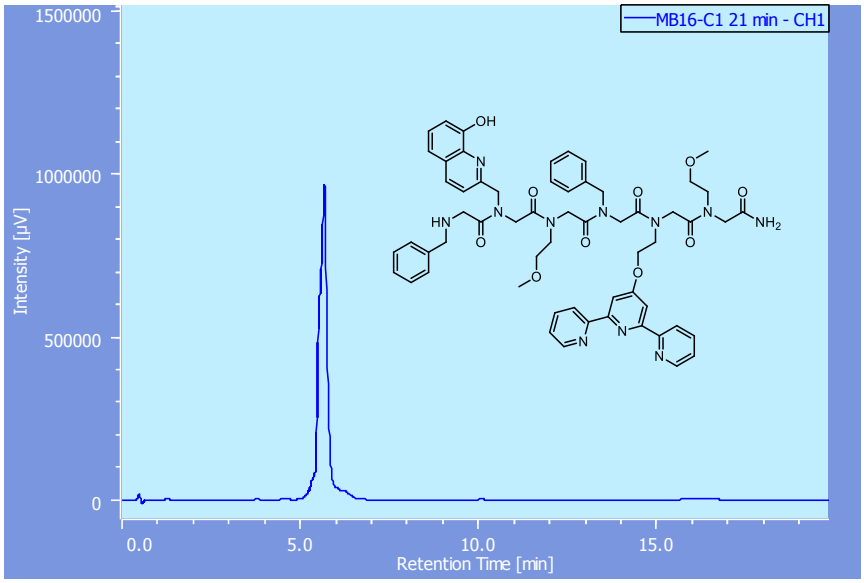

Figure S4. HPLC traces of purified peptoid oligomer **Nonhelix HQT i+3** at 214nm.

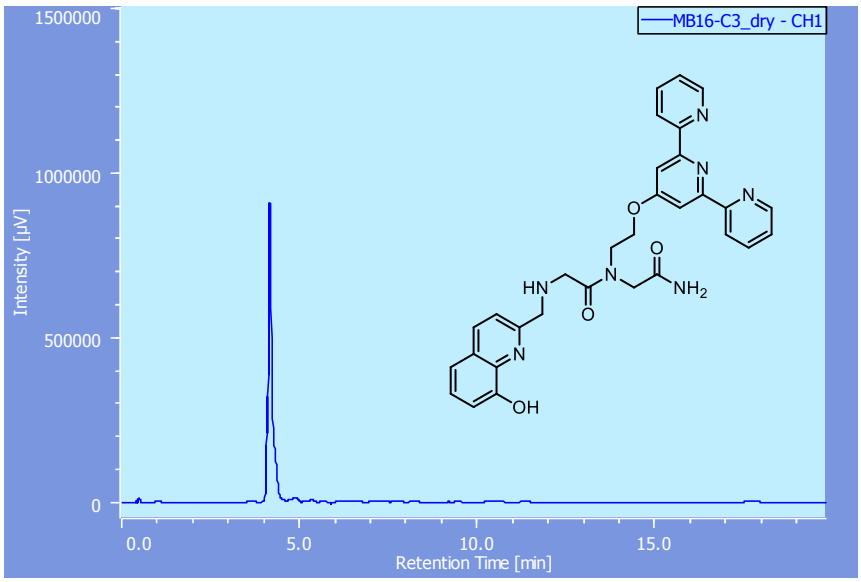

Figure S5. HPLC traces of purified peptoid oligomer **DI HQT** at 214nm.

CD data

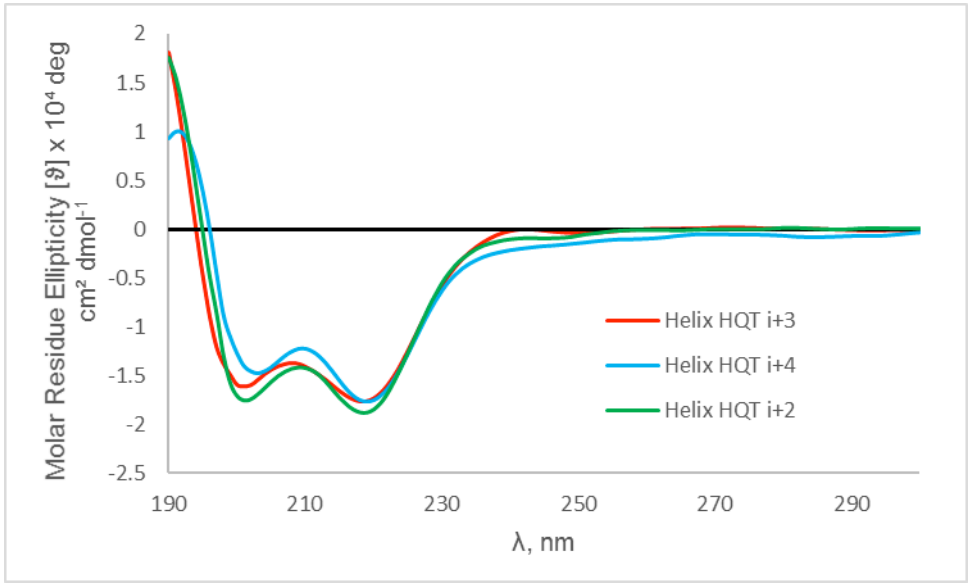

Figure S6. CD spectra of peptoid oligomers **Helix HQT i+3**, **Helix HQT i+4 and Helix HQT i+2**. The spectra were recorded at room temperature, at concentrations of 100 µM in MeOH:H_2O 4:1.

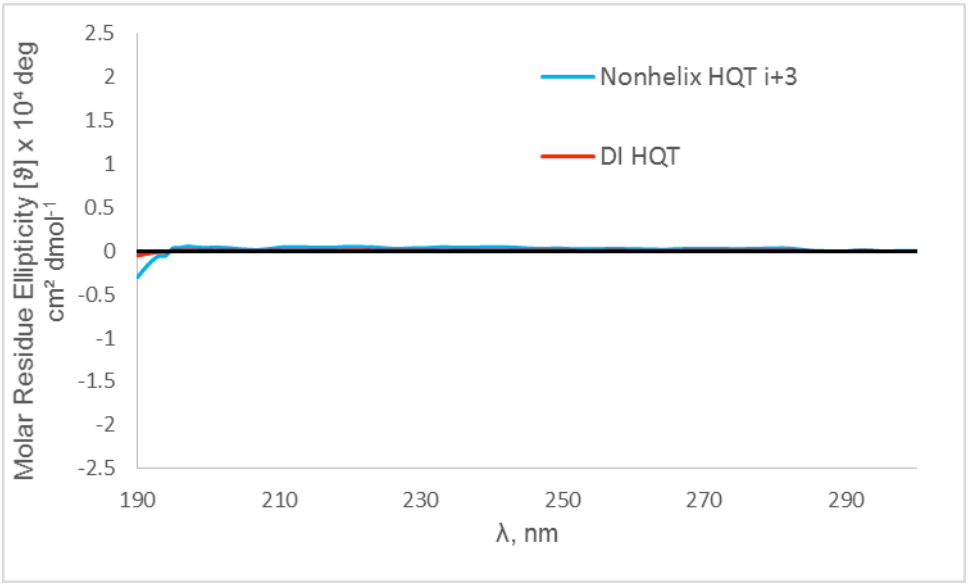

Figure S7. CD spectra of peptoid oligomers **Nonhelix HQT i+3** and **DI HQT**. The spectra were recorded at room temperature, at concentrations of 100 μM in MeOH:H_2O 4:1.

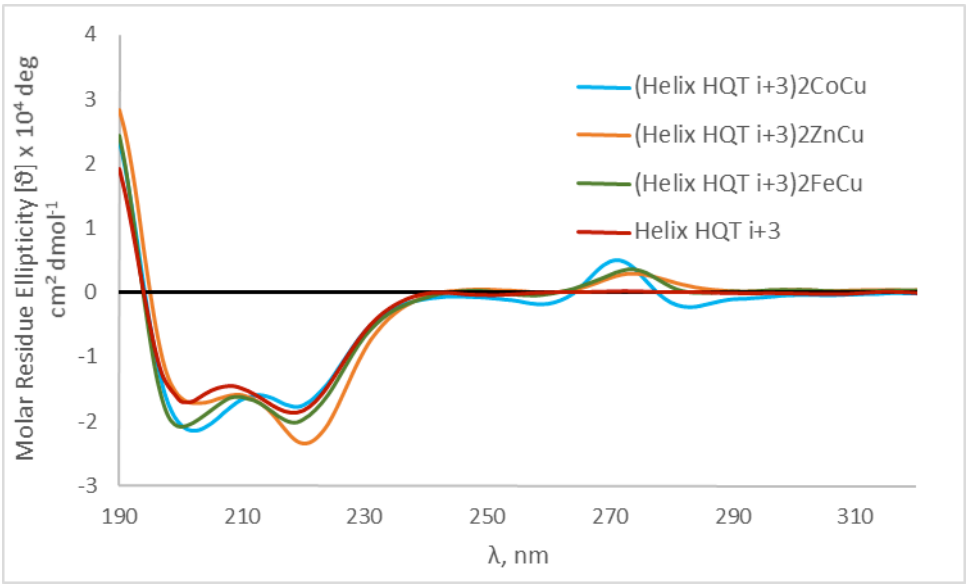

Figure S8. CD spectra of hetero bimetallic complexes (**Helix HQT i+3**)$_2$CoCu, (**Helix HQT i+3**)$_2$ZnCu and (**Helix HQT i+3**)$_2$FeCu. The spectra were recorded at room temperature, at concentrations of 100 μM in ACN.

UV-Vis data

UV-Vis of **Helix HQT i+3** and its metal complexes in MeOH/H_2O

Table S1. UV-Vis absorbance data of peptoid oligomer **Helix HQT i+3** and it metal complexes in MeOH/H_2O 4:1.

(**Helix HQT i+3**)M complex	λmax (nm)	Figure #
Co^{2+}	262, 309	S9
Zn^{2+}	265, 310, 322	S10
Mn^{2+}	266, 311, 322	S11
Ni^{2+}	268, 312, 325	S12
Fe^{3+}	249, 316, 556	S13

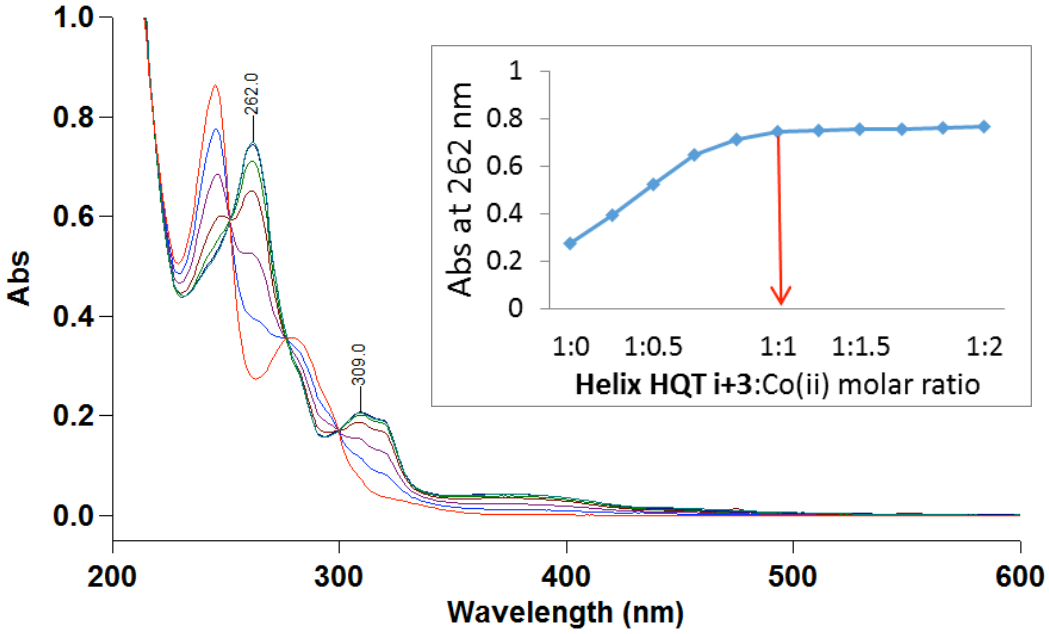

Figure S9. UV-Vis titration and a peptoid-to-metal ratio plot of **Helix HQT i+3** (17 μM) with Co^{2+} acetate (5mM) in 3 ml MeOH:H_2O 4:1.

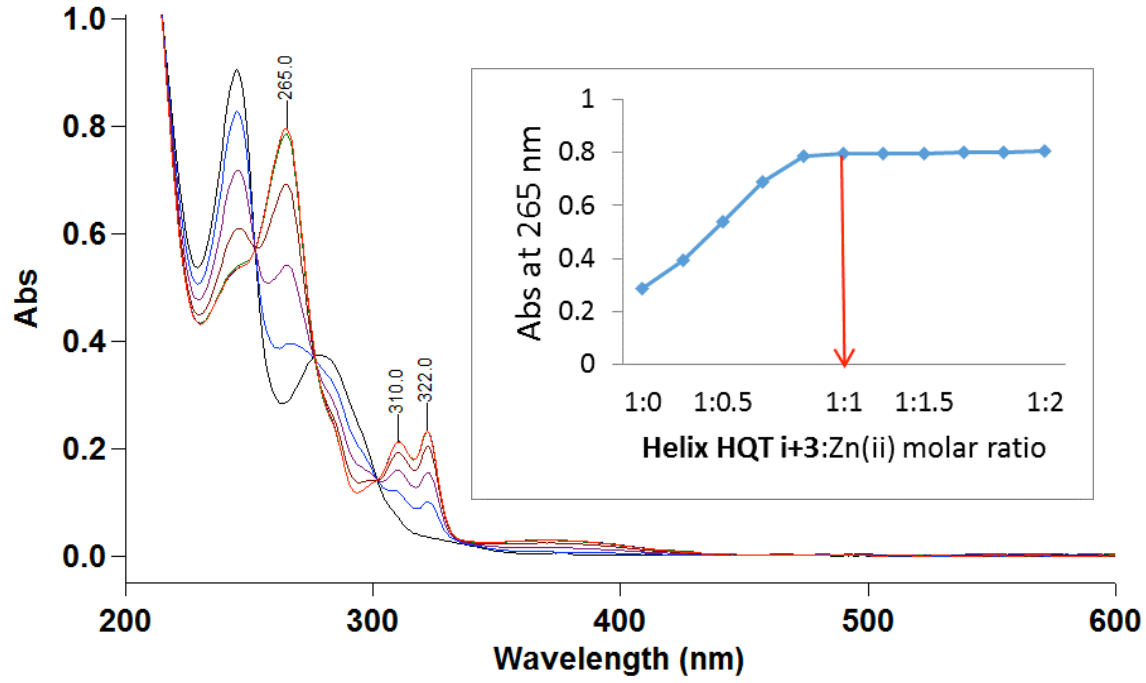

Figure S10. UV-Vis titration and a peptoid-to-metal ratio plot of **Helix HQT i+3** (17 μM) with Zn^{2+} acetate (5mM) in 3ml MeOH:H_2O 4:1.

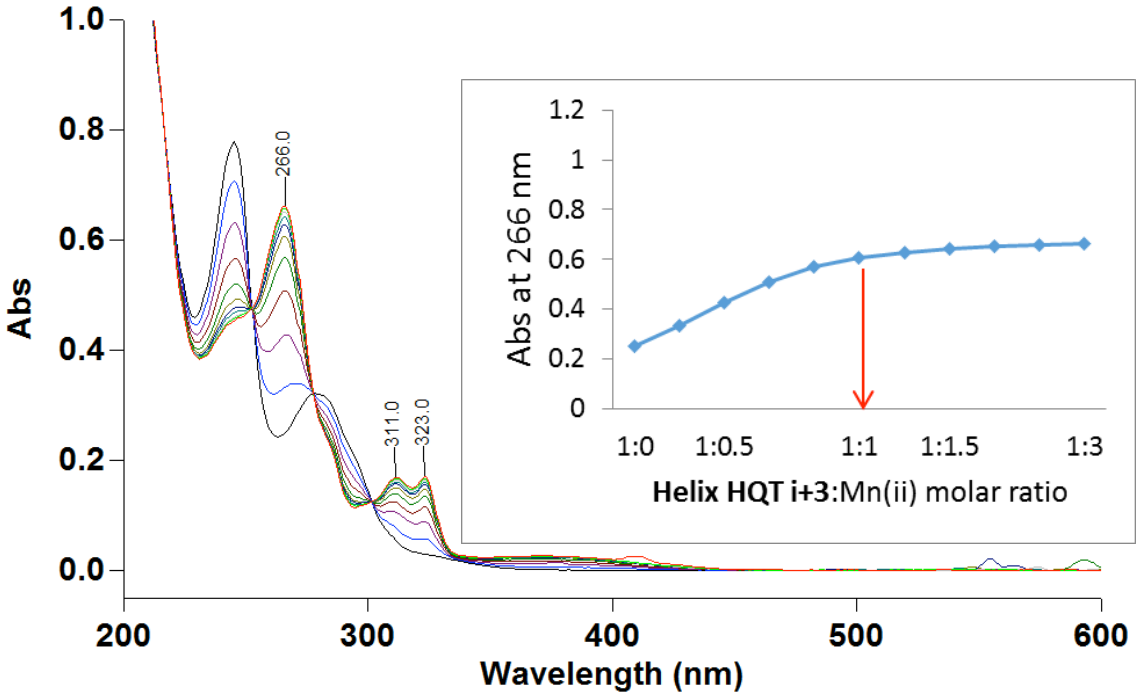

Figure S11. UV-Vis titration and a peptoid-to-metal ratio plot of **Helix HQT i+3** (17 μM) with Mn^{2+} acetate (5mM) in 3ml MeOH:H_2O 4:1.

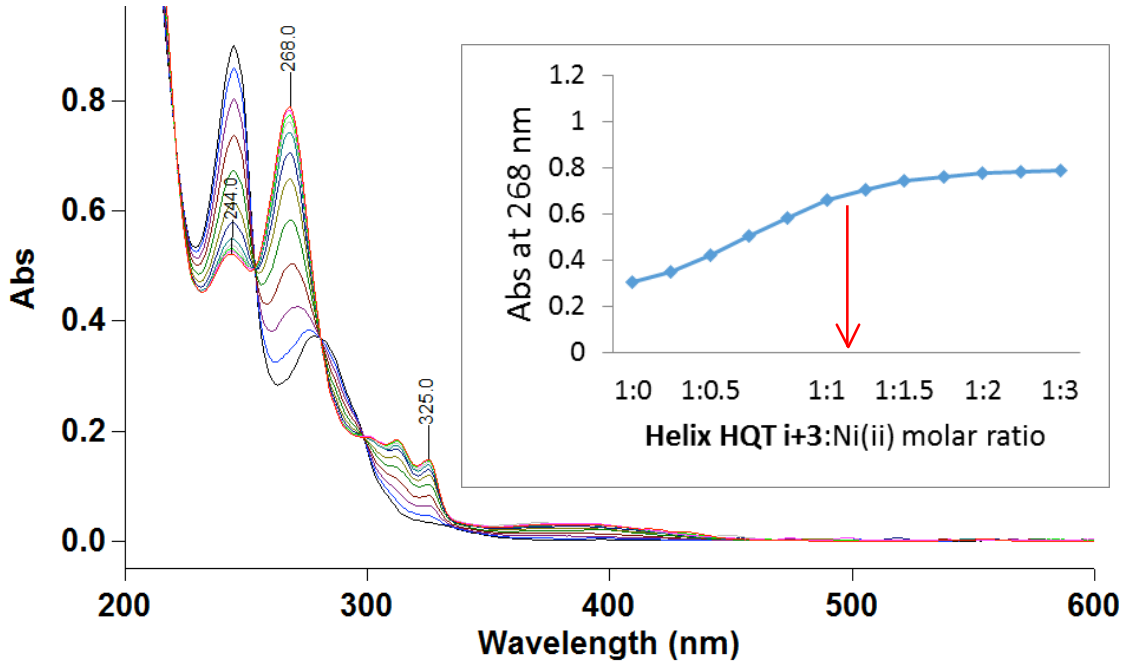

Figure S12. UV-Vis titration and a peptoid-to-metal ratio plot of **Helix HQT i+3** (17 μM) with Ni^{2+} acetate (5mM) in 3ml MeOH:H_2O 4:1.

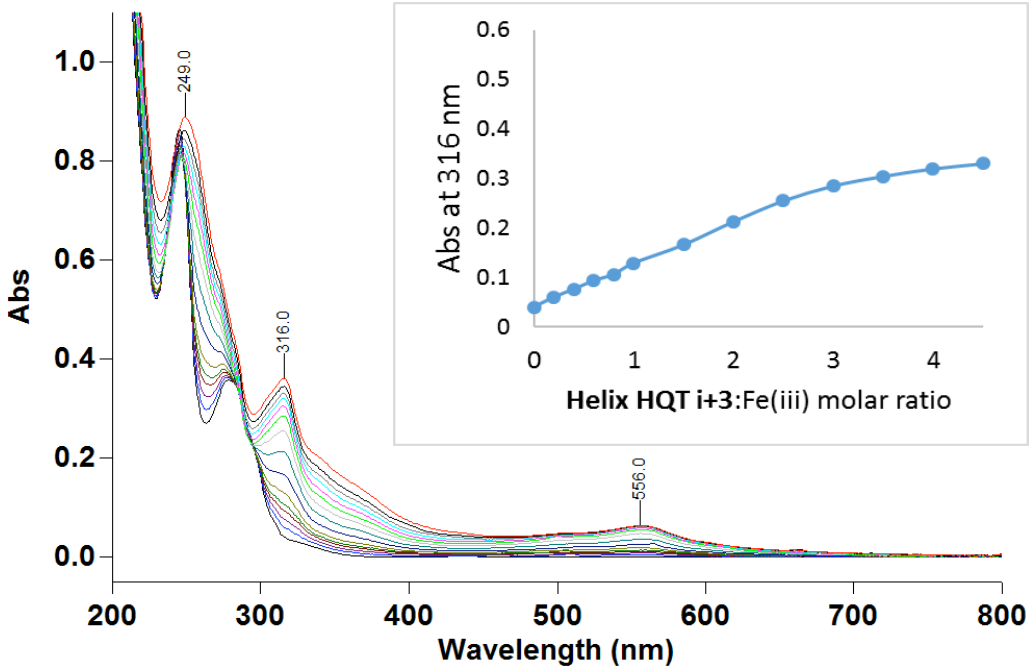

Figure S13. UV-Vis titration and a peptoid-to-metal ratio plot of **Helix HQT i+3** (17 μM) with Ni^{2+} acetate (5mM) in 3ml MeOH:H_2O 4:1. The peptoid-to-metal ratio plot in this case does not provide information about the binding.

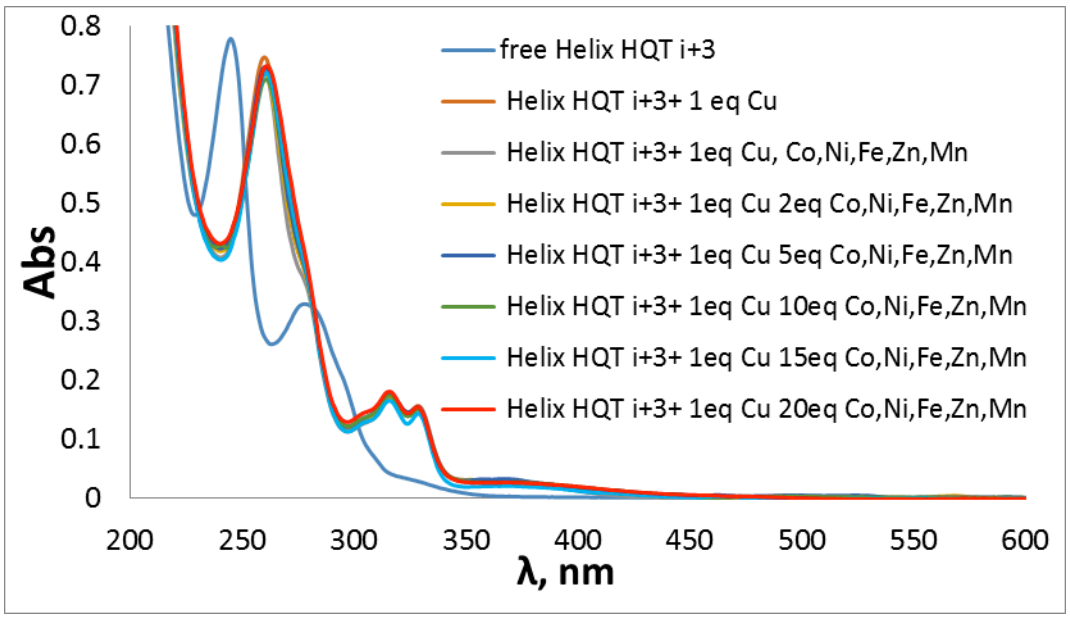

Figure S14. UV of **Helix HQT i+3** (17 μM) with 1 equiv. Cu^{2+} and 1-20 equiv. of Co^{2+}, Ni^{2+}, Fe^{3+},Zn^{2+}, Mn^{2+} in MeOH:H_2O 4:1. Absorption bands off all spectra were 259, 316, 328 nm.

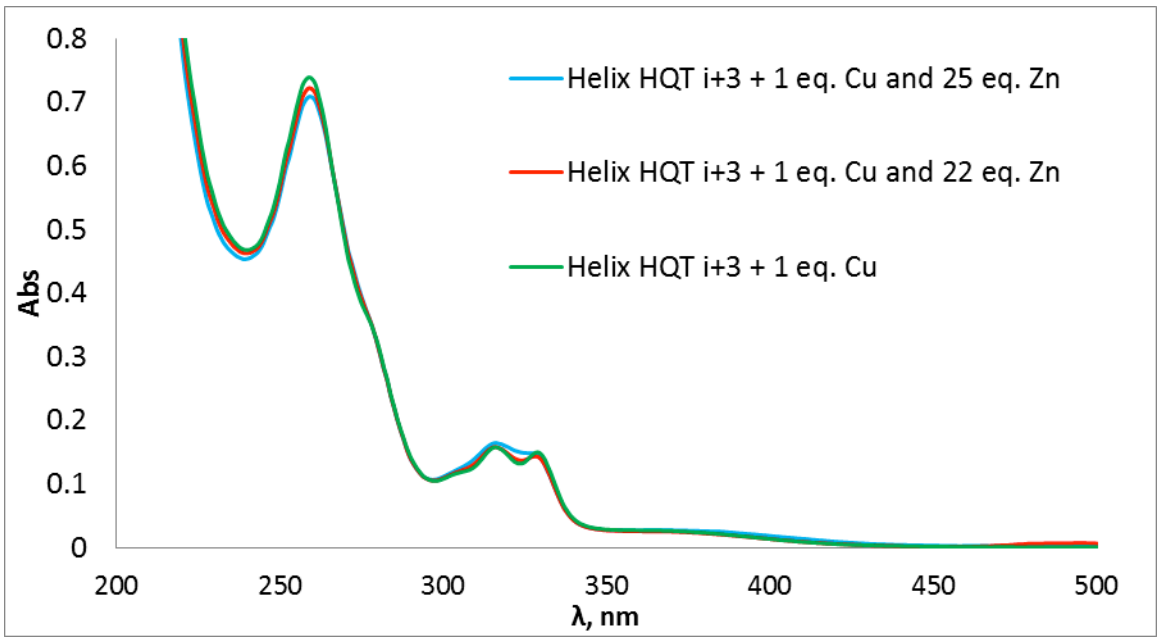

Figure S15. UV-VIs of **Helix HQT i+3** (17 μM) in 5:1 H_2O:MeOH solution containing Cu^{2+} only or mix of 1 equiv. Cu^{2+} and 25 or 22 equiv. Zn^{2+}.

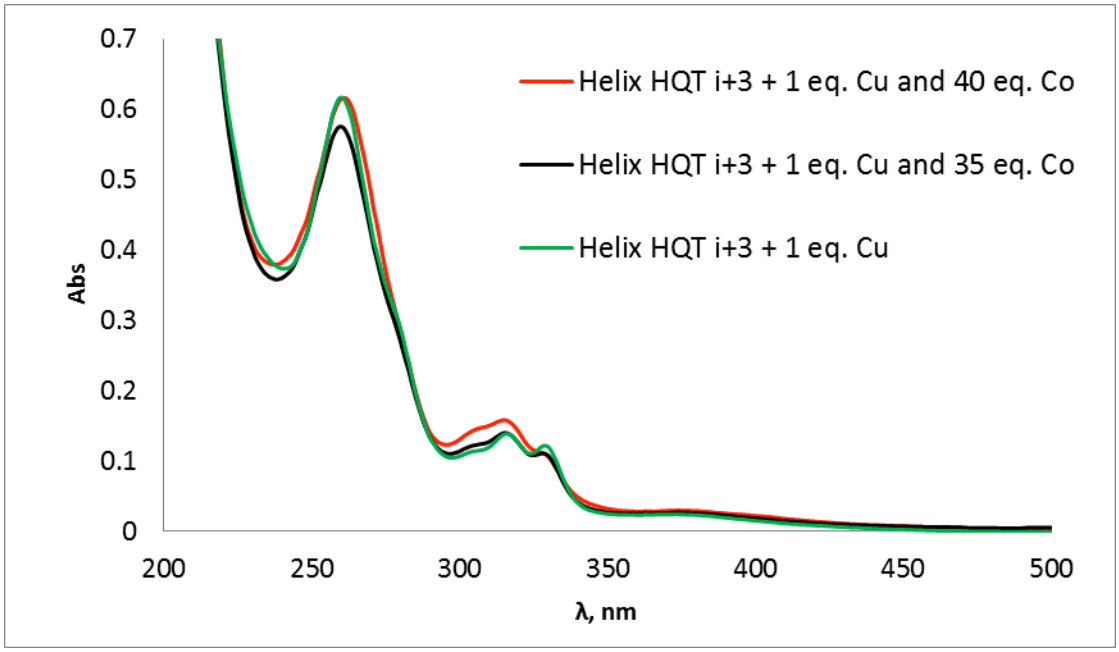

Figure S16. UV-Vis of **Helix HQT i+3** (17 μM) in 5:1 H_2O:MeOH solution containing 1 equiv. Cu^{2+} only or mix of 1 equiv. Cu^{2+} and 35 or 40 equiv. of Co^{2+}.

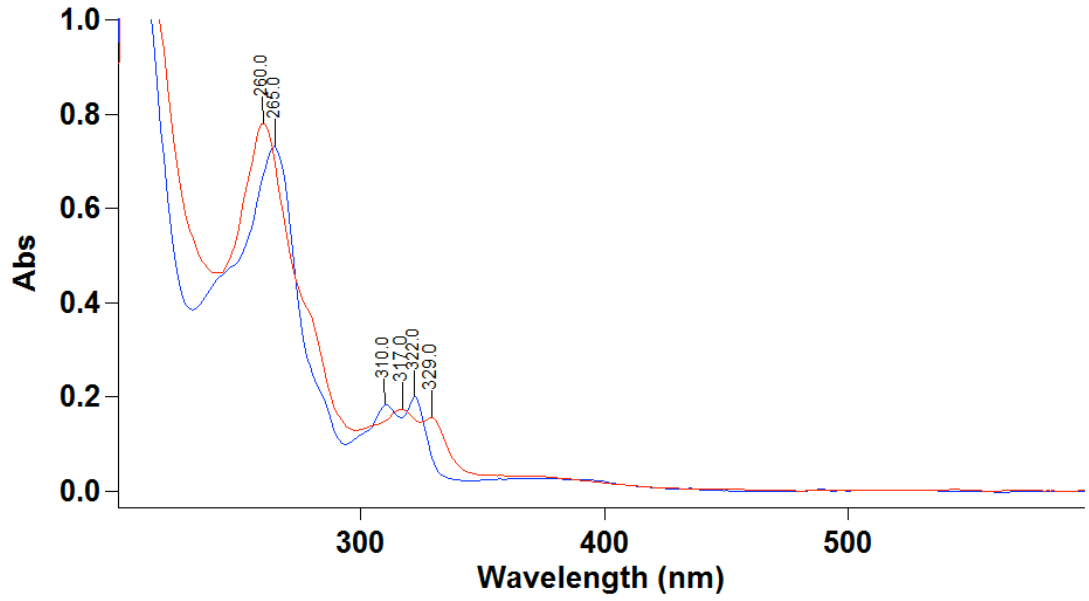

Figure S17. UV-Vis of (**Helix HQT i+3**)Zn (blue, 17 μM) followed by addition of 1 equiv. of Cu^{+2} (red) in MeOH/H_2O 4:1.

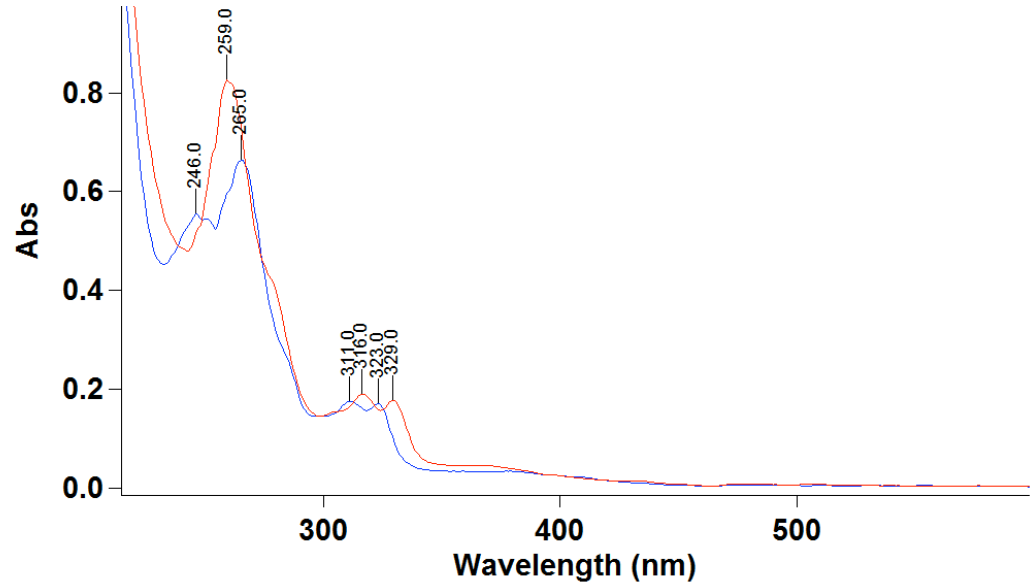

Figure S18. UV-Vis of (**Helix HQT i+3**)Mn (blue, 17 μM) followed by addition of 1 equiv. of Cu^{+2} (red) in MeOH/H_2O 4:1.

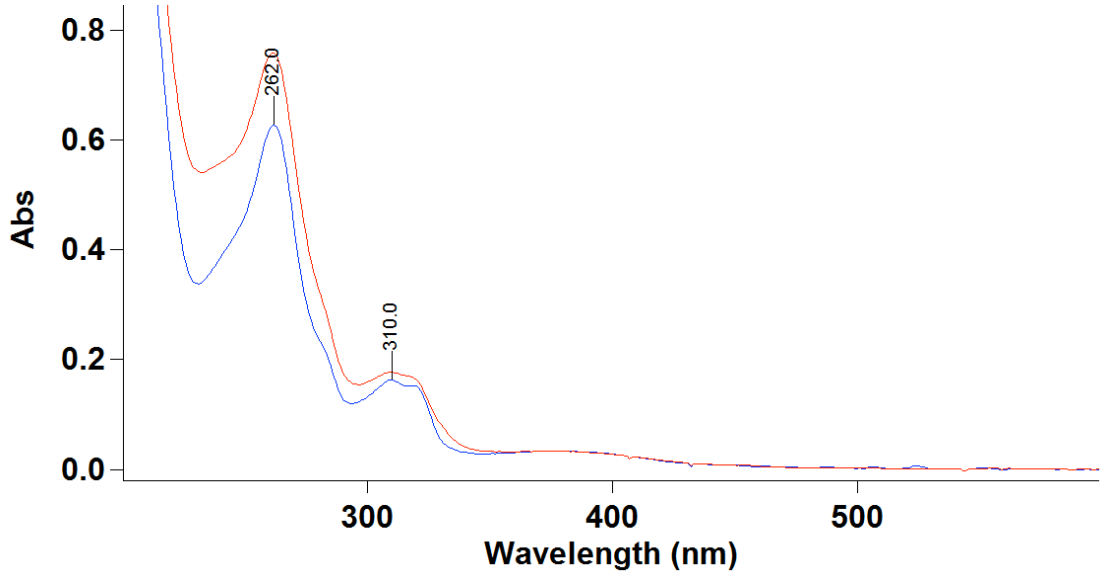

Figure S19. UV-Vis of (**Helix HQT i+3**)Co (blue, 17 μM) followed by addition of 1 equiv. of Cu^{+2} (red) in MeOH/H_2O 4:1.

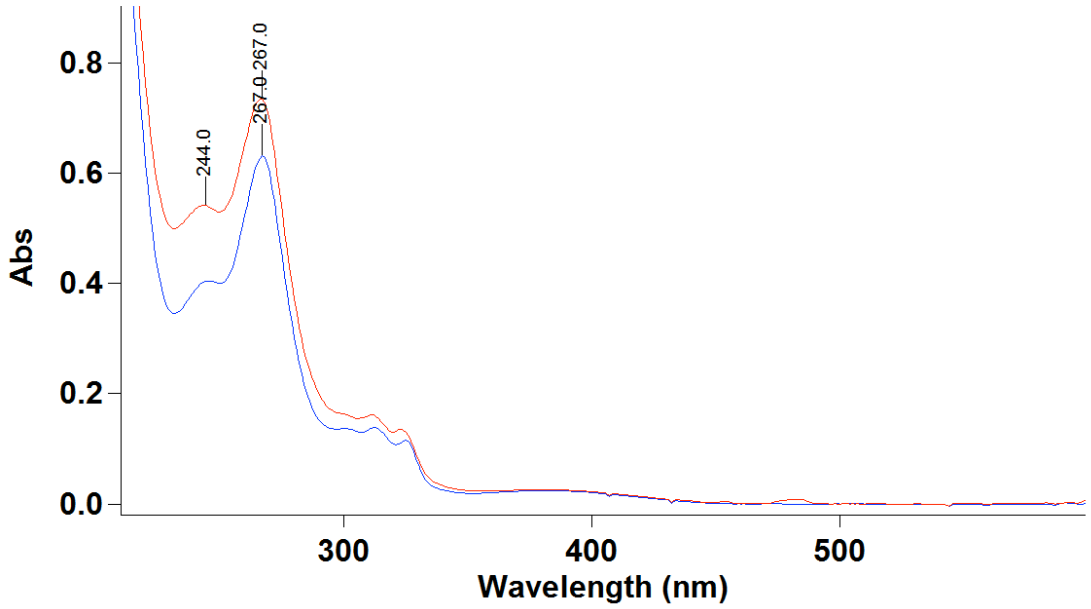

Figure S20. UV-Vis of (**Helix HQT i+3**)Ni (blue, 17 μM) followed by addition of 1 equiv. of Cu^{+2} (red) in MeOH/H_2O 4:1.

UV-Vis of control peptoids with mixture of metal ions in MeOH:H_2O

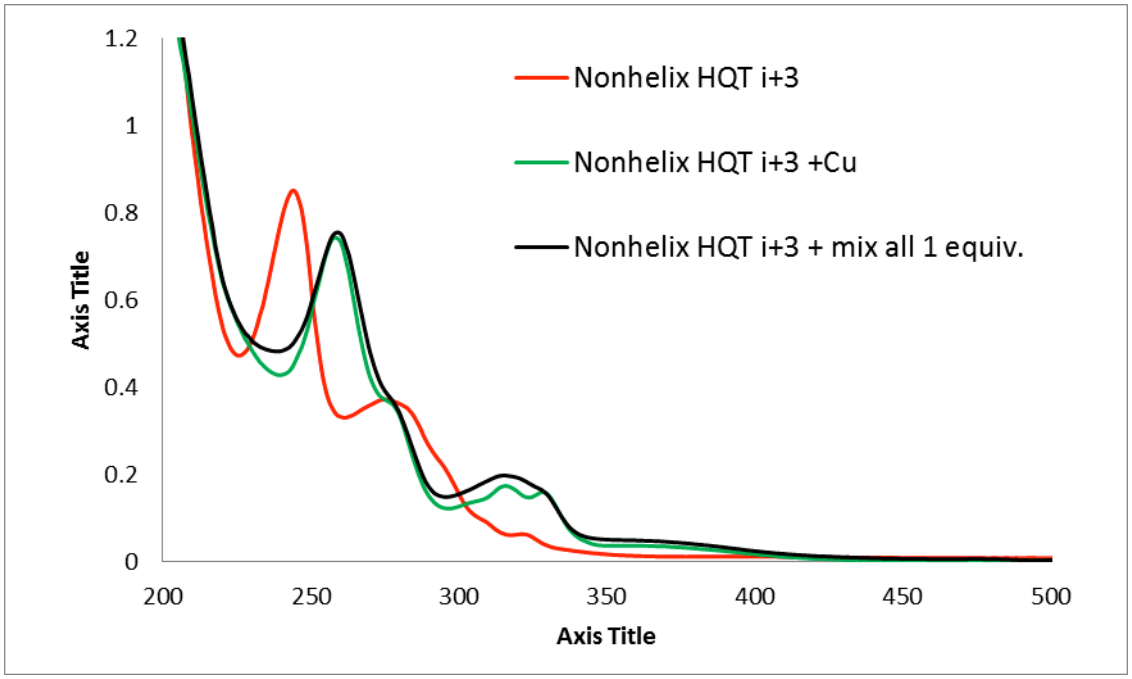

Figure S21. UV-Vis of **Nonhelix HQT i+3** (17 μM) with 1 equiv. Cu^{2+} and 1 equiv. of Cu^{2+} ,Co^{2+}, Ni^{2+}, Fe^{3+}, Zn^{2+}, Mn^{2+} in 3ml MeOH:H_2O 4:1.

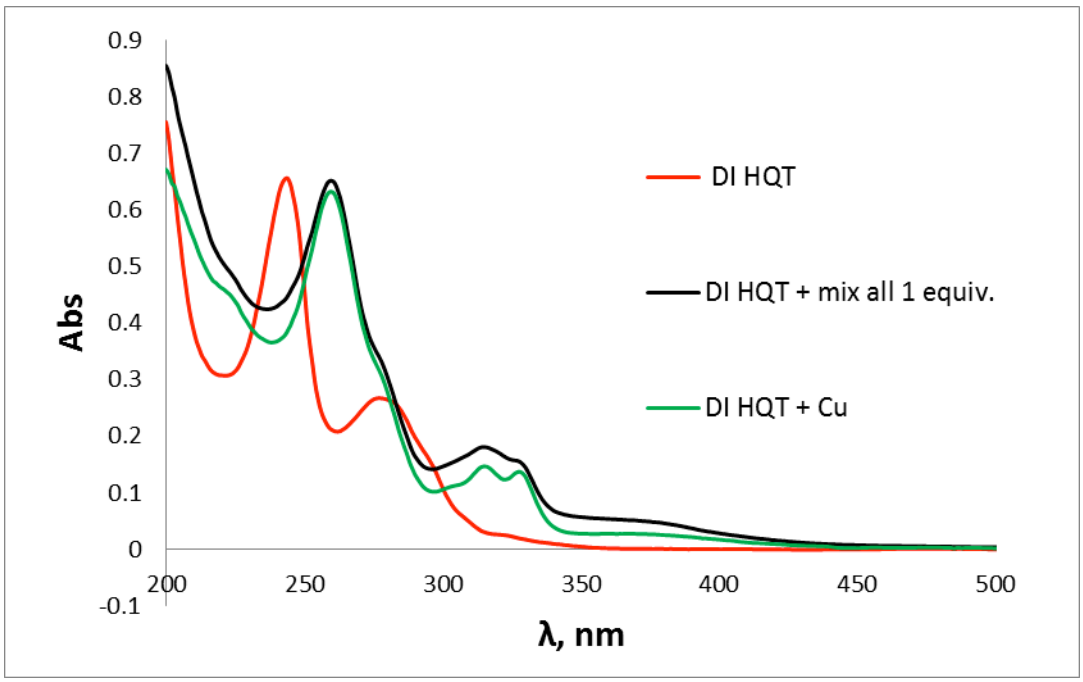

Figure S22. UV-Vis of **DI HQT** (17 μM) with 1 equiv. Cu^{2+} and 1 equiv. of Cu^{2+} ,Co^{2+}, Ni^{2+}, Fe^{3+}, Zn^{2+}, Mn^{2+} in 3ml MeOH:H_2O 4:1.

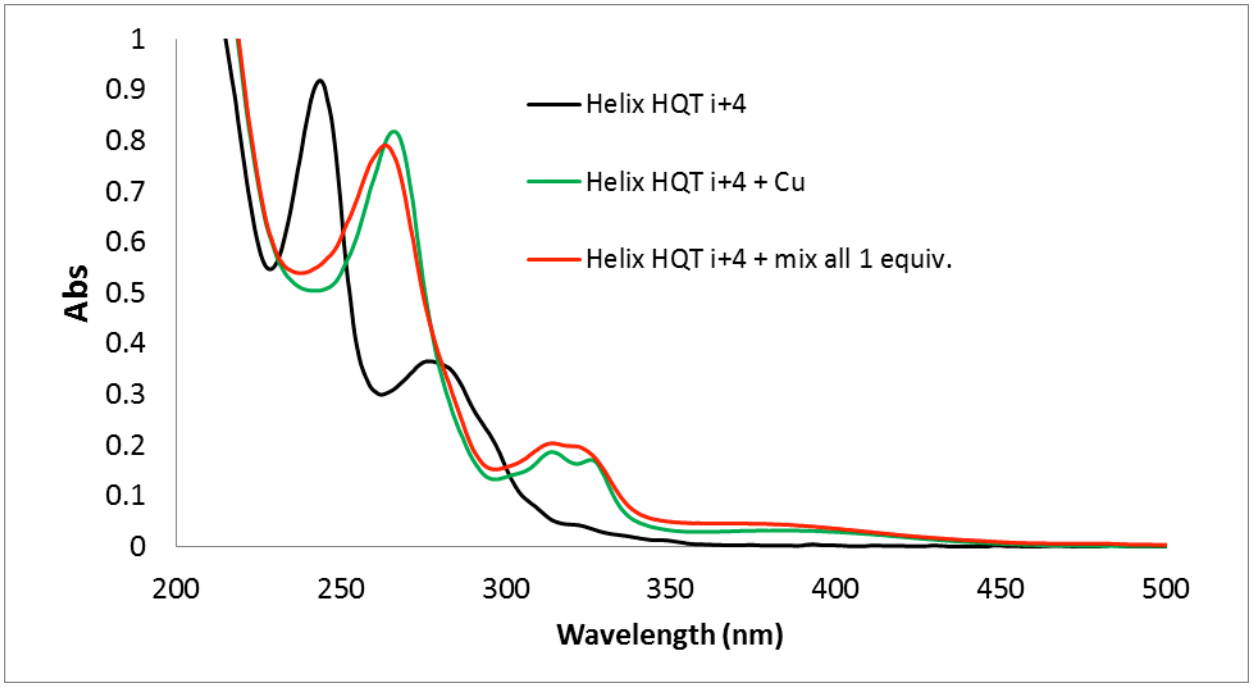

Figure S23. UV-Vis of **Helix HQT i+4** (17 μM) with 1 equiv. Cu^{2+} and 1 equiv. of Cu^{2+} ,Co^{2+}, Ni^{2+}, Fe^{3+}, Zn^{2+}, Mn^{2+} in 3ml MeOH:H_2O 4:1.

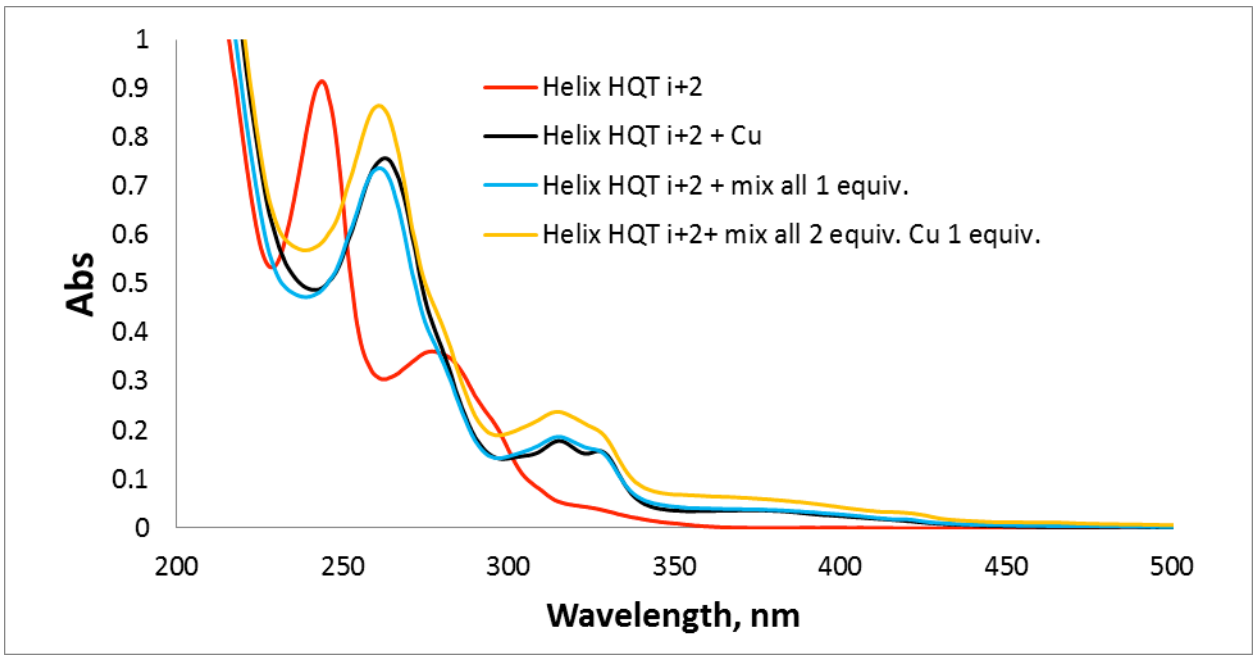

Figure S24. UV-Vis of **Helix HQT i+2** (17 μM) with 1 equiv. Cu^{2+} and 1 and 2 equiv. of Cu^{2+} ,Co^{2+}, Ni^{2+}, Fe^{3+}, Zn^{2+}, Mn^{2+} in 3ml MeOH:H_2O 4:1.

UV-Vis of **Helix HQT i+3** and its metal complexes in ACN

Table S2. Absorbance data of peptoid oligomer **Helix HQT i+3** and it metal complexes in ACN.

(**Helix HQT i**+3)M complex	λmax (nm)	Figure #
Cu^{2+}	263, 316, 329	S27
Co^{2+}	264, 308	S28
Zn^{2+}	268, 311, 323	S29
Fe^{3+}	253, 315, 560	S30
Ni^{2+}	270, 312, 325	S31
Mn^{2+}	263, 312, 323	S32

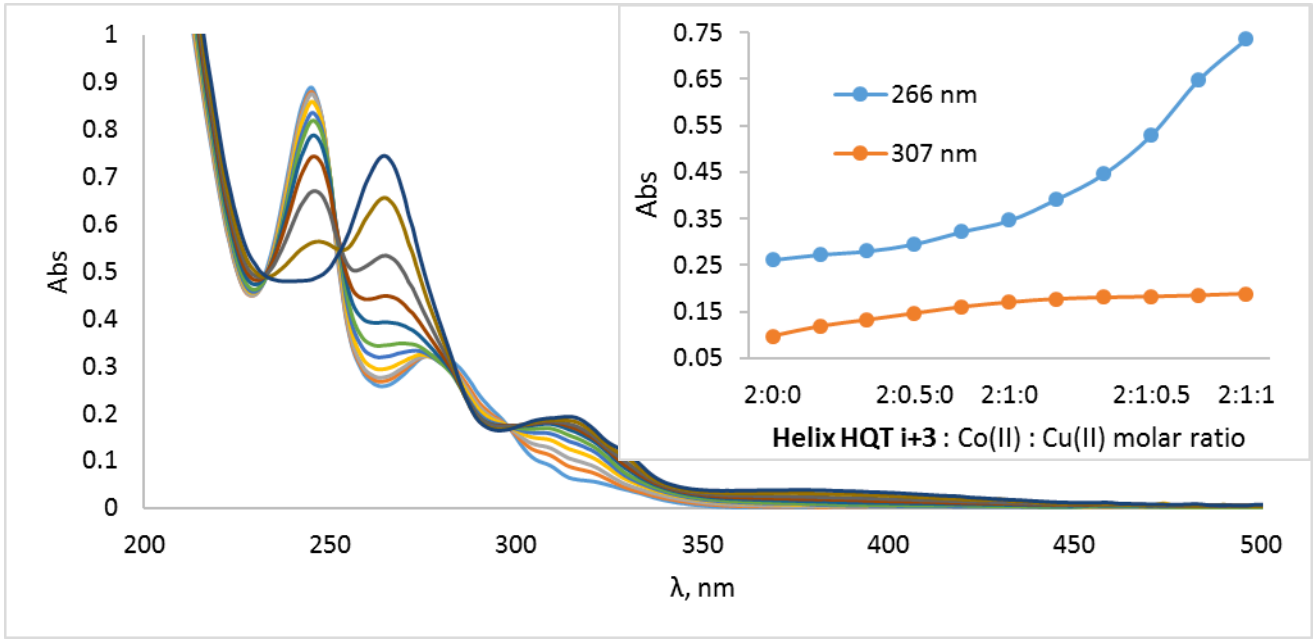

Figure S25. UV-Vis Titration and a peptoid-to-metal ratio plot of **Helix HQT i+3** (17 μM) with 0.5 equiv. of Co^{2+} (2.5 mM) followed by titration of 0.5 equiv. of Cu^{2+} (2.5 mM) in 3mL ACN.

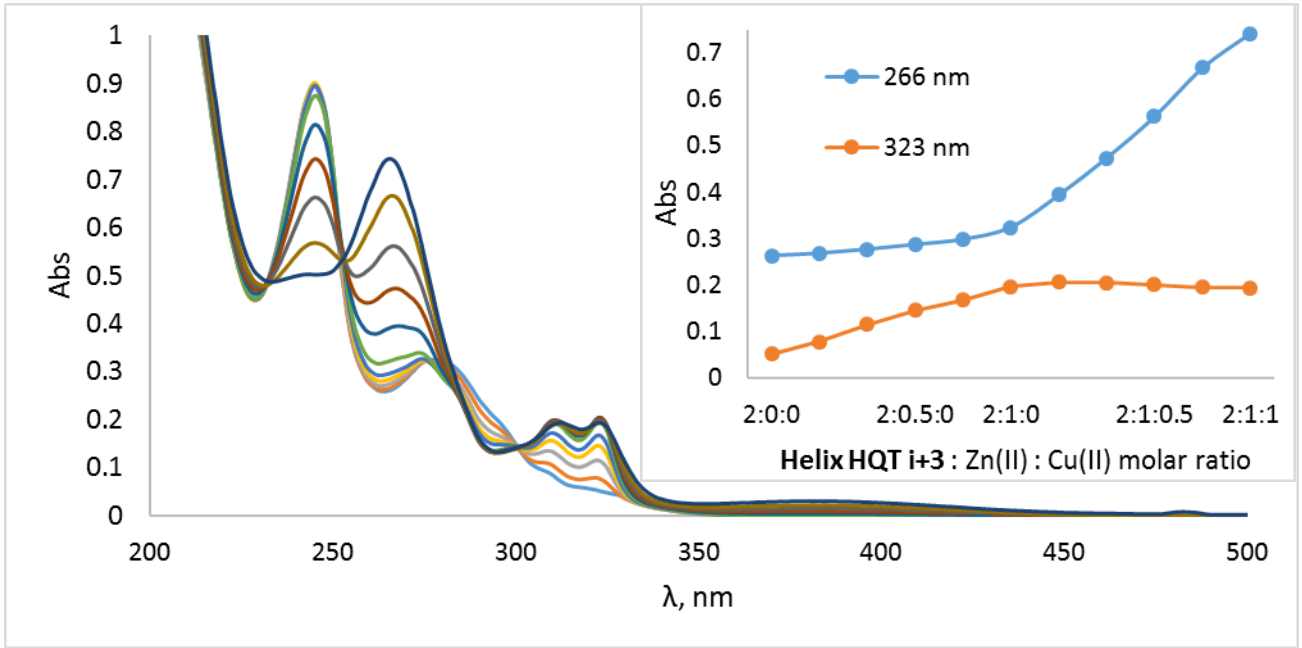

Figure S26. UV-Vis Titration and a peptoid-to-metal ratio plot of **Helix HQT i+3** (17 μM) with 0.5 equiv. of Zn^{2+} (2.5 mM) followed by titration of 0.5 equiv. of Cu^{2+} (2.5mM) in 3 ml ACN.

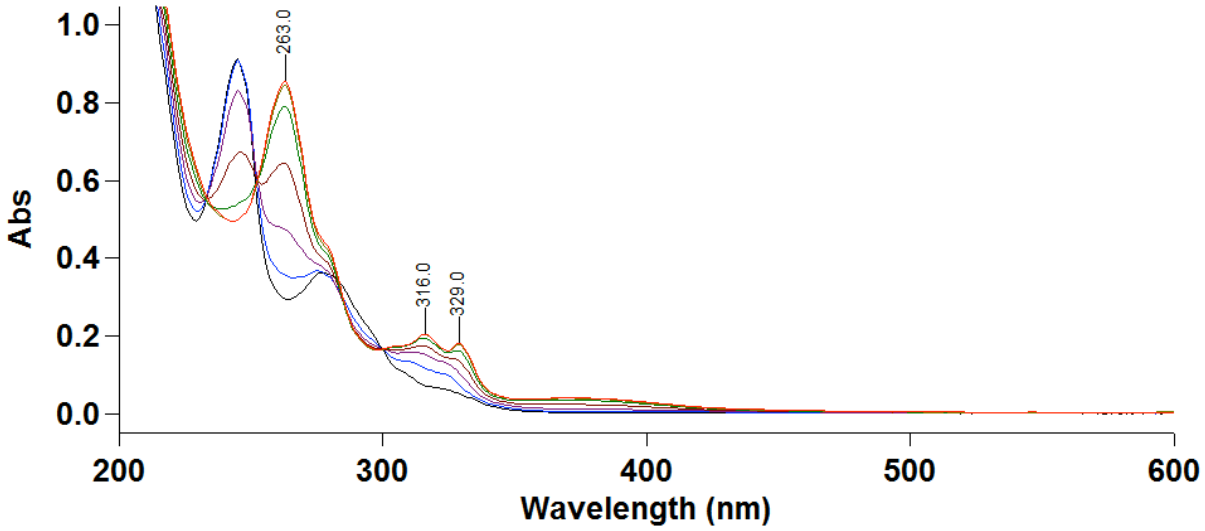

Figure S27. UV-Vis titration of **Helix HQT i+3** (17 µM) with Cu^{2+} acetate (5mM) in 3ml ACN.

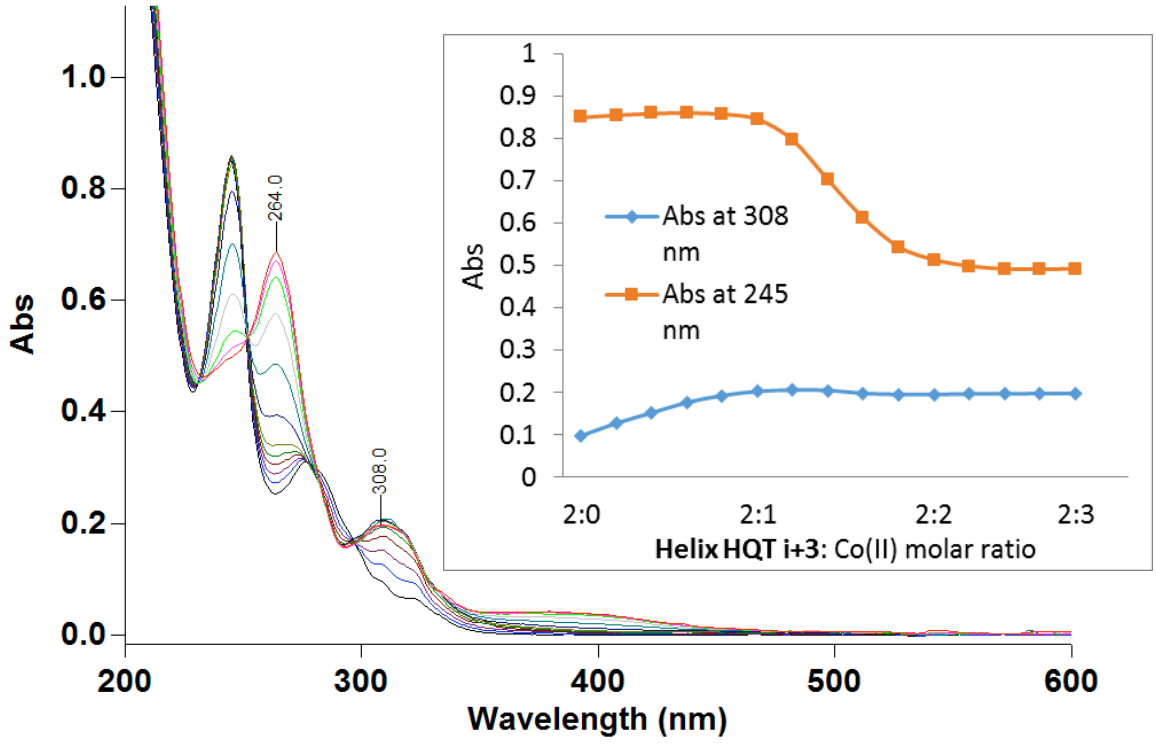

Figure S28. UV-Vis titration and a peptoid-to-metal ratio plot of **Helix HQT i+3** (17 µM) with Co^{2+} acetate (2.5mM) in 3ml ACN.

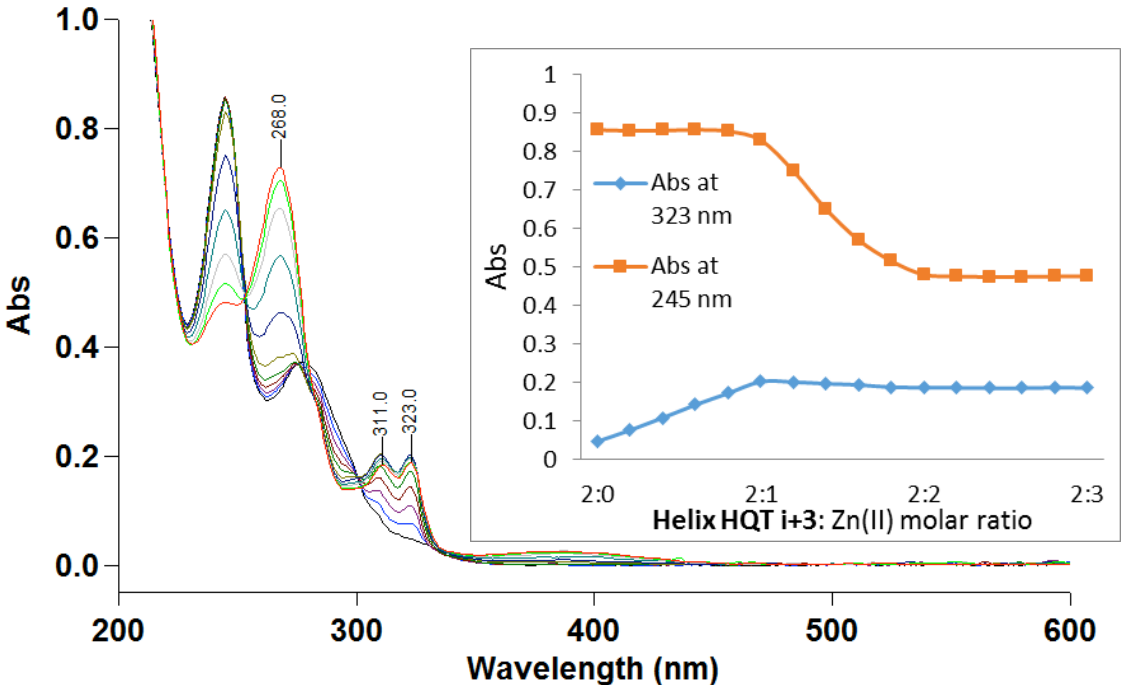

Figure S29. UV-Vis titration and a peptoid-to-metal ratio plot of **Helix HQT i+3** (17 μM) with Zn^{+2} acetate (2.5mM) in 3ml ACN.

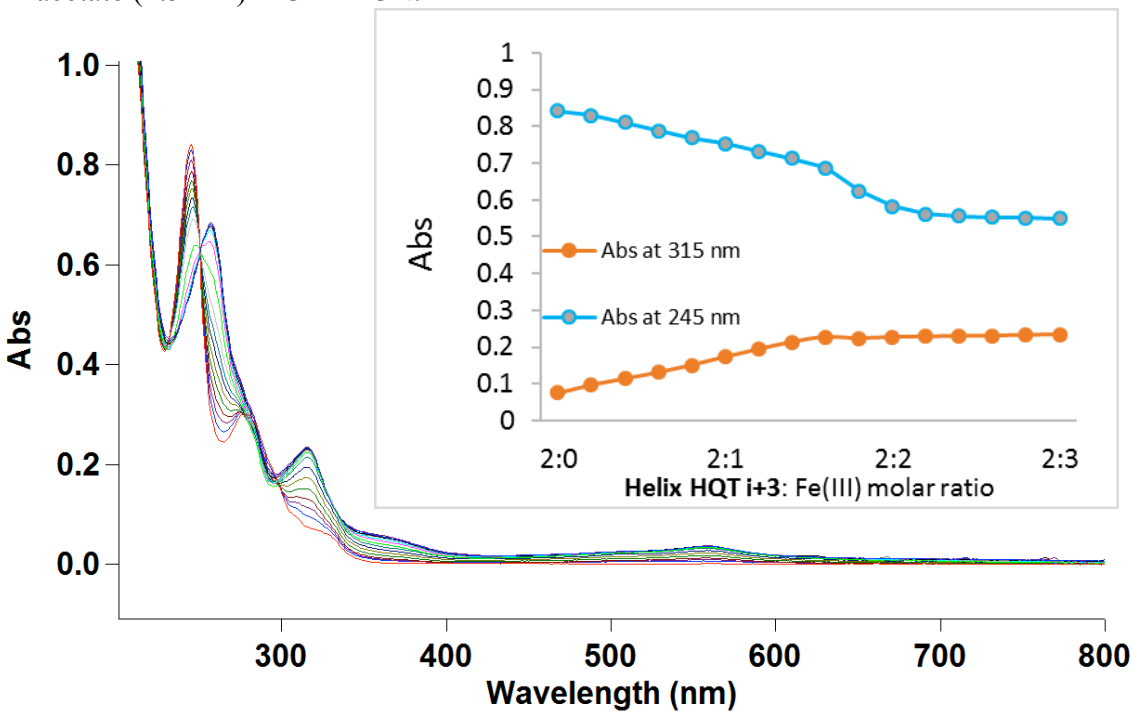

Figure S30. UV-Vis titration and a peptoid-to-metal ratio plot of **Helix HQT i+3** (17 μM) with Fe^{3+} perchlorate (2.5mM) in 3ml ACN.

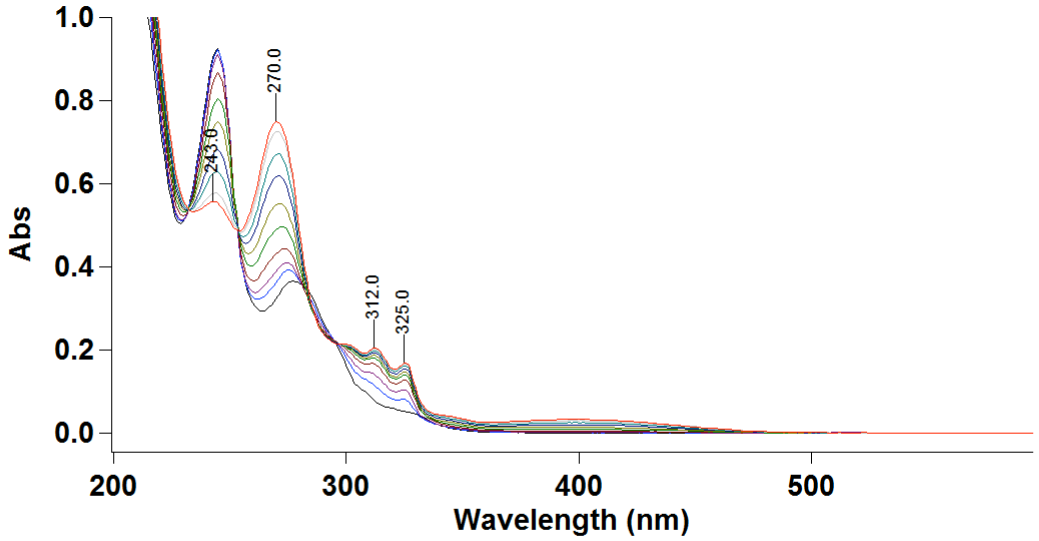

Figure S31. UV-Vis titration of **Helix HQT i+3** (17 µM) with Ni^{2+} acetate (2.5mM) in 3ml ACN.

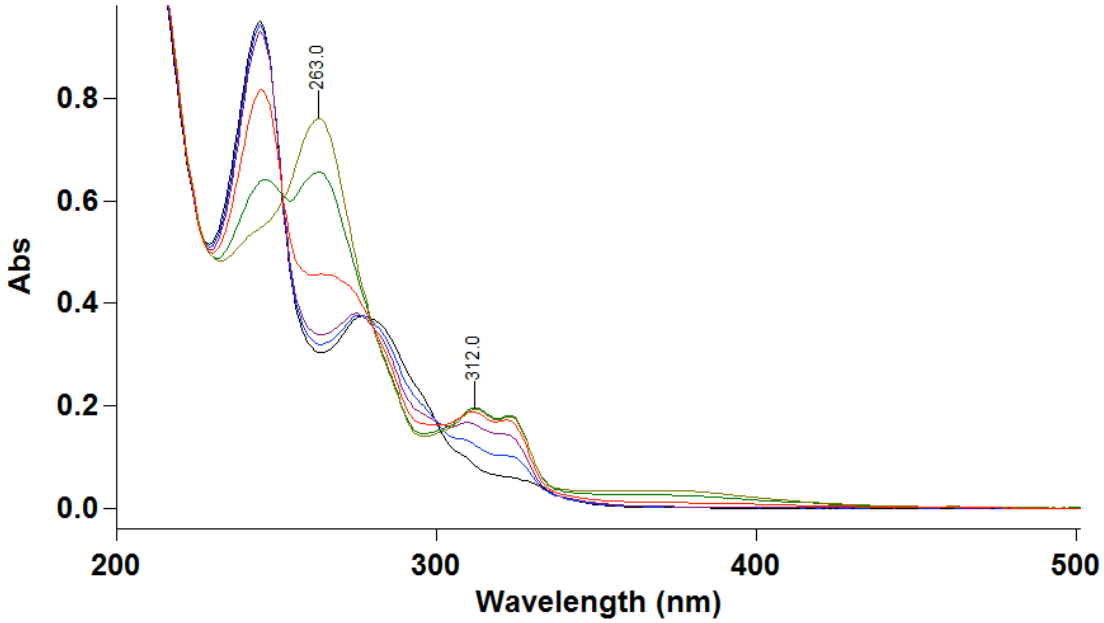

Figure S32. UV-Vis titration of **Helix HQT i+3** (17 µM) with Mn^{2+} acetate (5mM) in 3ml ACN.

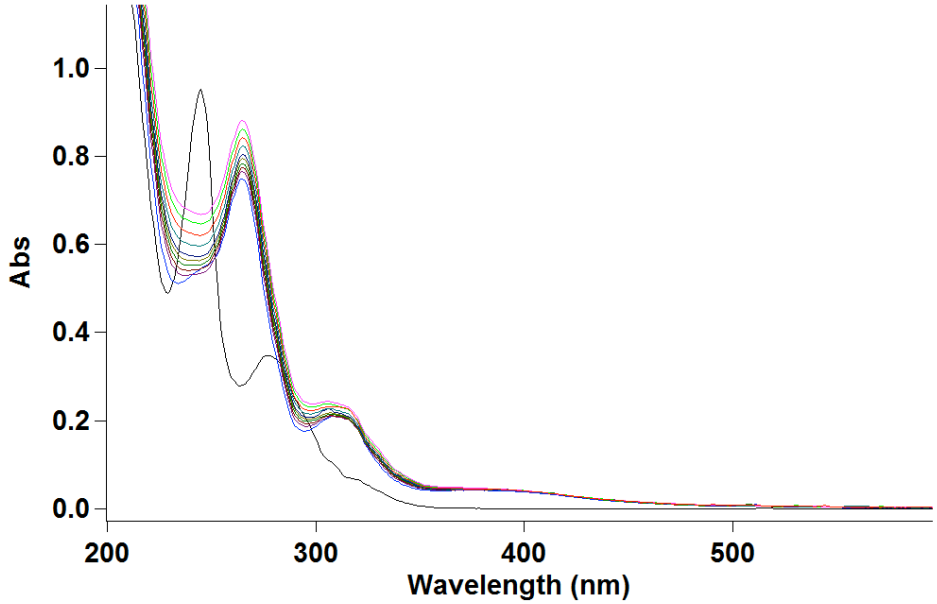

Figure S33. UV-Vis of free peptoid **Helix HQT i+3** (black, 17 µM), formation of (**Helix HQT i+3**)$_2$CoCu (blue) followed by titration with Cu^{+2} (2.5mM) in 3ml ACN.

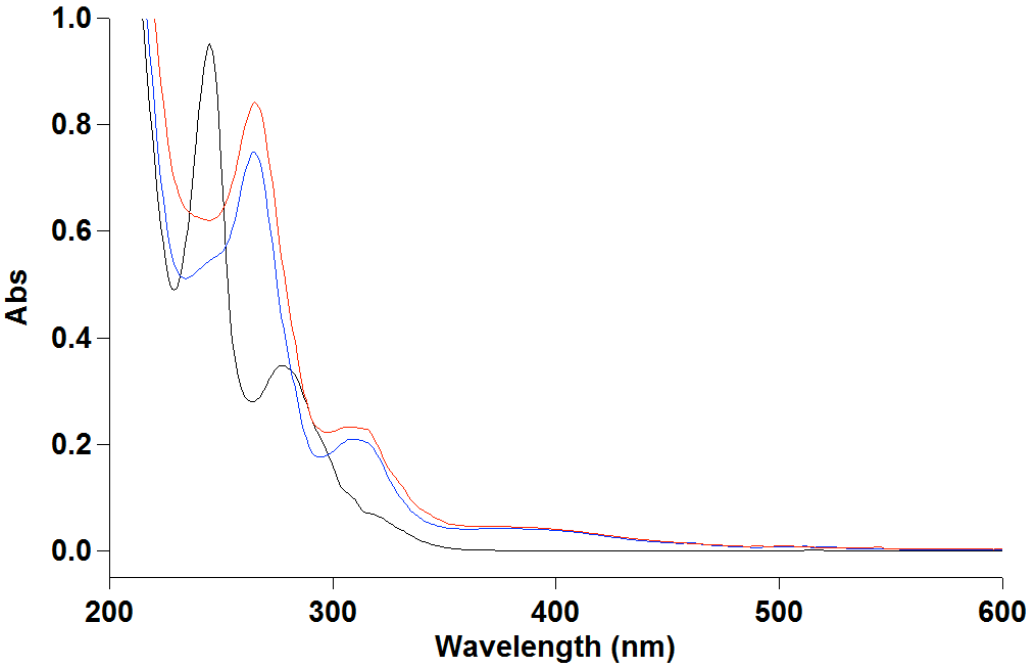

Figure S34. UV-Vis of **Helix HQT i+3** (black, 17 µM), (**Helix HQT i+3**)$_2$CoCu (blue) followed by addition of 2 equiv. of Cu^{+2} (red) in ACN.

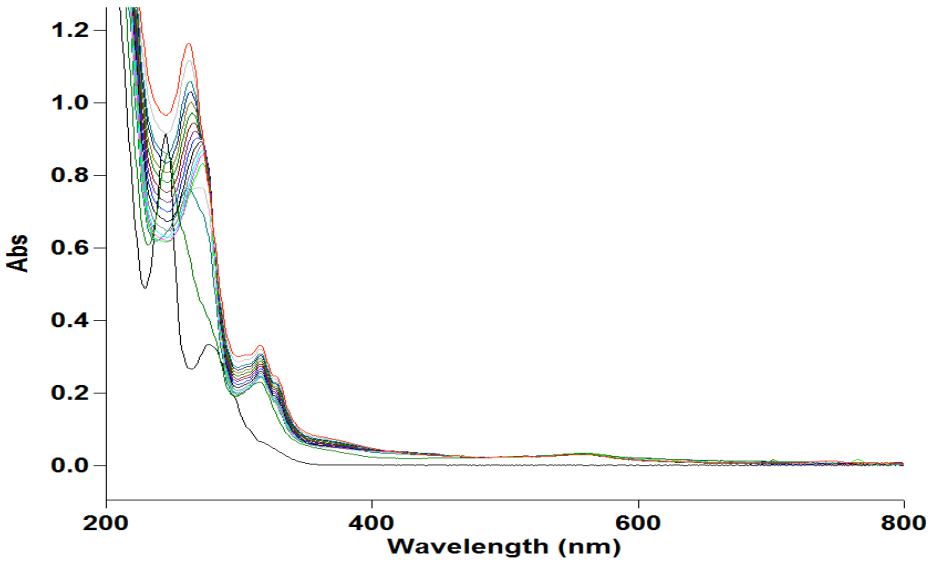

Figure S35. UV-Vis of free peptoid **Helix HQT i+3** (black, 17 µM), formation of (**Helix HQT i+3**)$_2$FeCu (blue) followed by titration with Cu^{+2} (2.5mM) in 3ml ACN.

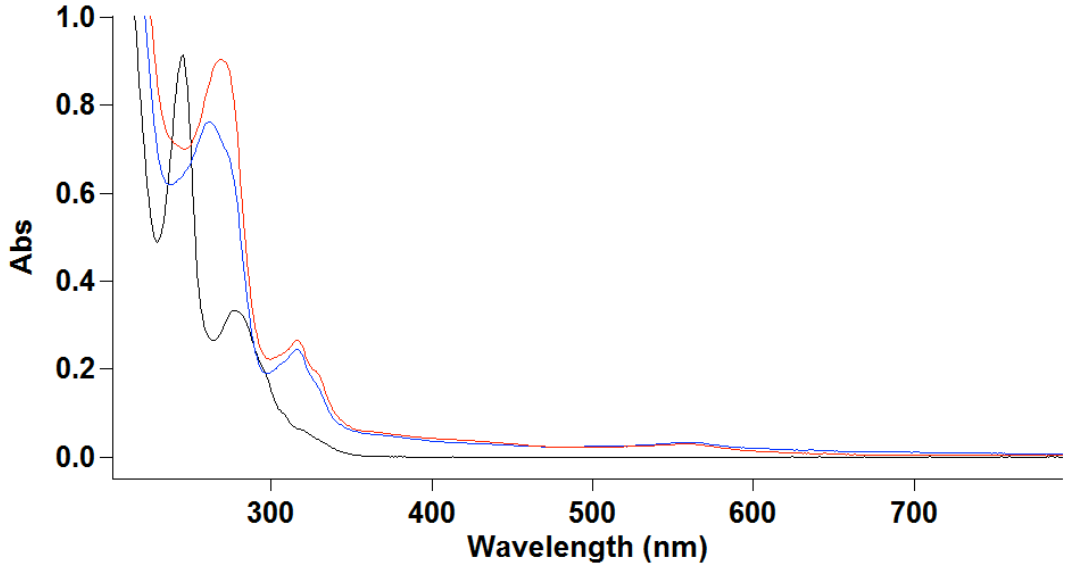

Figure S36. UV-Vis of **Helix HQT i+3** (black, 17 µM), (**Helix HQT i+3**)$_2$FeCu (blue line) followed by addition of 3 equiv. of Cu^{+2} (red) in 3ml ACN.

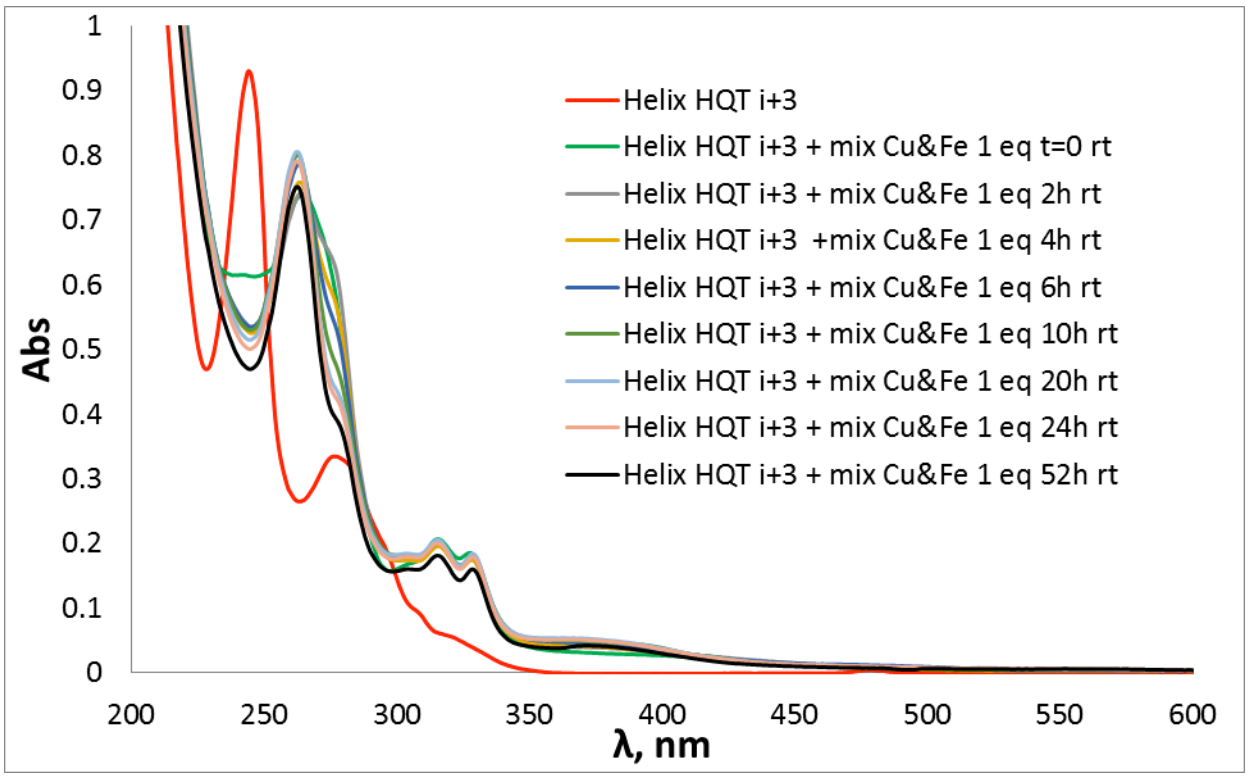

Figure S37. UV-Vis of **Helix HQT i+3** (17 µM) with mixture of 1 equiv. Cu^{2+} and Fe^{3+} in ACN at room temperature at different time points.

UV-Vis of control peptoids in ACN

Table S3. UV-Vis absorbance data of control peptoid oligomers and their metal complexes in ACN.

peptoid	Cu	Co	Zn	mix Cu&Co	mix Cu&Zn
Non helix HQT i+3	263, 316, 329 (Fig S38)	264, 30 (Fig S39)	268, 311, 323 (Fig S40)	262, 309 (Fig S41)	264, 314 (Fig S42)
DI HQT	263, 315, 328 (Fig S43)	264, 307 (Fig S44)	367, 311, 322 (Fig S45)	263, 315 (Fig S46)	264, 313 (Fig S47)
Helix HQT i+2	264, 314 (Fig S48)	266, 310 (Fig S49)	268, 310, 321 (Fig S50)	265, 311 (Fig S51)	267, 310 (Fig S52)
Helix HQT i+4	265, 316 (Fig S53)	266, 314 (Fig S54)	267, 309, 321 (Fig S55)	265, 310 (Fig S56)	267, 310, 321 (Fig S57)

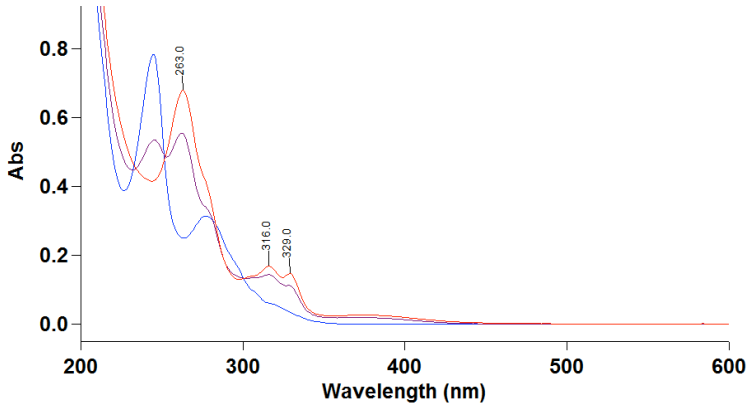

Figure S38. UV-Vis of **Nonhelix HQT i+3** (blue, 17 μM) in ACN with 0.5 (purple) and 1 equiv. of Cu^{2+} (red).

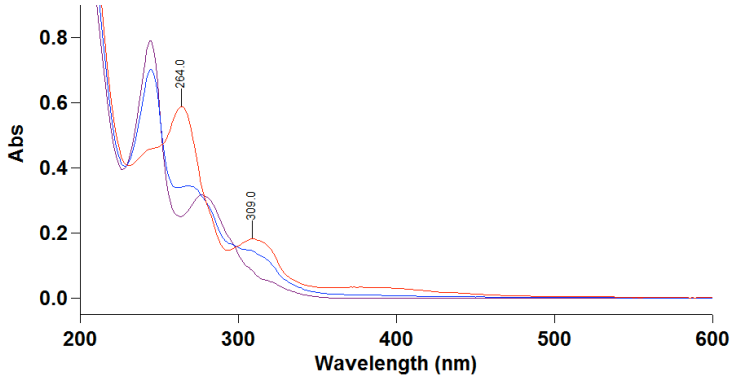

Figure S39. UV-Vis of **Nonhelix HQT i+3** (purple, 17 μM) in ACN with 0.5 (blue) and 1.5 equiv. of Co^{2+} (red).

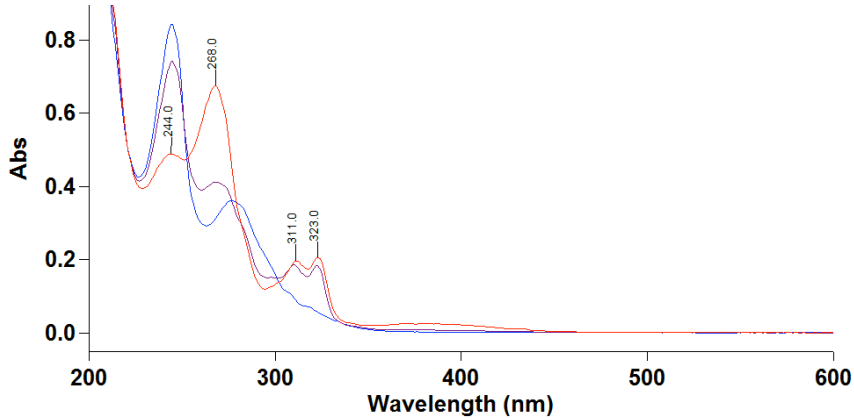

Figure S40. UV-Vis of **Nonhelix HQT i+3** (blue, 17 μM) in ACN with 0.5 (purple) and 1 equiv. of Zn^{2+} (red).

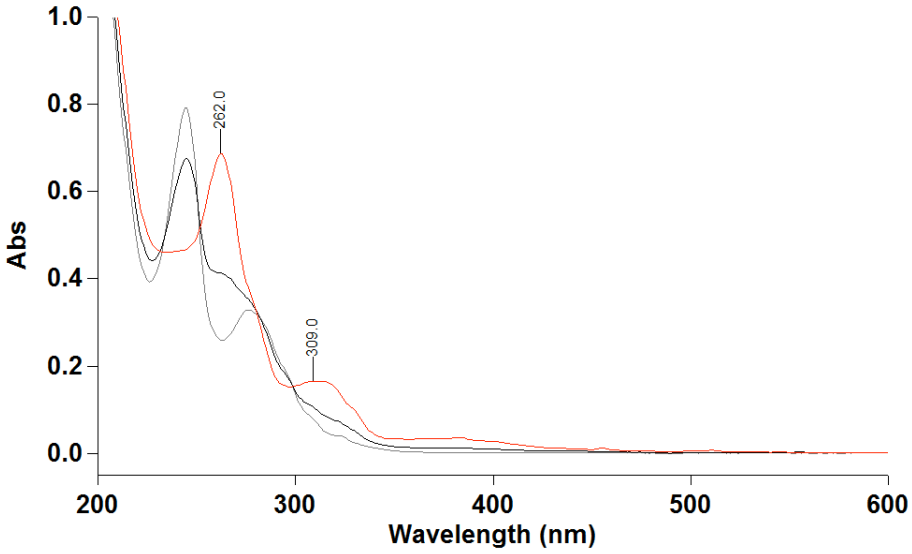

Figure S41. UV-Vis of free **NonHelix HQT i+3** (gray, 17 μM) with 0.5 equiv. mix of Cu^{2+} and Co^{2+} (black) and 1equiv. mix of Cu^{2+} and Co^{2+} (red) in ACN.

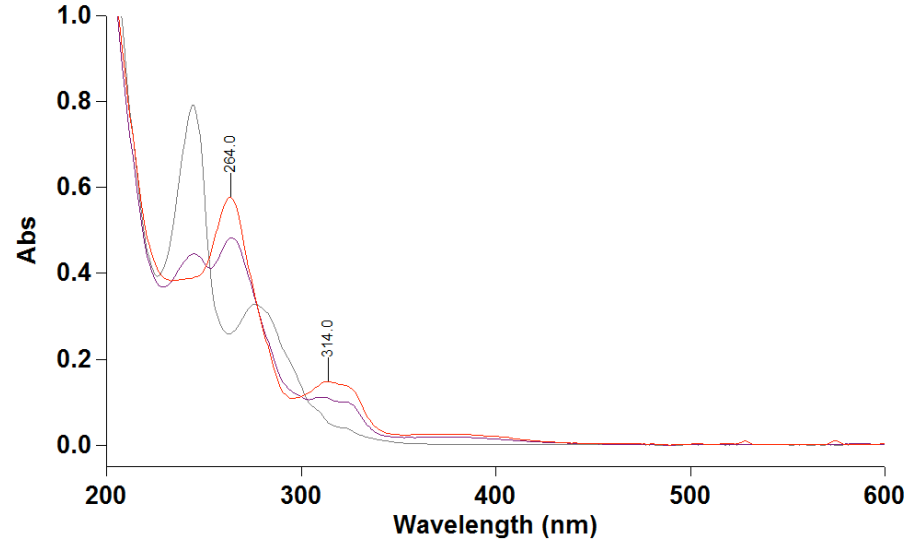

Figure S42. UV-Vis of free **NonHelix HQT i+3** (gray, 17 μM) with 0.5 equiv. mix of Cu^{2+} and Zn^{2+} (purple) and 1 equiv. mix of Cu^{2+} and Zn^{2+} (red) in ACN.

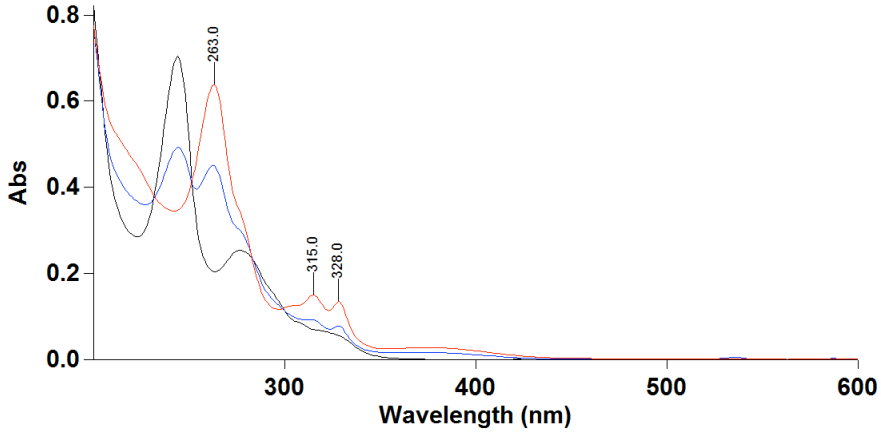

Figure S43. UV-Vis of **DI HQT** (black, 17 µM) in ACN with 0.5 (blue) and 1equiv. of Cu^{2+} (red).

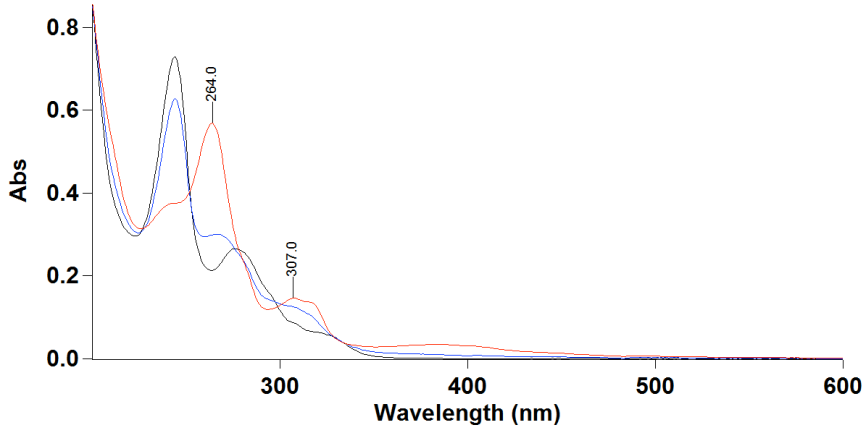

Figure S44. UV-Vis of **DI HQT** (black, 17 µM) in ACN with 0.5 (blue) and 1.5 equiv. of Co^{2+} (red).

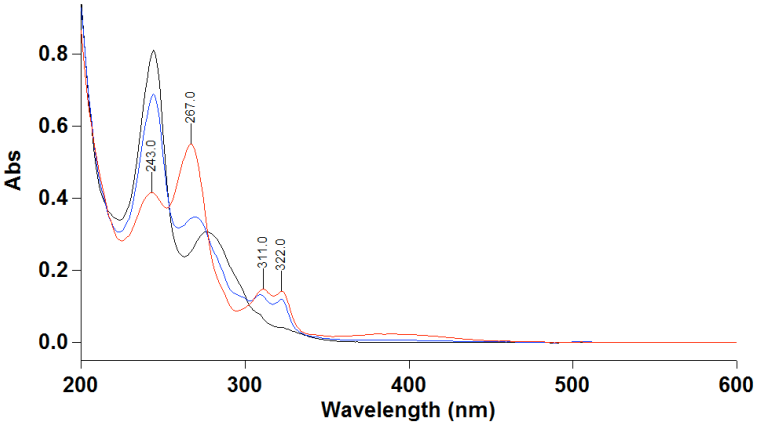

Figure S45. UV-Vis of **DI HQT** (black, 17 µM) in ACN with 0.5 (blue) and 1.5 equiv. of Zn^{2+} (red).

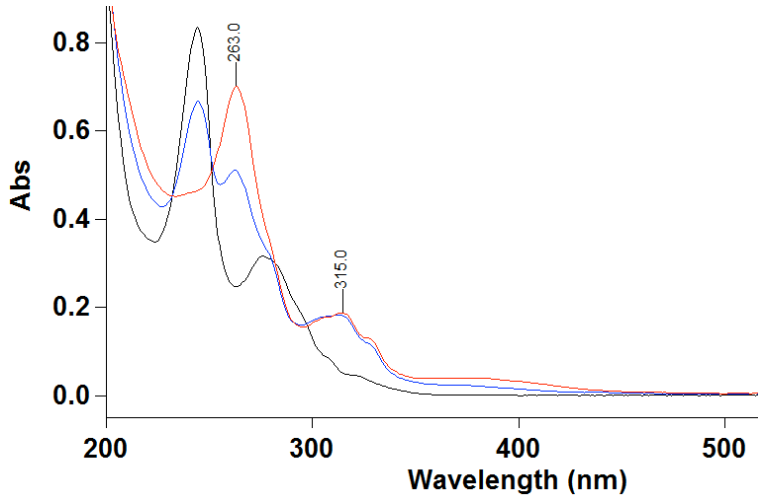

Figure S46. UV-Vis of free **DI HQT** (black, 17 µM) with 0.5 equiv. mix of Cu^{+2} and Co^{+2} (blue) and 1 mix of Cu^{+2} and Co^{+2} (red) in ACN.

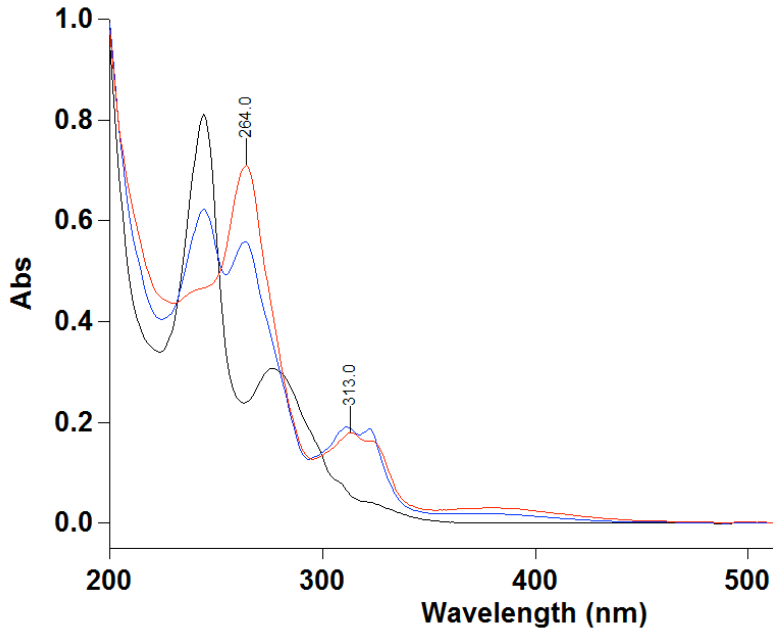

Figure S47. UV-Vis of free **DI HQT** (black, 17 µM) with 0.5 equiv. mix of Cu^{2+} and Zn^{2+} (blue) and 1 equiv. mix of Cu^{2+} and Zn^{2+} (red) in ACN.

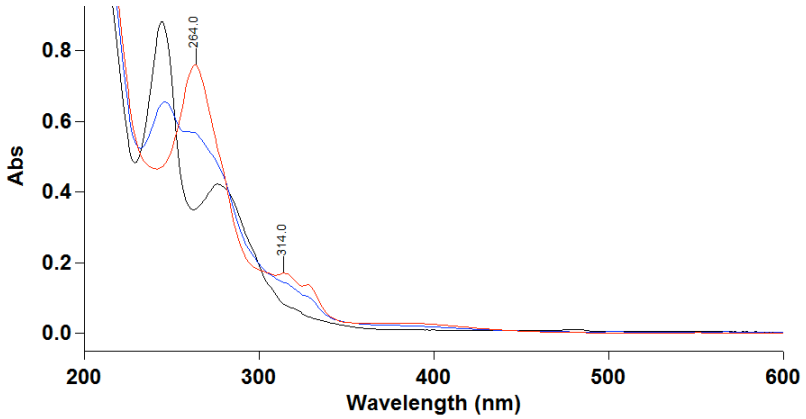

Figure S48. UV-Vis of **Helix HQT i+2** (black, 17 µM) in ACN with 0.5 (blue) and 1 equiv. of Cu^{2+} (red).

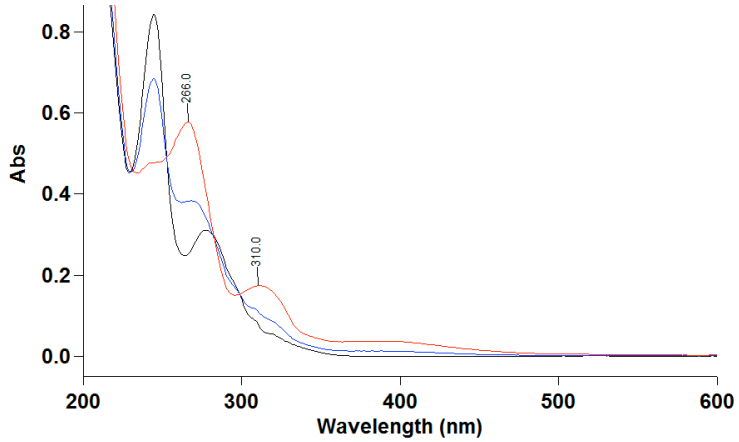

Figure S49. UV-Vis of **Helix HQT i+2** (black, 17 µM) in ACN with 0.5 (blue) and 1.5 equiv. of Co^{2+} (red).

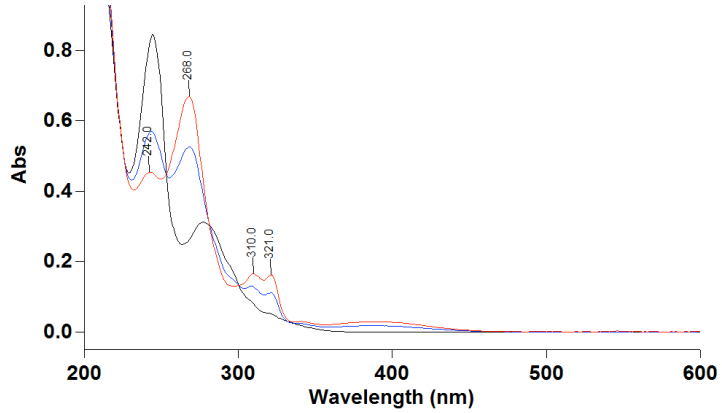

Figure S50. UV-Vis of **Helix HQT i+2** (black, 17 µM) in ACN with 0.5 (blue) and 1 equiv. of Zn^{2+} (red).

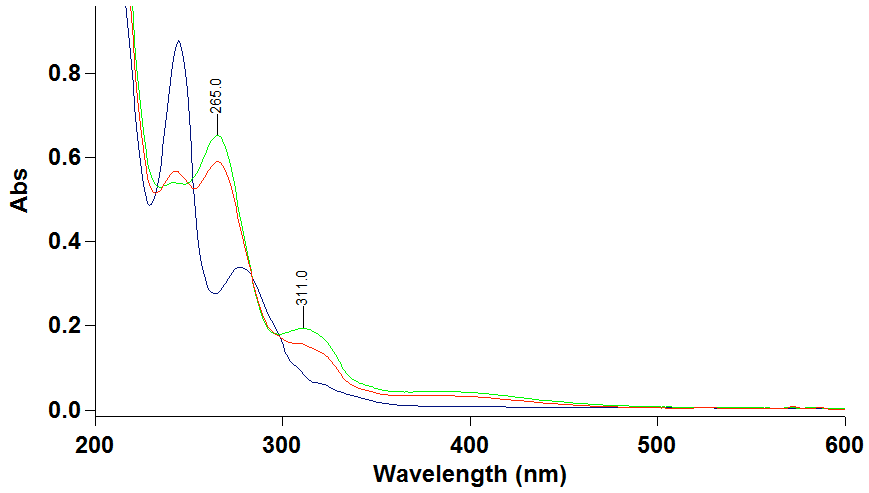

Figure S51. UV-Vis of free **Helix HQT i+2** (blue, 17 µM) with 0.5 equiv. mix of Cu^{2+} and Co^{2+} (red) and 1equiv. mix of Cu^{2+} and Co^{2+} (green) in ACN.

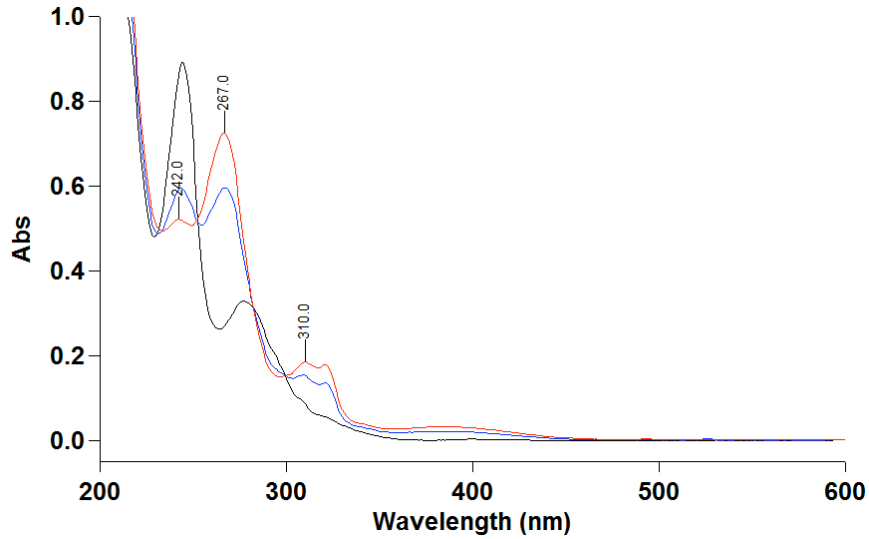

Figure S52. UV-Vis of free **Helix HQT i+2** (black, 17 µM) with 0.5 equiv. mix of Cu^{2+} and Zn^{2+} (blue) and 1 equiv. mix of Cu^{2+} and Zn^{2+} (red) in ACN.

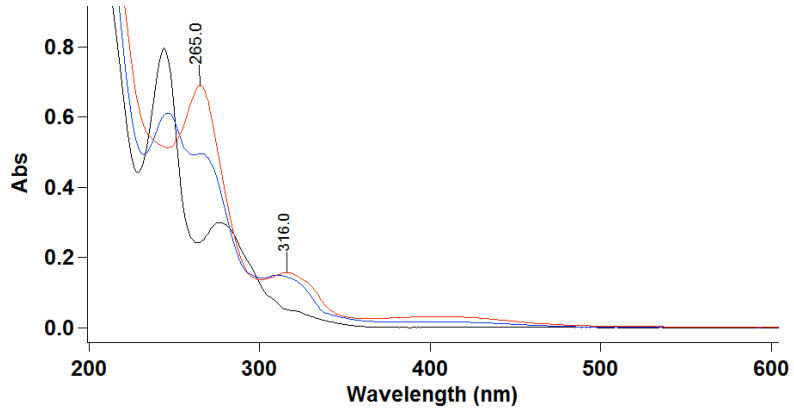

Figure S53. UV-Vis of **Helix HQT i+4** (black, 17 μM) in ACN with 0.5 (blue) and 1 equiv. of Cu^{2+} (red).

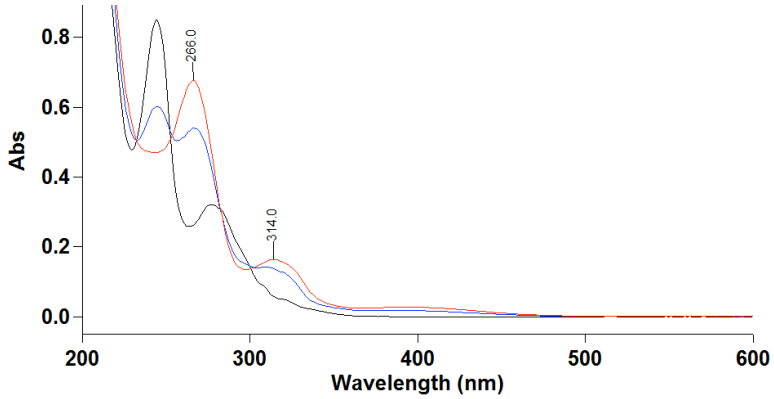

Figure S54. UV-Vis of **Helix HQT i+4** (black, 17 μM) in ACN with 0.5 (blue) and 1 equiv. of Co^{2+} (red).

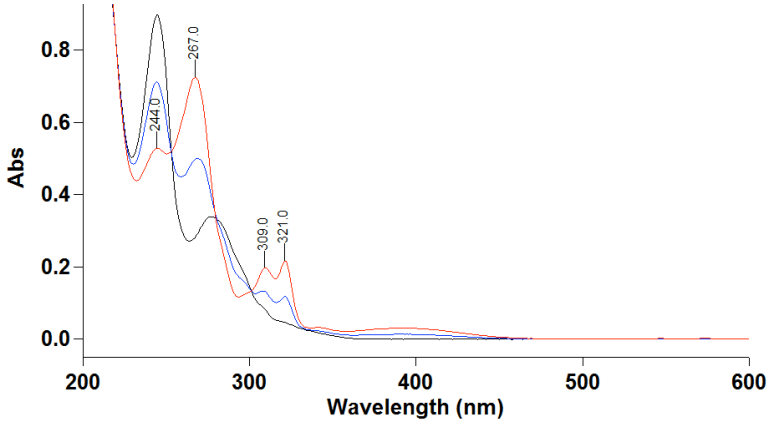

Figure S55. UV-Vis of **Helix HQT i+4** (black, 17 μM) in ACN with 0.5 (blue) and 1 equiv. of Zn^{2+} (red).

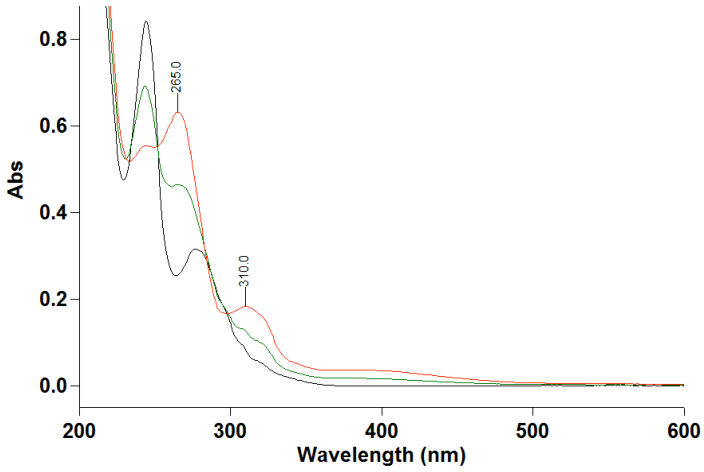

Figure S56. UV-Vis of free **Helix HQT i+4** (black, 17 µM) with 0.5 equiv. mix of Cu^{2+} and Co^{2+} (green) and 1 equiv. mix of Cu^{2+} and Co^{2+} (red) in ACN.

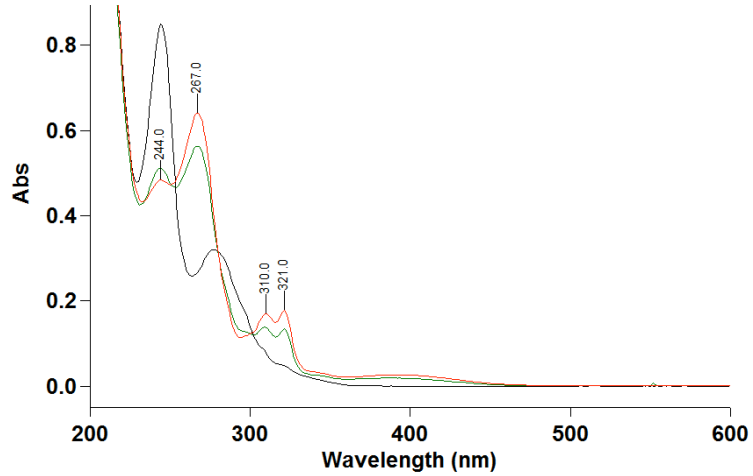

Figure S57. UV-Vis of free **Helix HQT i+4** (black, 17 µM) with 0.5 equiv. mix of Cu^{2+} and Zn^{2+} (green) and 1 equiv. mix of Cu^{2+} and Zn^{2+} (red) in 3ml ACN.

Association constants

Table S4. The association constants for metal binding were obtained by fitting the UV titrations results to the equation below using a nonlinear regression (curve fit) GraphPad Prism® software. Where A_0 and A_{max} are the minimum and maximum absorbance measured for the free ligand respectively, L_0 is the initial concentration of the free ligand (typically 7 µM) and M is the concentration of metal ions that was added (0-290 µM).

$$A = A_0 + \frac{1}{2[L_0]}(A_{max} - A_0) \times \left[\left([L_0] + [M] + \frac{1}{K} \right) \pm \sqrt{\left([L_0] + [M] + \frac{1}{K} \right)^2 - 4[L_0][M]} \right]$$

(Peptoid)M	A_0, A_{max}	Binding constant K [M^{-1}]	R square
(**Helix HQT i+3**)Cu	0.426, 0.303	$(1.03 \pm 0.49)\times10^{13}$	0.9986
(**Helix HQT i+3**)Zn	0.378, 0.187	$(3.60 \pm 0.46)\times10^{11}$	0.9938
(**Helix HQT i+3**)Co	0.350, 0.176	$(2.53 \pm 0.35)\times10^{11}$	0.9916
(**Helix HQT i+3**)Ni	0.373, 0.149	$(1.52 \pm 0.09)\times10^{10}$	0.9971
(**Helix HQT i+3**)Mn	0.362, 0.162	$(1.13 \pm 0.06)\times10^{10}$	0.9981
(**DI HQT**)Cu	0.292, 0.136	$(1.36\pm0.66)\times10^{12}$	0.9773
(**DI HQT**)Zn	0.330, 0.184	$(1.28\pm0.49)\times10^{12}$	0.9806
(**DI HQT**)Co	0.324, 0.226	$(5.15\pm0.76)\times10^{11}$	0.9984
(**DI HQT**)Ni	0.333, 0.174	$(1.33 \pm 0.18)\times10^{9}$	0.9916
(**DI HQT**)Mn	0.316, 0.214	$(1.04 \pm 0.28)\times10^{9}$	0.9742
(**Nonhelix HQT i+3**)Cu	0.398, 0.297	$(1.16\pm0.53)\times10^{12}$	0.9874
(**Nonhelix HQT i+3**)Zn	0.312, 0.193	$(1.07\pm0.68)\times10^{12}$	0.9467
(**Nonhelix HQT i+3**)Co	0.305, 0.175	$(1.69\pm0.56)\times10^{12}$	0.9895
(**Nonhelix HQT i+3**)Ni	0.316, 0.154	$(6.03 \pm 0.69)\times10^{10}$	0.9892
(**Nonhelix HQT i+3**)Mn	0.316, 0.203	$(2.65 \pm 0.28)\times10^{10}$	0.9952
(**Helix HQT i+4**)Cu	0.321, 0.248	$(4.12\pm0.84)\times10^{11}$	0.9939
(**Helix HQT i+4**)Zn	0.375, 0.261	$(1.04\pm0.17)\times10^{11}$	0.9878

(**Helix HQT i+4**)Co	0.298, 0.224	$(1.40\pm0.39)\times10^{11}$	0.9803
(**Helix HQT i+4**)Ni	0.316, 0.199	$(2.67 \pm 0.75)\times10^{10}$	0.9551
(**Helix HQT i+4**)Mn	0.293, 0.171	$(8.13 \pm 1.77)\times10^{10}$	0.9629
(**Helix HQT i+2**)Cu	0.373, 0.221	$(1.50\pm0.37)\times10^{12}$	0.9933
(**Helix HQT i+2**)Zn	0.379, 0.278	$(1.00\pm0.37)\times10^{12}$	0.9823
(**Helix HQT i**+2)Co	0.366, 0.228	$(6.01\pm2.23)\times10^{11}$	0.9815
(**Helix HQT i**+2)Ni	0.363, 0.247	$(1.15 \pm 0.39)\times10^{10}$	0.9681
(**Helix HQT i**+2)Mn	0.381, 0.221	$(5.37 \pm 0.64)\times10^{10}$	0.9913
(**$H_2$6**)Cu	0.319, 0.119	$(1.43\pm0.46)\times10^{12}$	0.9896

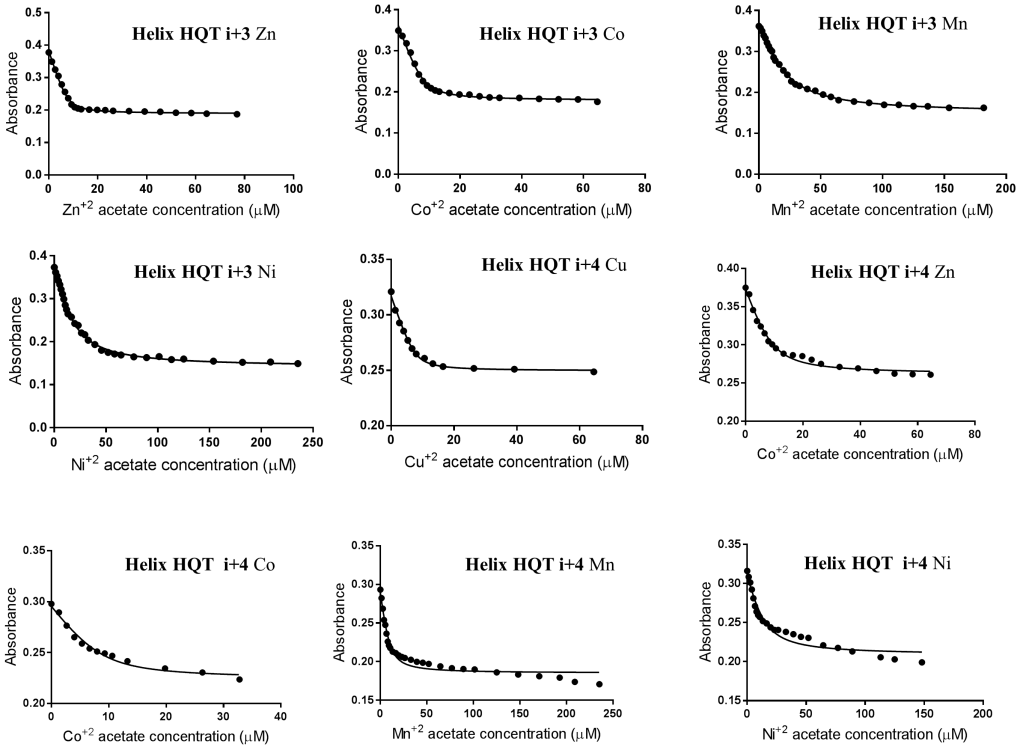

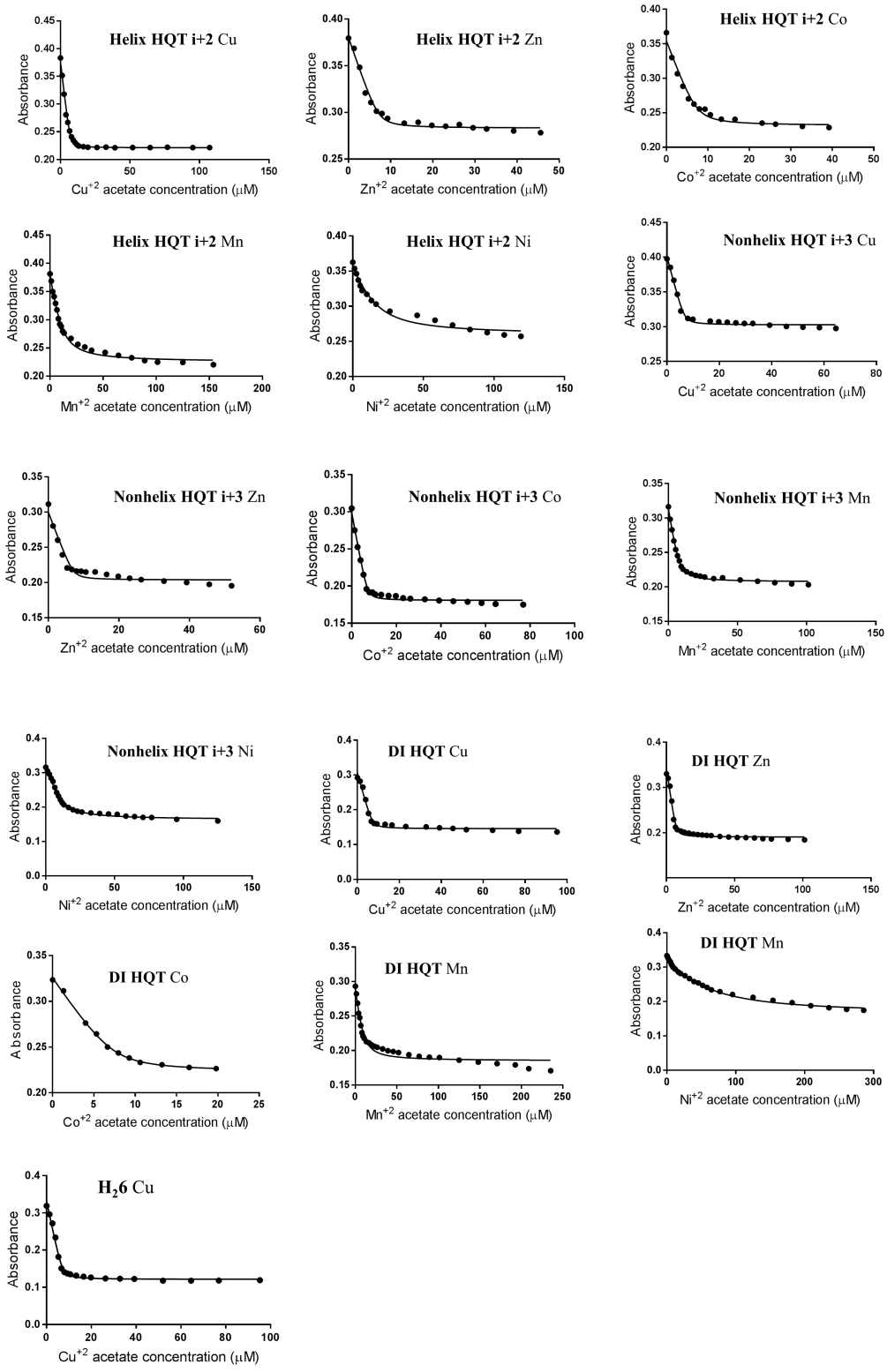

Figure S58. Association curve (dots) and fit (line) for the formation of peptoid metal complexes. The fitting was done using a nonlinear regression (curve fit) GraphPad Prism® software.

EPR

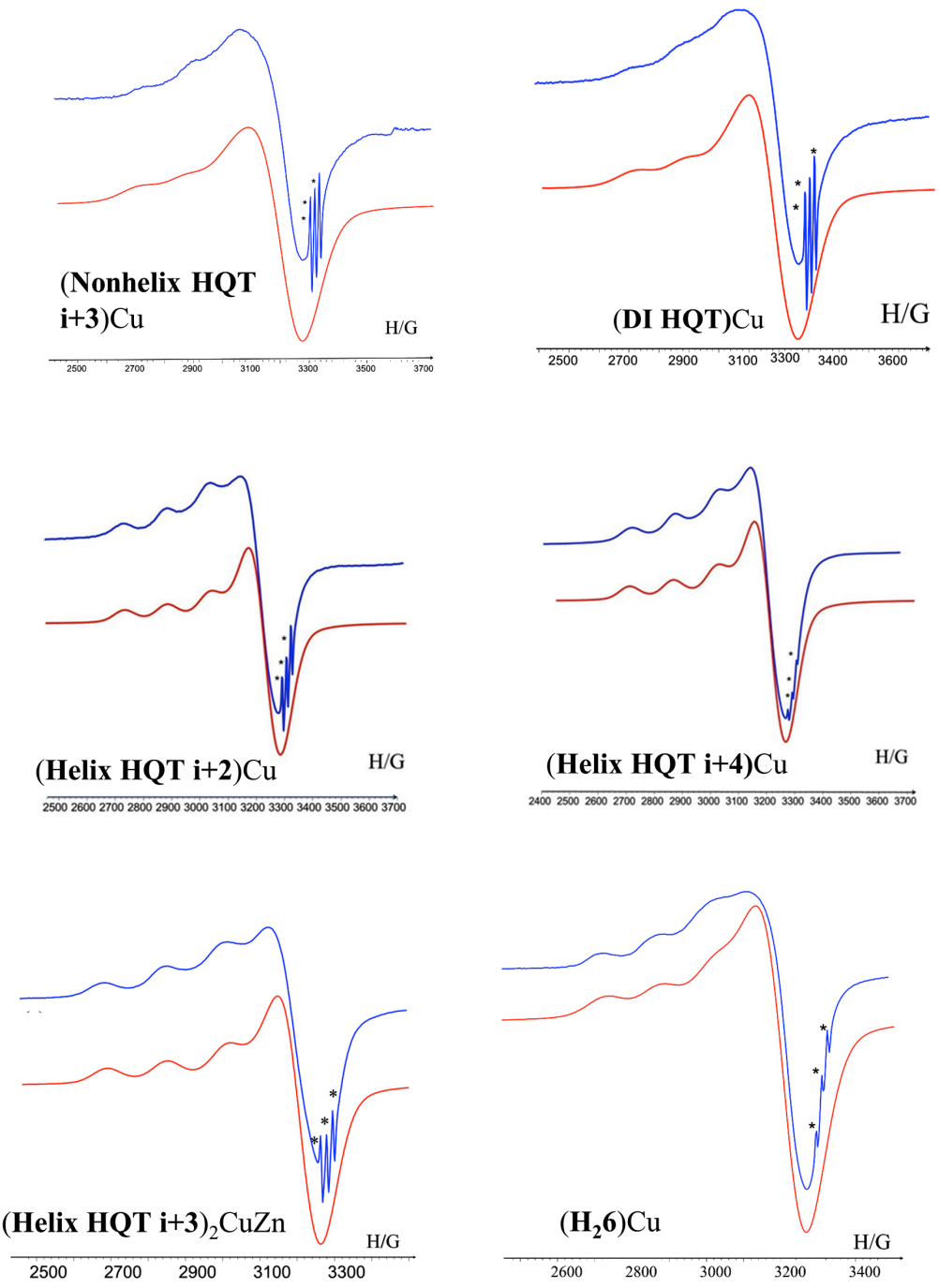

Figure S59. Room temperature X-band EPR spectra of copper(II) complexes (blue lines) and corresponding simulated spectra (red lines). Reference- TEMPO marked by*, g = 2.0058.

ESI-MS

Table S5. Peptoid oligomer sequences and ESI-MS analysis. *N*hq = 8-hydroxy-2-quinolinemethylamine, *Nspe* = (S)-(-)-1-Phenylethylamine, *Nterpy* = 2,2':6',2''-Terpyridineamine. *Npm* = N-benzylamine and *Nme* = N-methoxyamine.

Peptoid	Molecular weight Calc.: Found (gr/mol)	Figure #
Nspe-Nterpy-Nspe-Nspe-Nhq-Nspe (**Helix HQT i+3**)	1208.4 : 1208.0	S60
Nme-Nterpy-Npm-Nme-Nhq-Npm (**Nonhelix HQT i+3**)	1088.2 : 1087.8	S61
Nterpy-Nhq **(DI HQT)**	563.6 : 564.1	S62
Nspe- Nspe-Nspe- Nterpy-Nspe -Nhq (**Helix HQT i+2**)	1208.4 : 1209.0	S63
Nspe-Nterpy-Nspe-Nspe- Nspe -Nhq **(Helix HQT i+4)**	1208.4 : 1209.0	S64

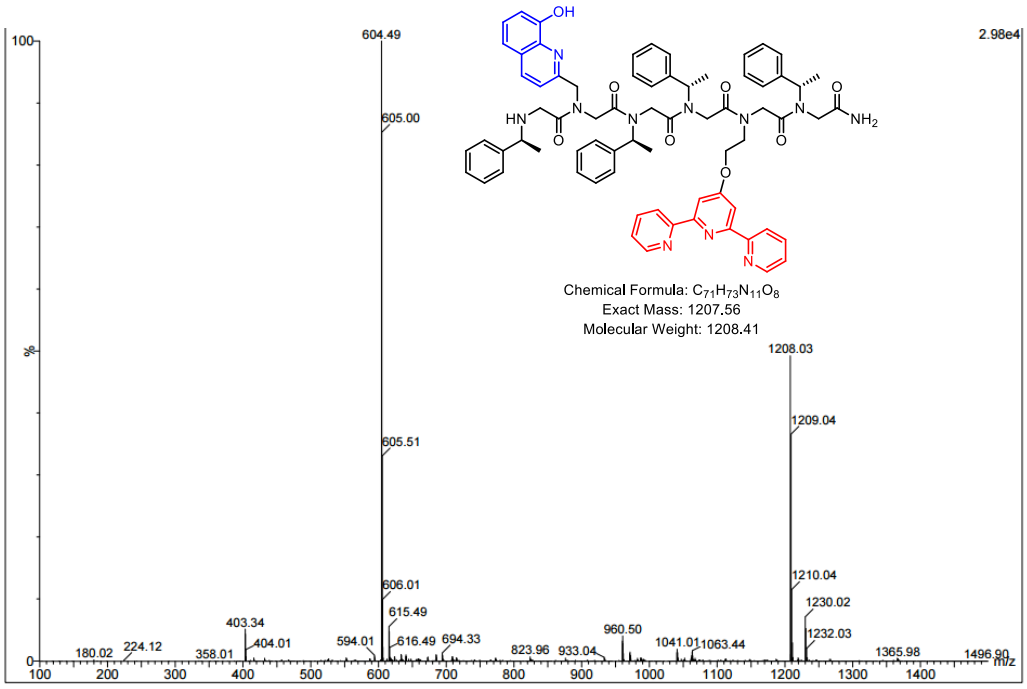

Figure S60. ESI-MS traces of peptoid oligomer **Helix HQT i+3**.

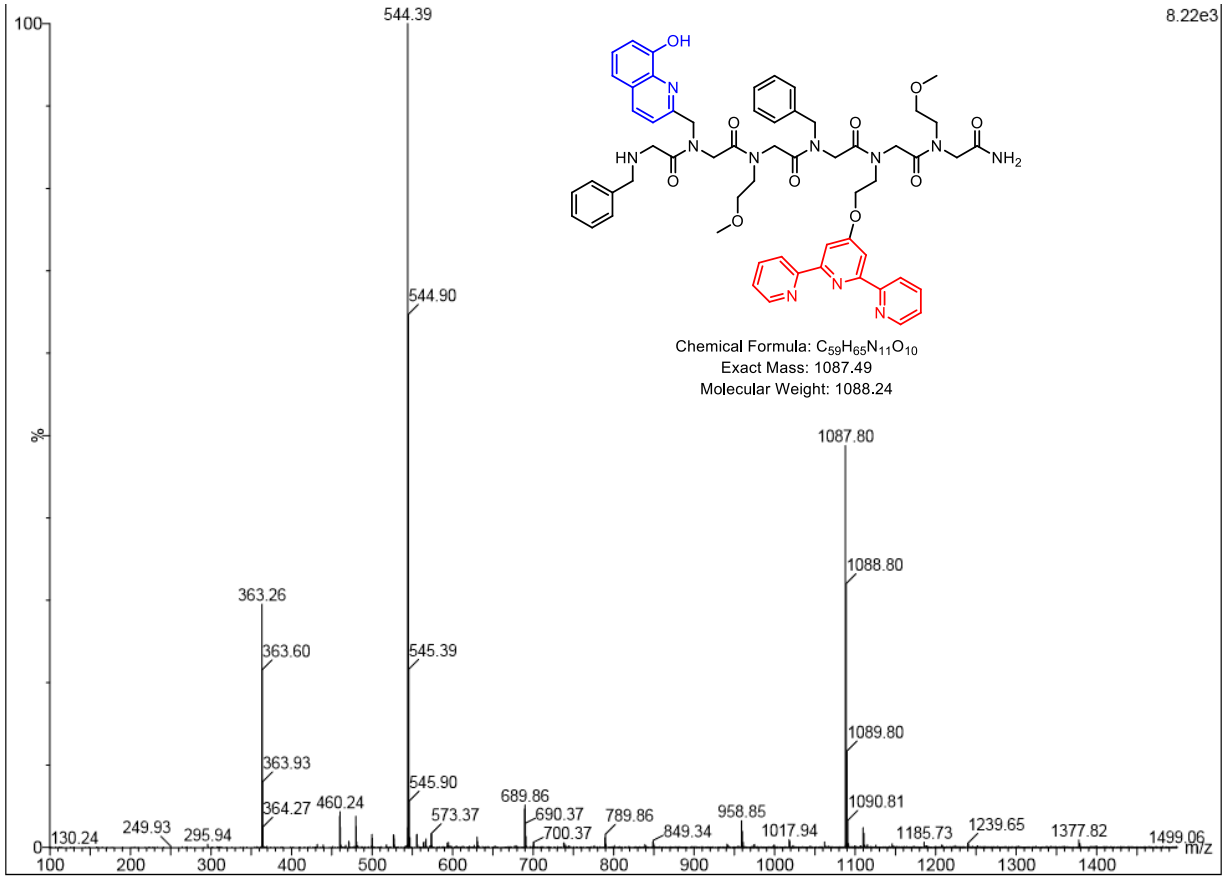

Figure S61. ESI-MS traces of peptoid oligomer **Nonhelix HQT i+3**.

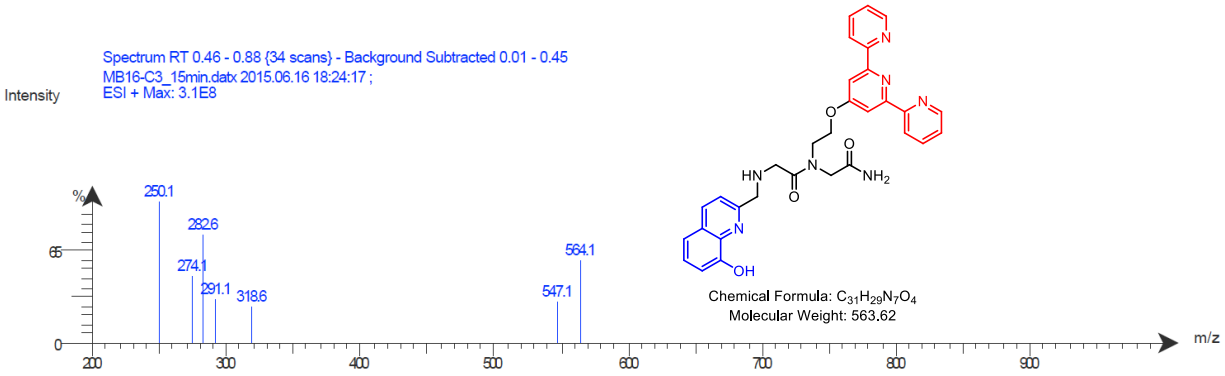

Figure S62. ESI-MS traces of peptoid oligomer **DI HQT**.

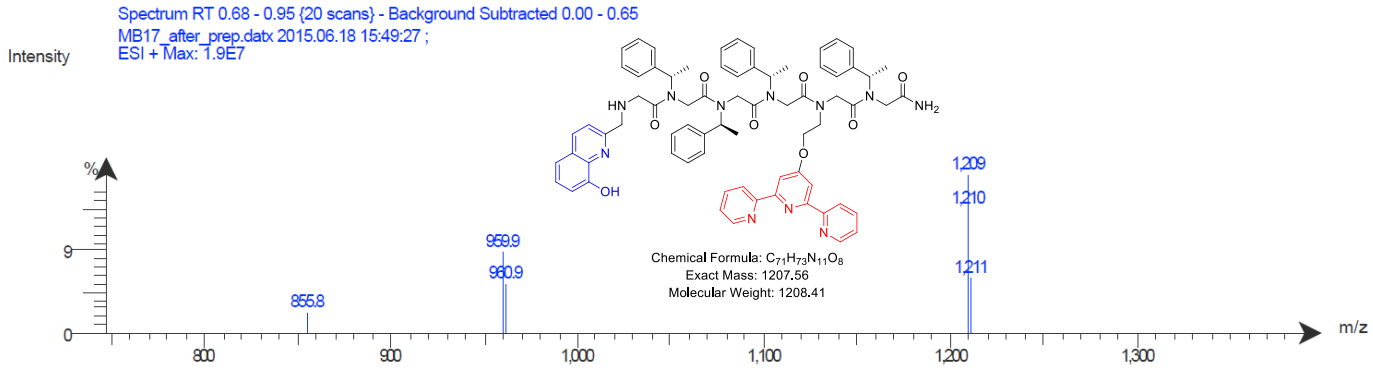

Figure S63. ESI-MS traces of peptoid oligomer **Helix HQT i+2**.

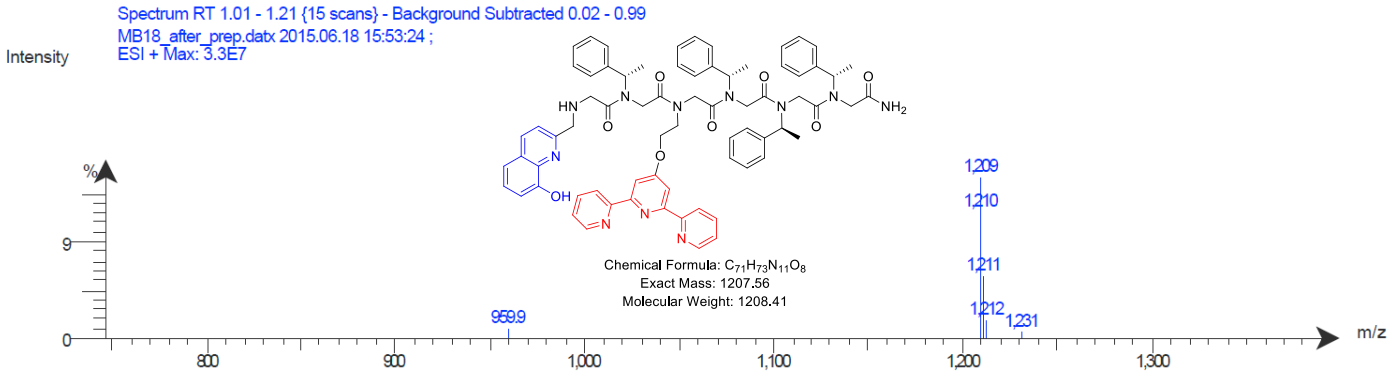

Figure S64. ESI-MS traces of peptoid oligomer **Helix HQT i+4**.

Table S6. ESI-MS analysis of **Helix HQT i and i+3** metal complexes

Metallopeptoid	Molecular weight Calc.: Found (gr/mol)	# Figure
(**Helix HQT i+3**)Cu	1269.49 : 1269.56	S65-66
(**Helix HQT i**+3)Co	1265.49 : 1265.40	S67-68
(**Helix HQT i**+3)Zn	1270.49 : 1270.41	S69-70
(**Helix HQT i+*3***)Fe	1362.39 (m/2z) : 1362.44 (m/2z)	S71-77
(**Helix HQT i+3**)Ni	1264.49 : 1264.41	S73-74
(**Helix HQT i**+3)Mn	1261.49: 1261.40	S75-S76
(**Helix HQT i+3**)$_2$CuCo	846.67(m/3z) : 846.58 (m/3z)	S85-86
(**Helix HQ i+3**)$_2$CuZn	848.33(m/3z) : 848.24 (m/3z)	S87-89
(**Helix HQT i+3**)$_2$CuFe	844.66(m/3z) : 844.61 (m/3z)	S90-91

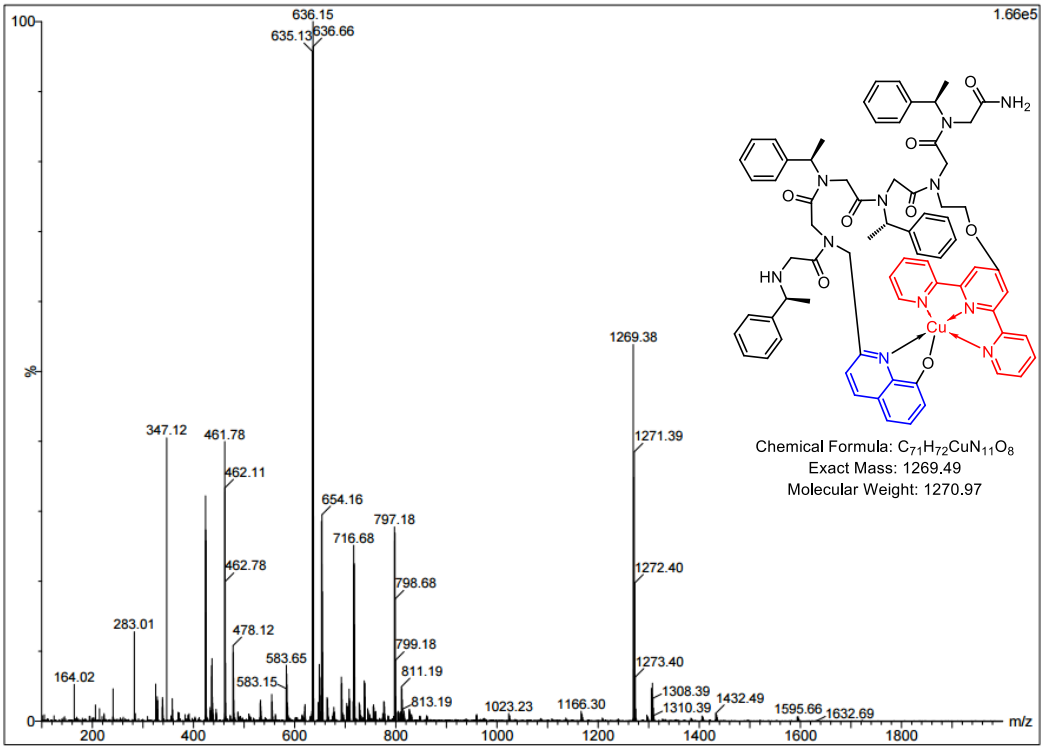

Figure S65. ESI-MS traces of (**Helix HQT i+3**)Cu complex.

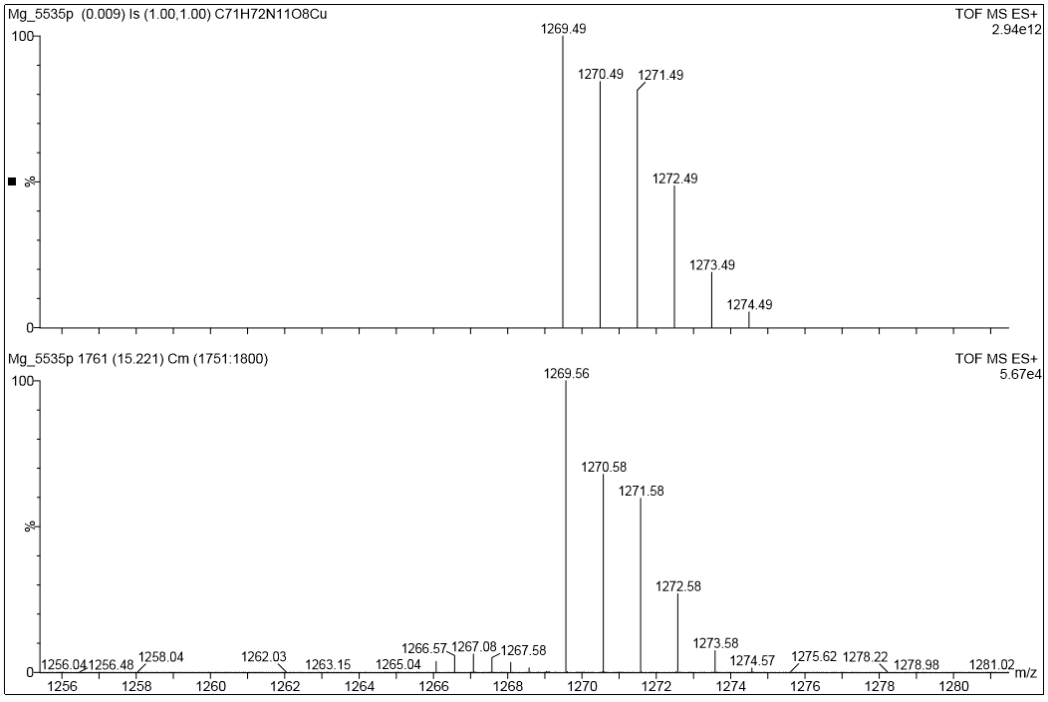

Figure S66. Experimental isotopic analysis by ESI-MS of (**Helix HQT i+3**)Cu complex (bottom) and calculated ESI-MS spectrum (top).

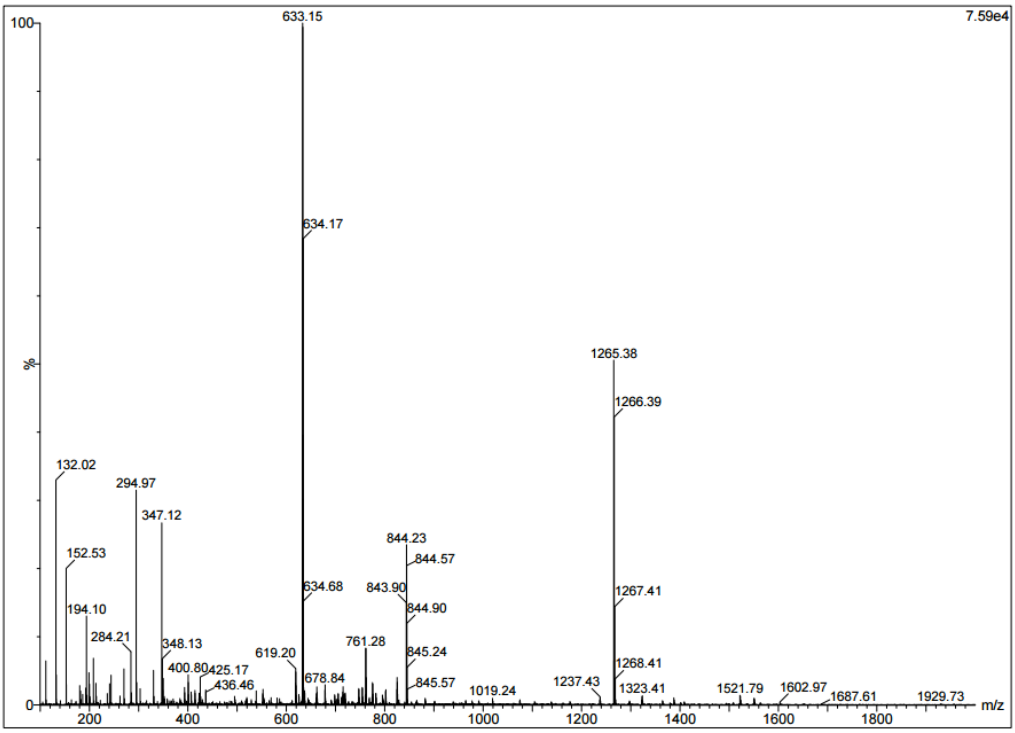

Figure S67. ESI-MS traces of (**Helix HQT i+3**)Co complex.

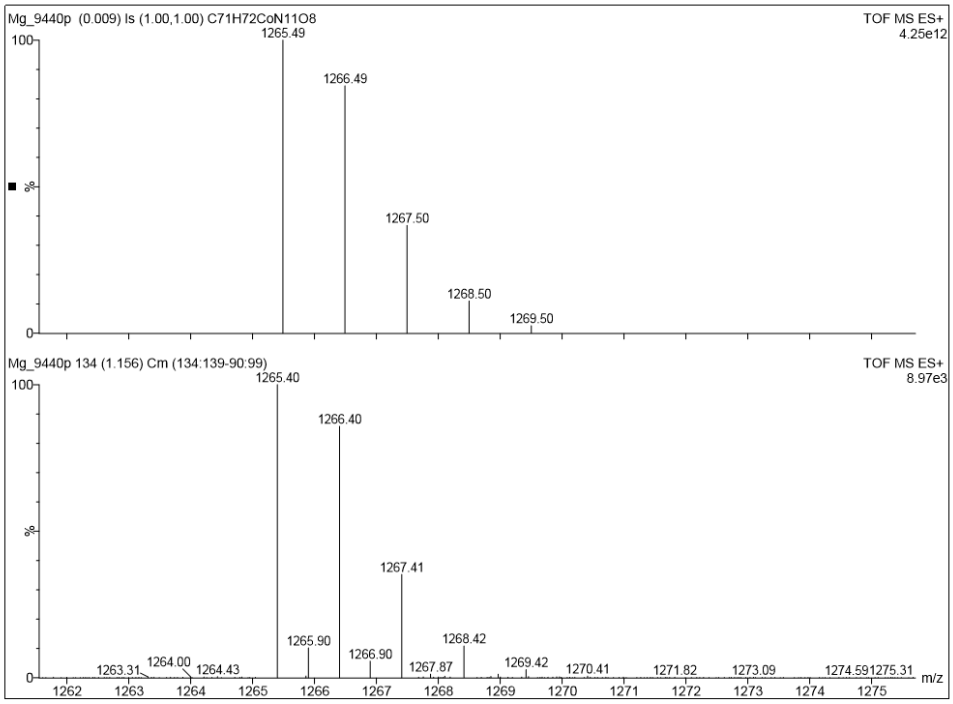

Figure S68. Experimental isotopic analysis by ESI-MS of (**Helix HQT i+3**)Co complex (bottom) and calculated ESI-MS spectrum (top).

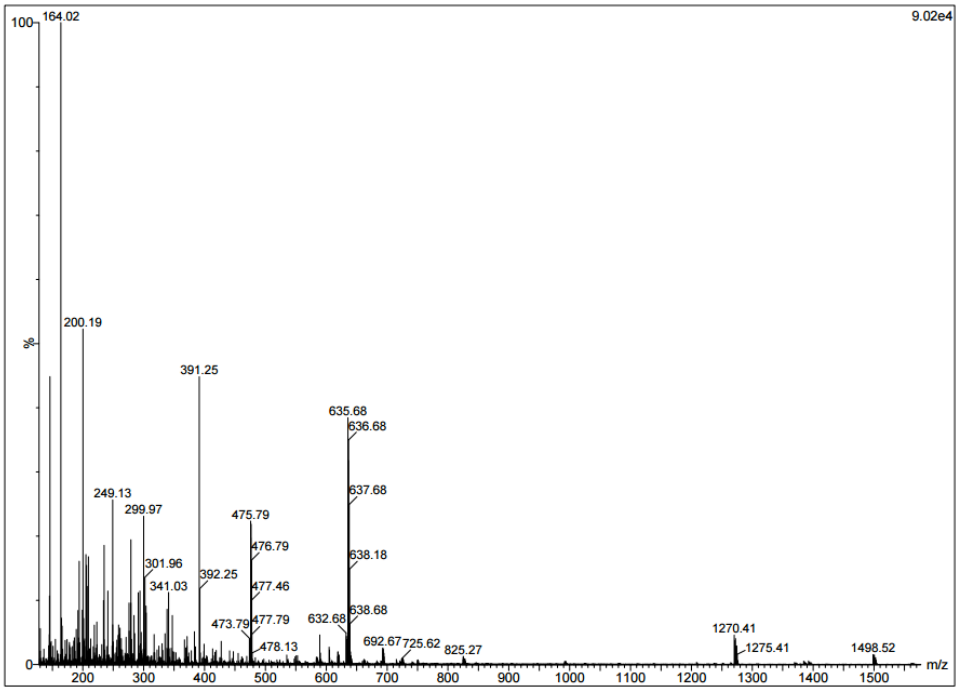

Figure S69. ESI-MS traces of (**Helix HQT i+3**)Zn complex.

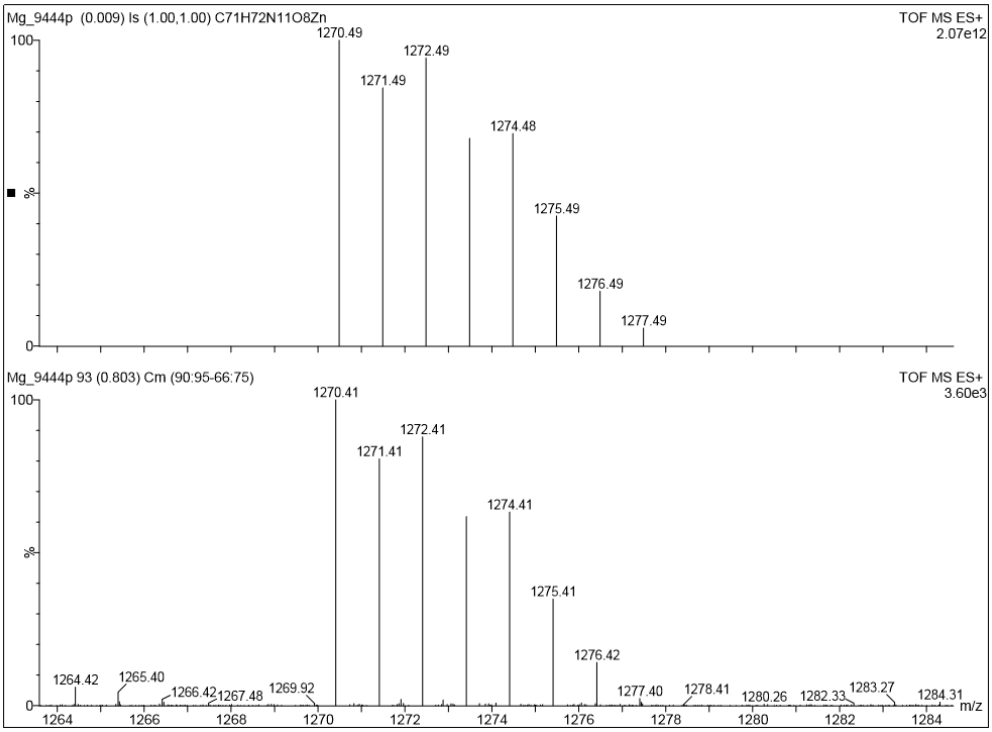

Figure S70. Experimental isotopic analysis by ESI-MS of (**Helix HQT i+3**)Zn complex (bottom) and calculated ESI-MS spectrum (top).

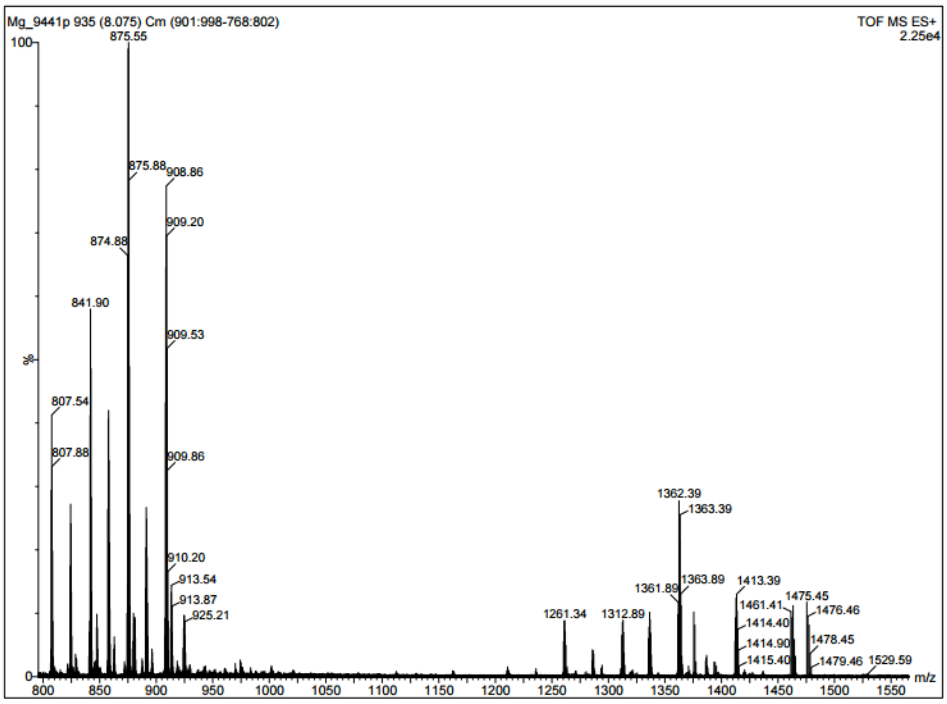

Figure S71. ESI-MS traces of (**Helix HQT i+3**)Fe complex.

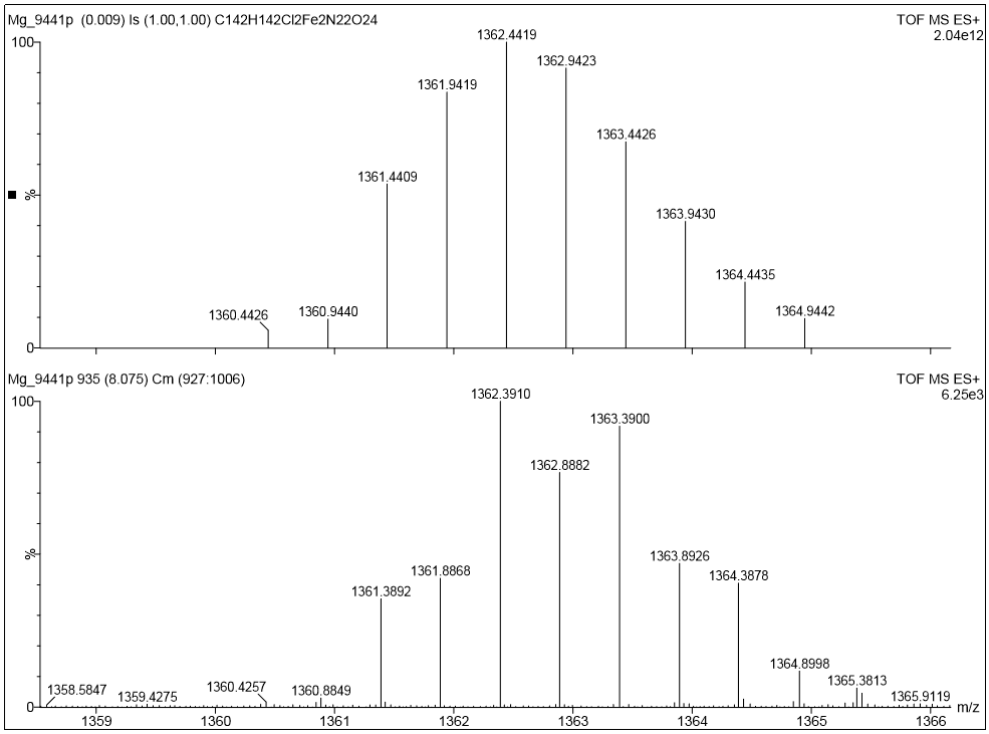

Figure S72. Experimental isotopic analysis by ESI-MS of (**Helix HQT i+3**)Fe complex (bottom) and calculated ESI-MS spectrum (top).

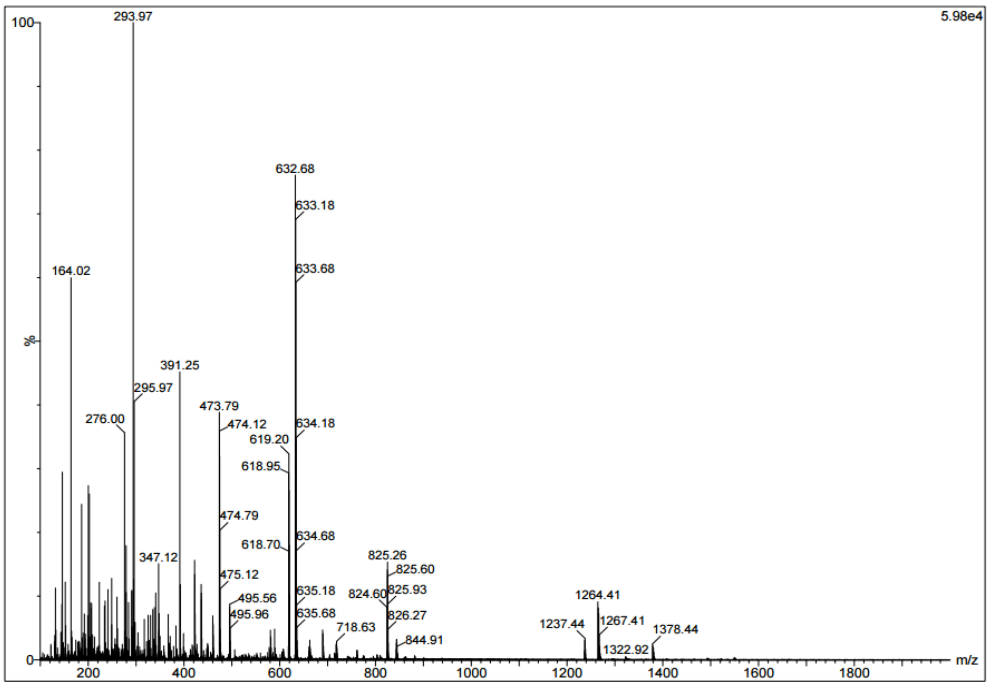

Figure S73. ESI-MS traces of (**Helix HQT i+3**)Ni complex.

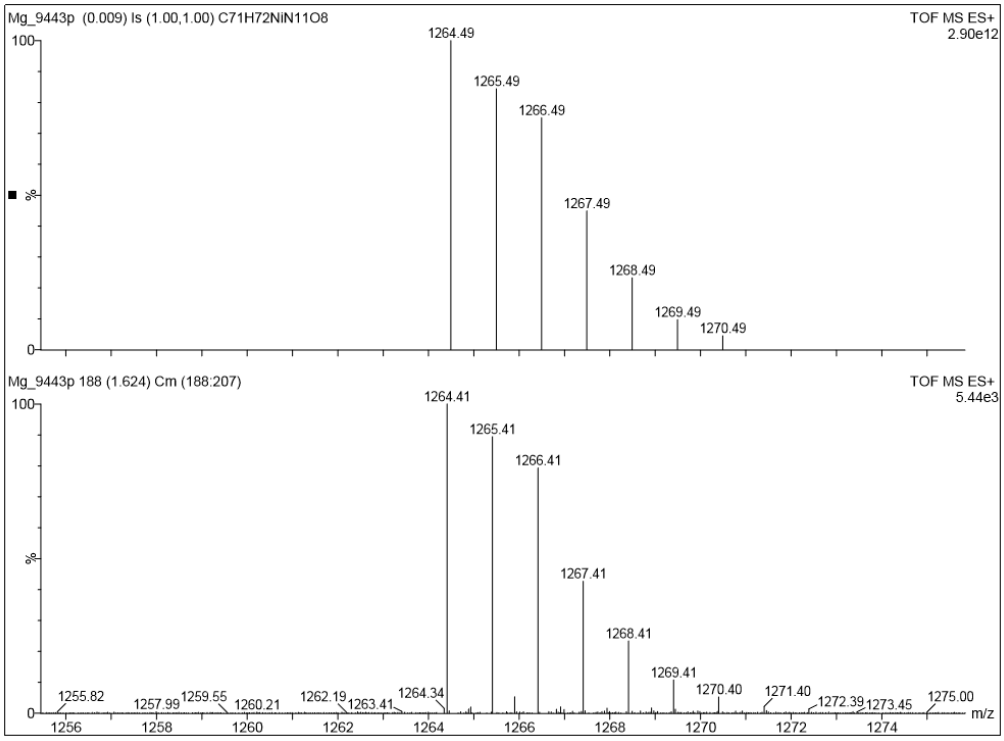

Figure S74. Experimental isotopic analysis by ESI-MS of (**Helix HQT i+3**)Ni complex (bottom) and calculated ESI-MS spectrum (top).

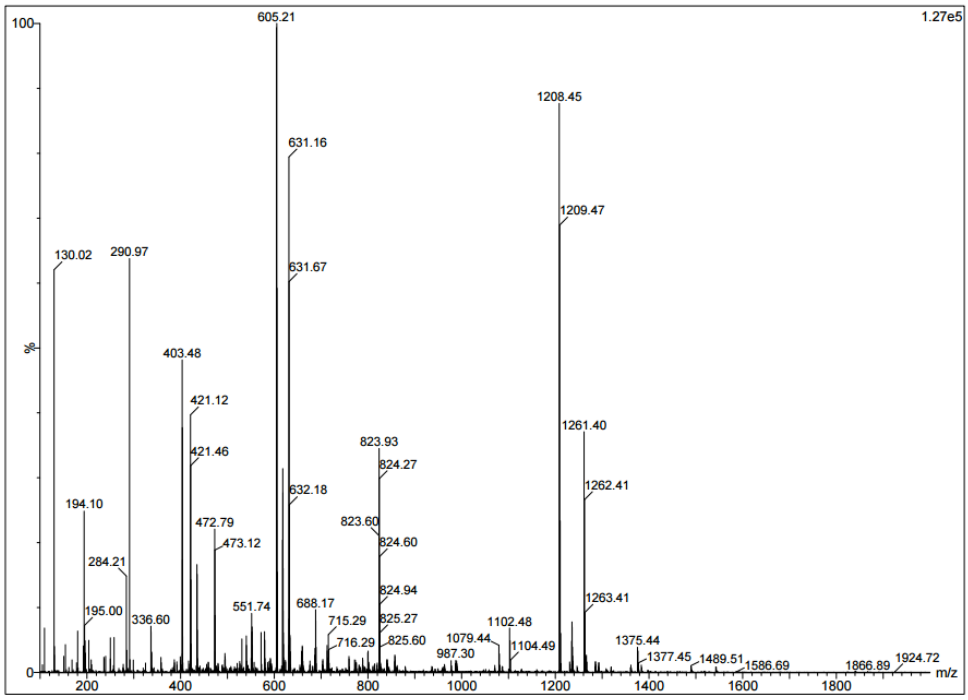

Figure S75. ESI-MS traces of (**Helix HQT i+3)**Mn complex.

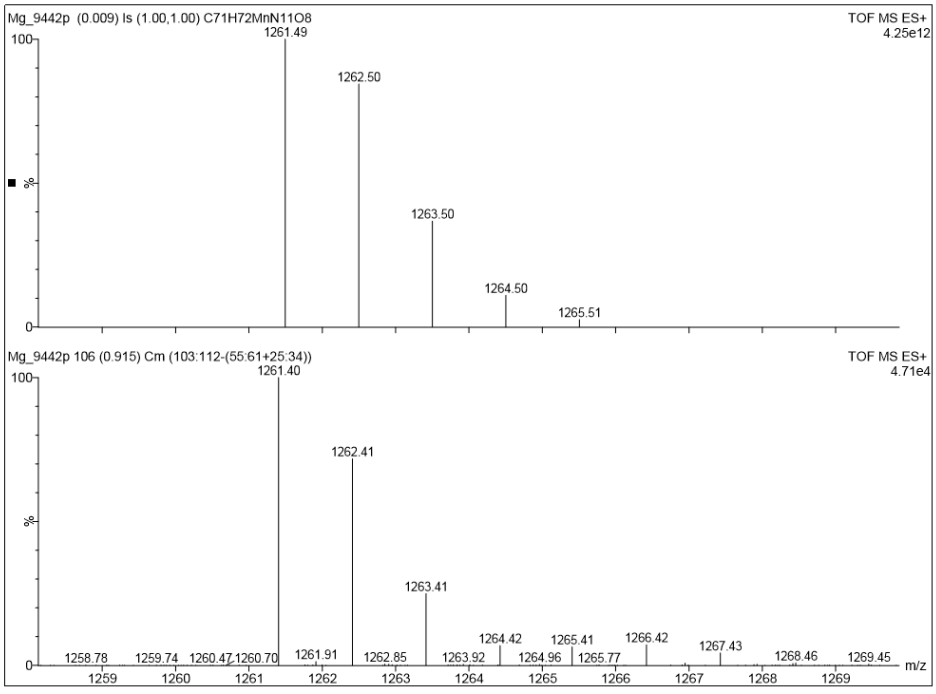

Figure S76. Experimental isotopic analysis by ESI-MS of (**Helix HQT i+3**)Mn complex (bottom) and calculated ESI-MS spectrum (top).

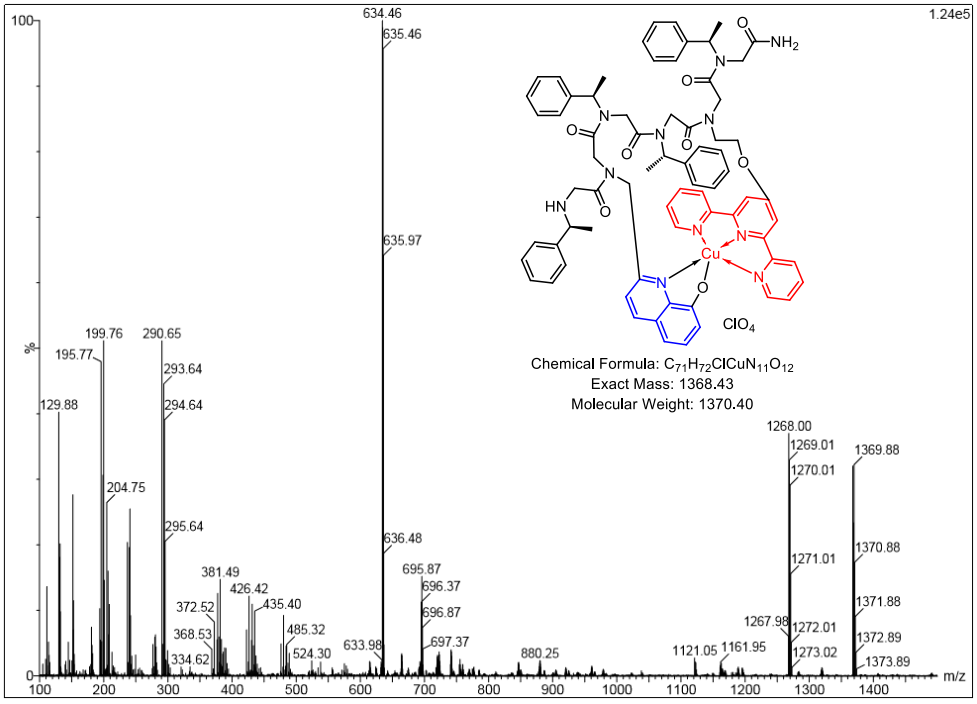

Figure S77. ESI-MS traces of peptoid oligomer **Helix HQT i+3** with 1 equiv. of Cu^{2+}, Co^{2+}, Ni^{2+}, Mn^{2+}, Fe^{3+}, Zn^{2+}.

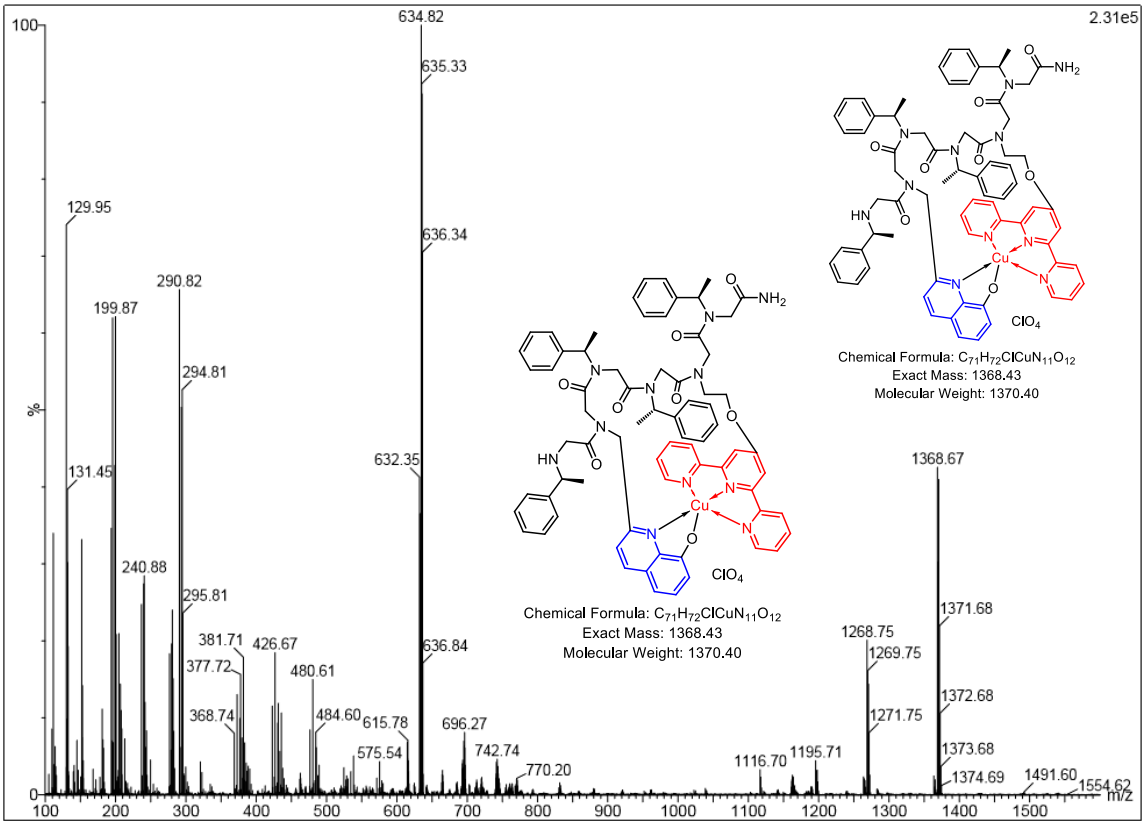

Figure S78. ESI-MS traces of peptoid oligomer **Helix HQT i+3** with 1 equiv. of Cu^{2+} and 10 equiv. Co^{2+}, Ni^{2+}, Mn^{2+}, Fe^{3+} and Zn^{2+}.

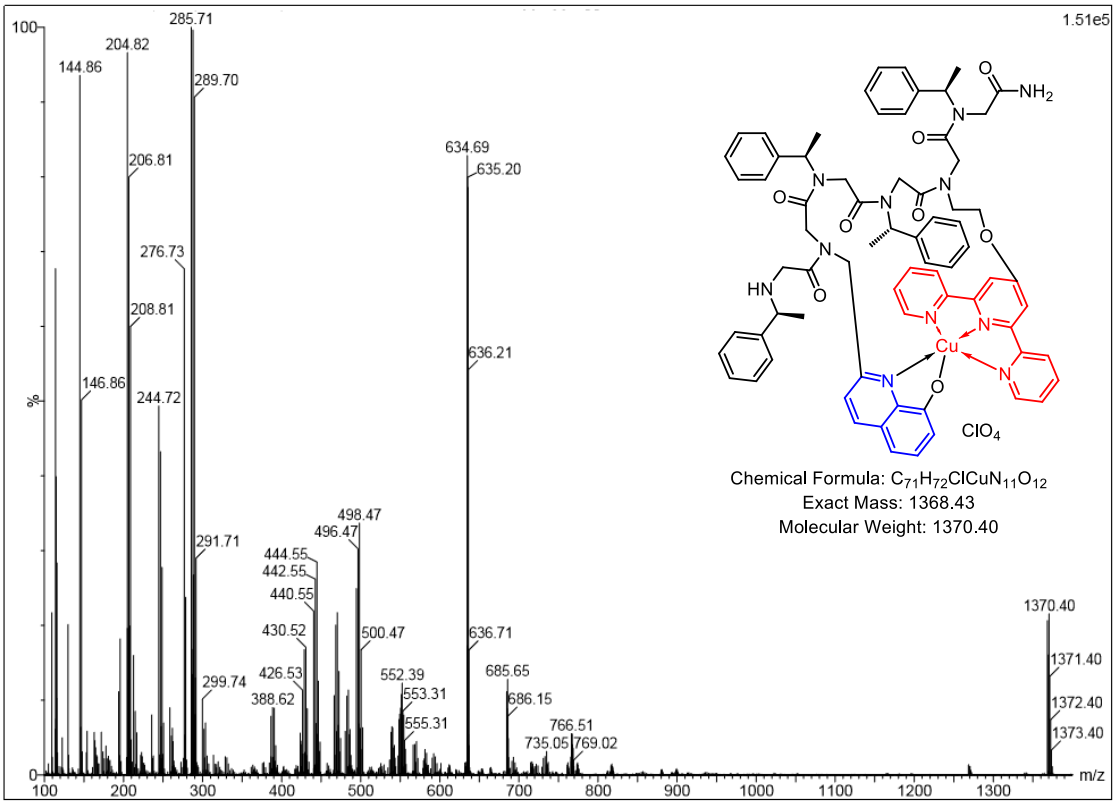

Figure S79. ESI-MS traces of peptoid oligomer **Helix HQT i+3** with 1 equiv. of Cu^{2+} and 20 equiv. Co^{2+}, Ni^{2+}, Mn^{2+}, Fe^{3+} and Zn^{2+}.

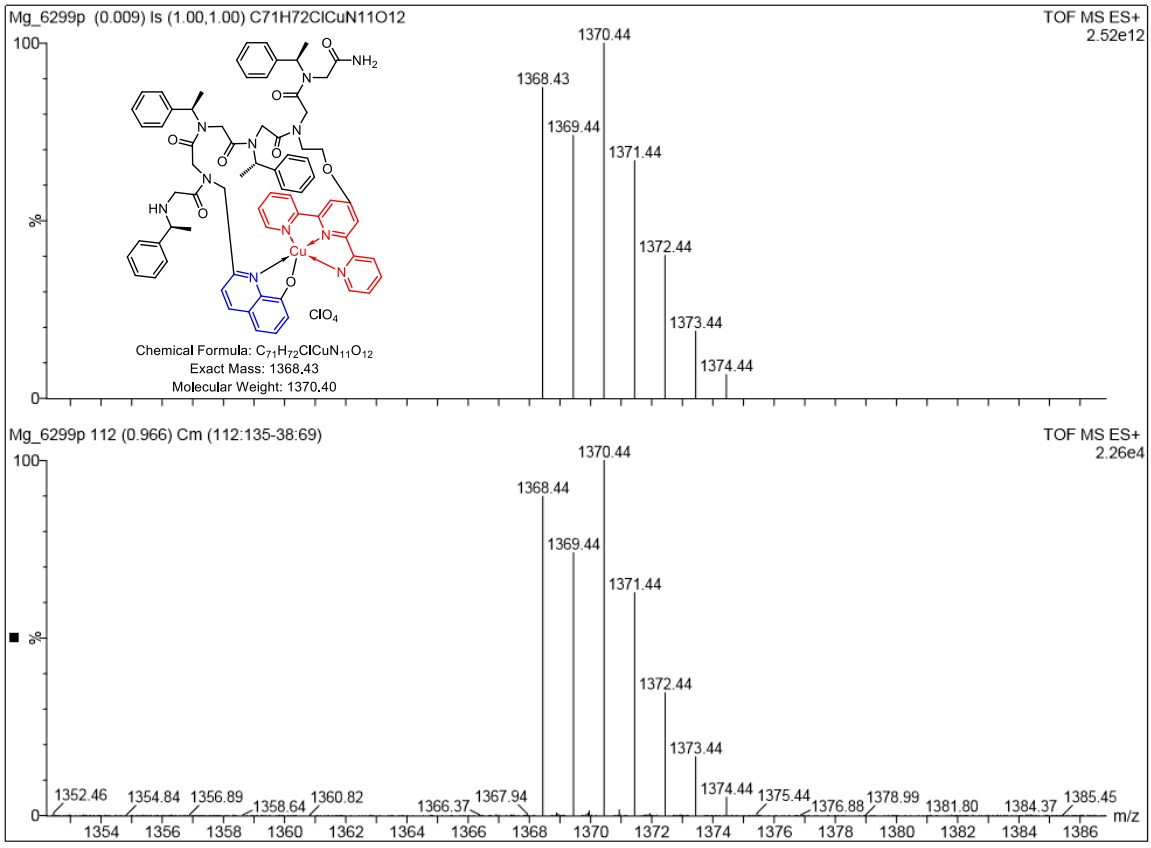

Figure S80. Experimental isotopic analysis by ESI-MS of (**Helix HQT i**+3)Cu-perchlorate complex (bottom) and calculated ESI-MS spectrum (top).

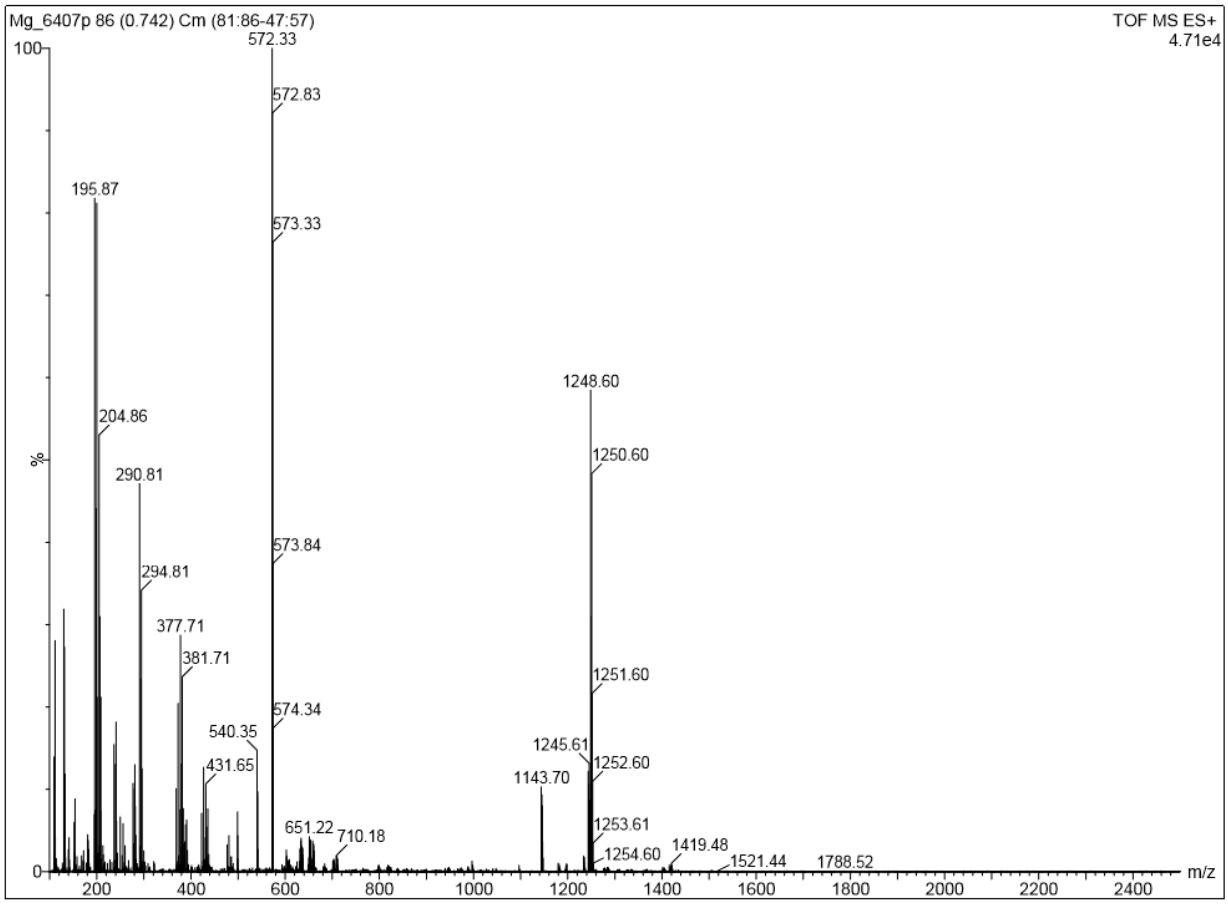

Figure S81. ESI-MS traces of peptoid oligomer **Nonhelix HQT i+3** with 1 equiv. of Cu^{2+}, Co^{2+}, Ni, Mn^{2+}, Fe^{3+} and Zn^{2+}.

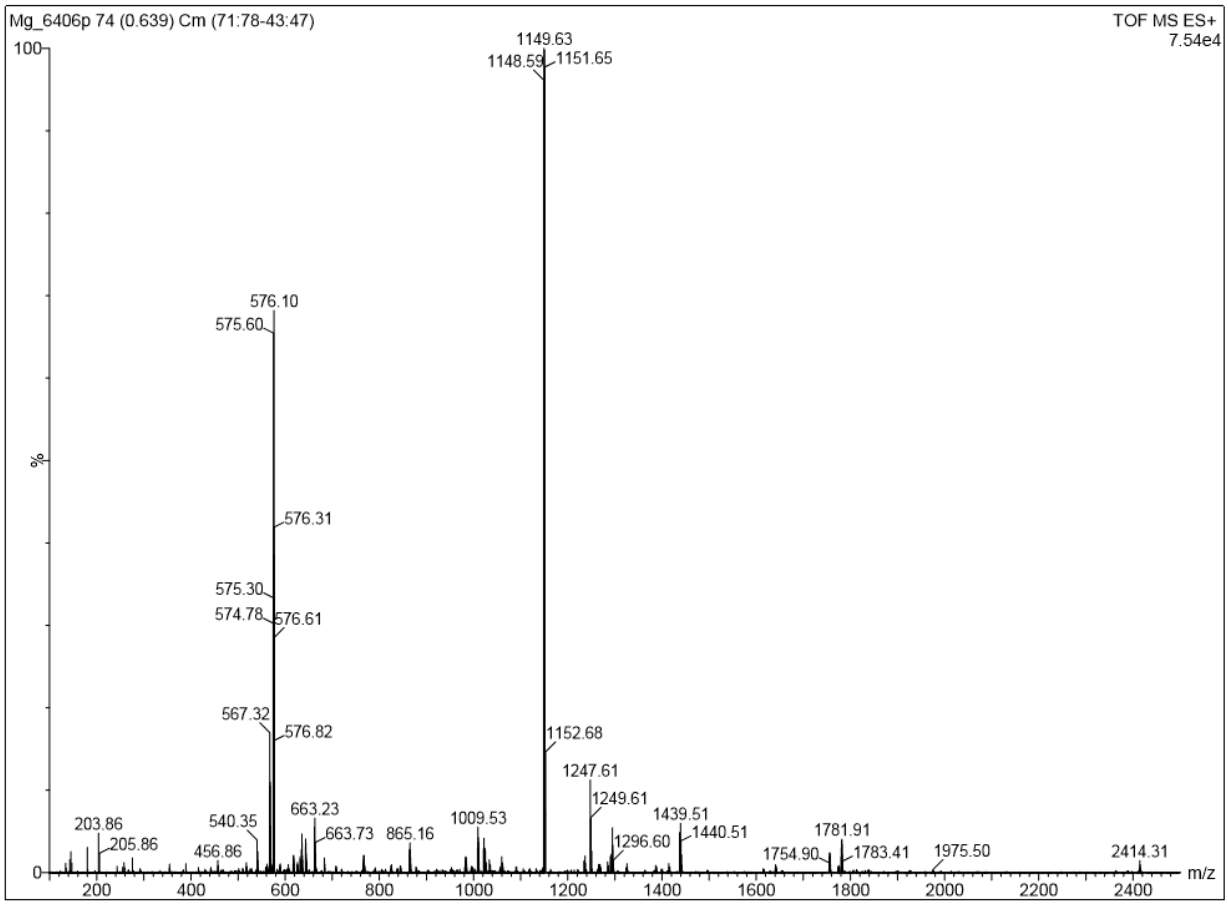

Figure S82. ESI-MS traces of peptoid oligomer **Nonhelix HQT i+3** with 1 equiv. of Cu^{2+}.

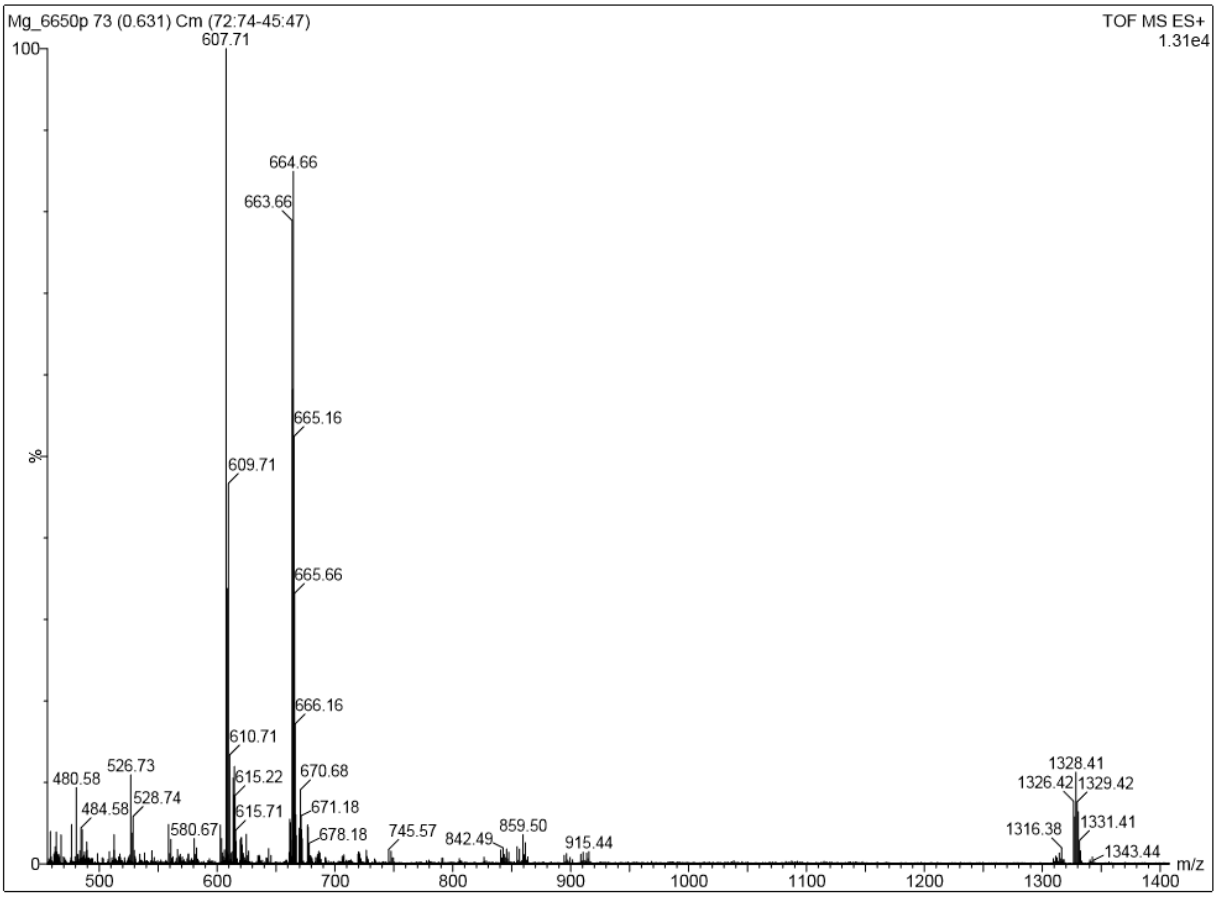

Figure S83. ESI-MS traces of peptoid oligomer **DI HQT** with 1 equiv. of Cu^{2+}, Co^{2+}, Ni^{2+}, Mn^{2+}, Fe^{3+} and Zn^{2+}.

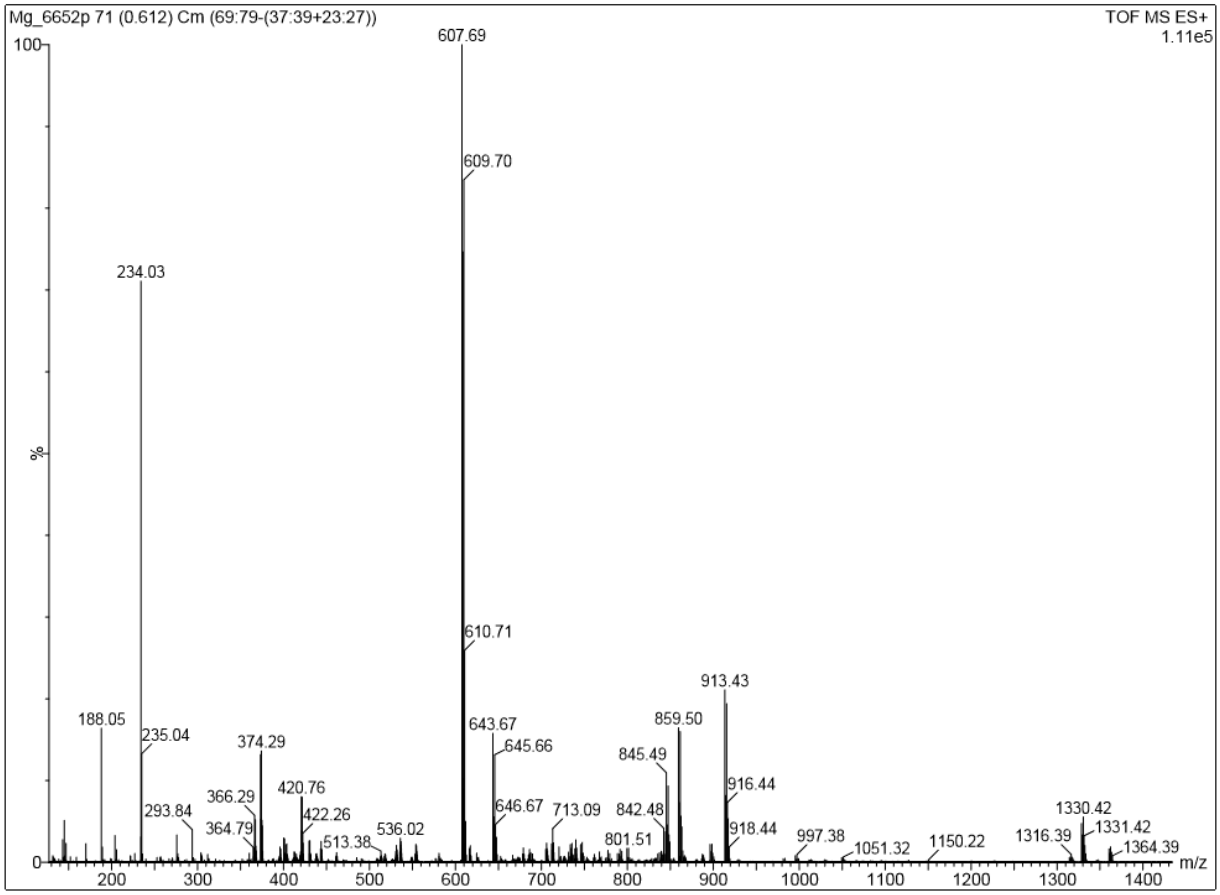

Figure S84. ESI-MS traces of peptoid oligomer **DI HQT** with 1 equiv. Cu^{2+}.

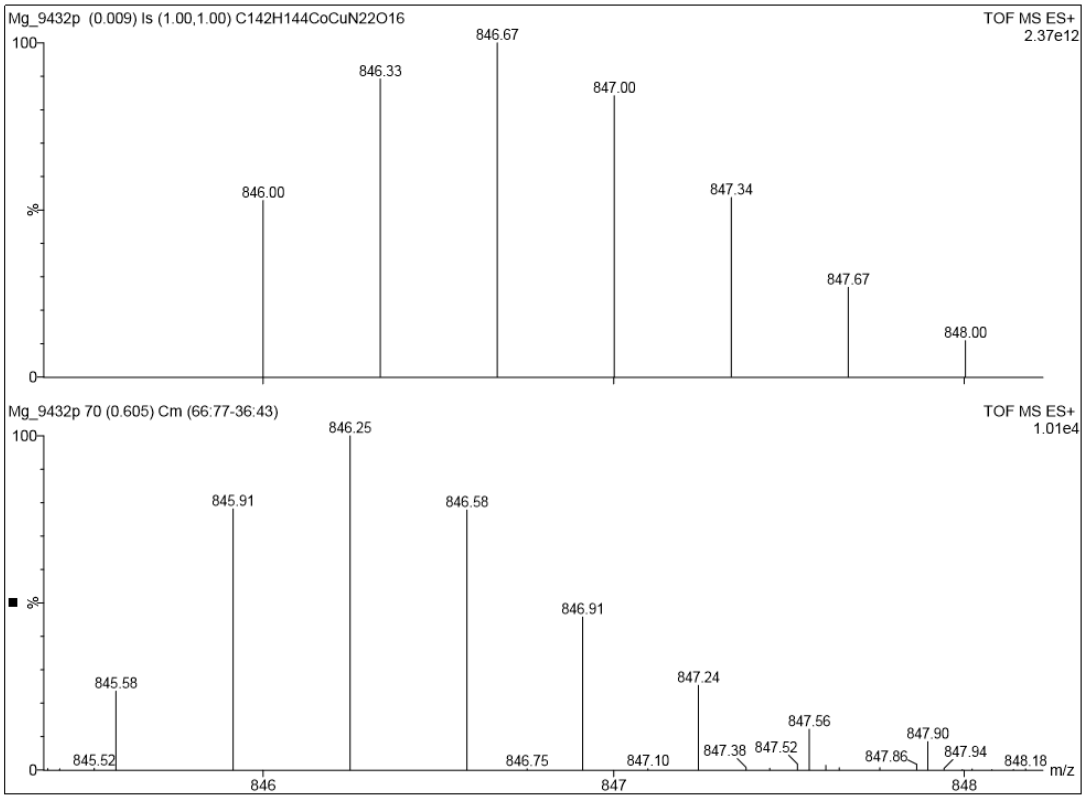

Figure S85. Experimental isotopic analysis by ESI-MS m/3z of (**Helix HQT i+3**)$_2$CoCu hetero bi-metallic peptoid complex synthesized by step approach (bottom) and calculated ESI-MS spectrum (top).

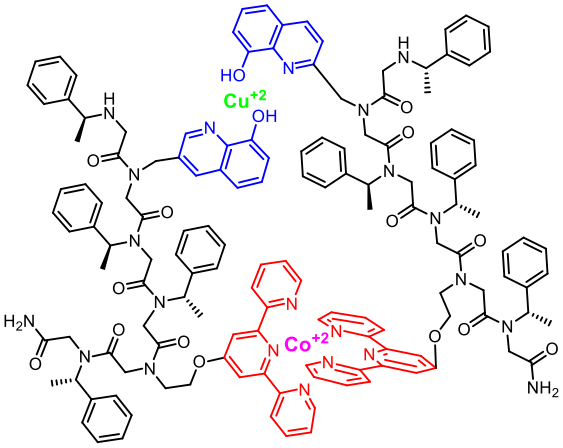

Chemical Formula: $C_{142}H_{146}CoCuN_{22}O_{16}^{4+}$
Exact Mass: 2536.99
Molecular Weight: 2539.29

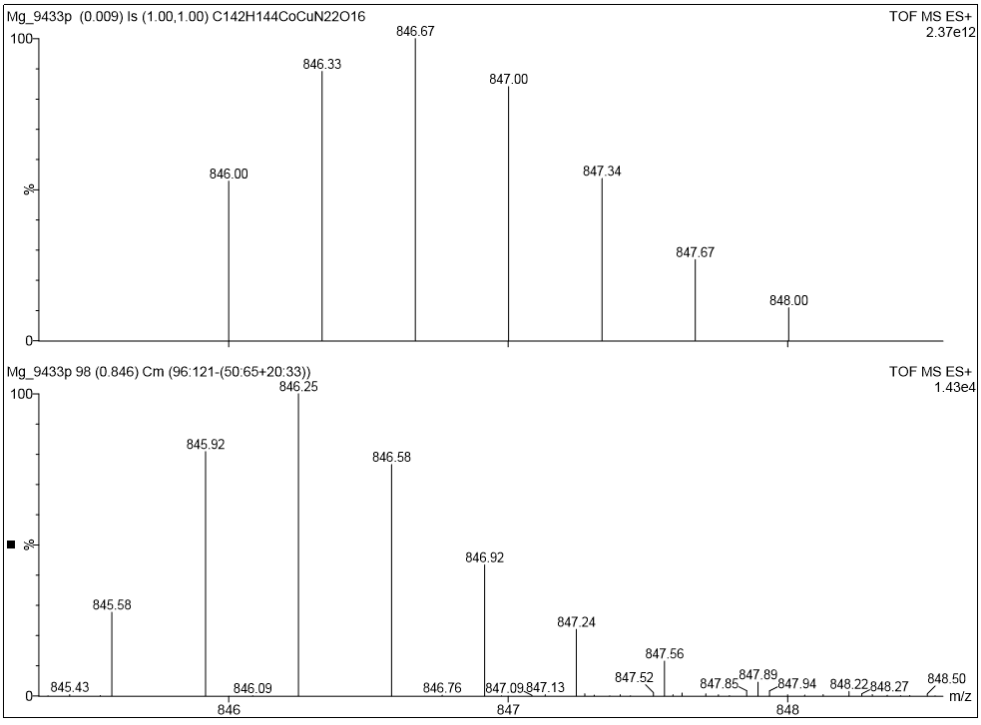

Figure S86. Experimental isotopic analysis by ESI-MS m/3z traces of (**Helix HQT i and i+3**)$_2$CoCu hetero bi-metallic peptoid duplex synthesized by mix approach (bottom) and calculated ESI-MS spectrum (top).

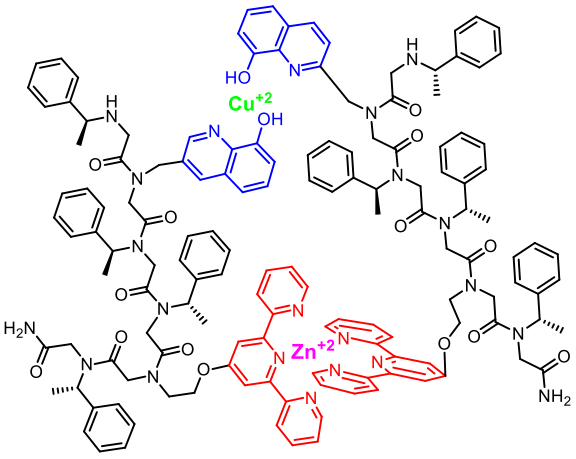

Chemical Formula: $C_{142}H_{146}CuN_{22}O_{16}Zn^{4+}$
Exact Mass: 2541.99
Molecular Weight: 2545.74

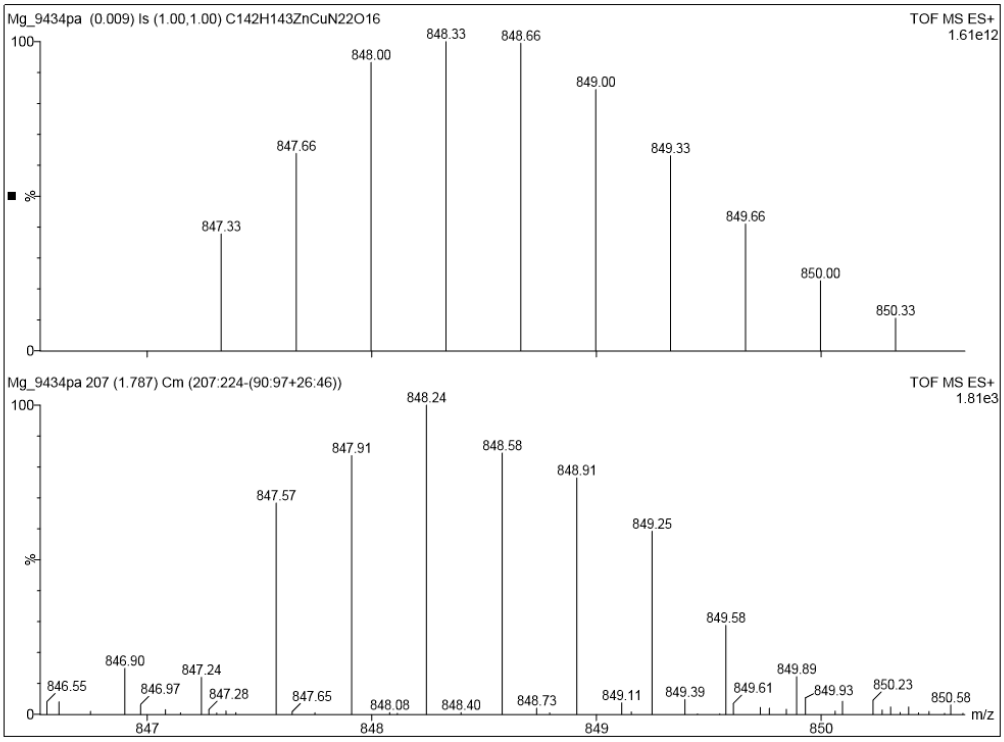

Figure S87. Experimental isotopic analysis by ESI-MS m/3z traces of (**Helix HQT i+3**)$_2$ZnCu hetero bi-metallic peptoid duplex synthesized by step approach (bottom) and calculated ESI-MS spectrum (top).

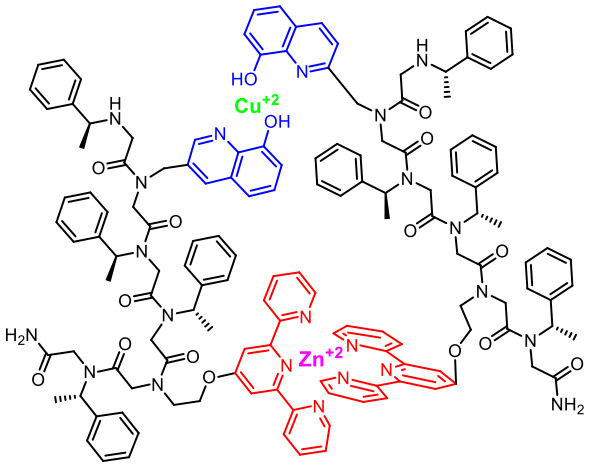

Chemical Formula: $C_{142}H_{146}CuN_{22}O_{16}Zn^{4+}$
Exact Mass: 2541.99
Molecular Weight: 2545.74

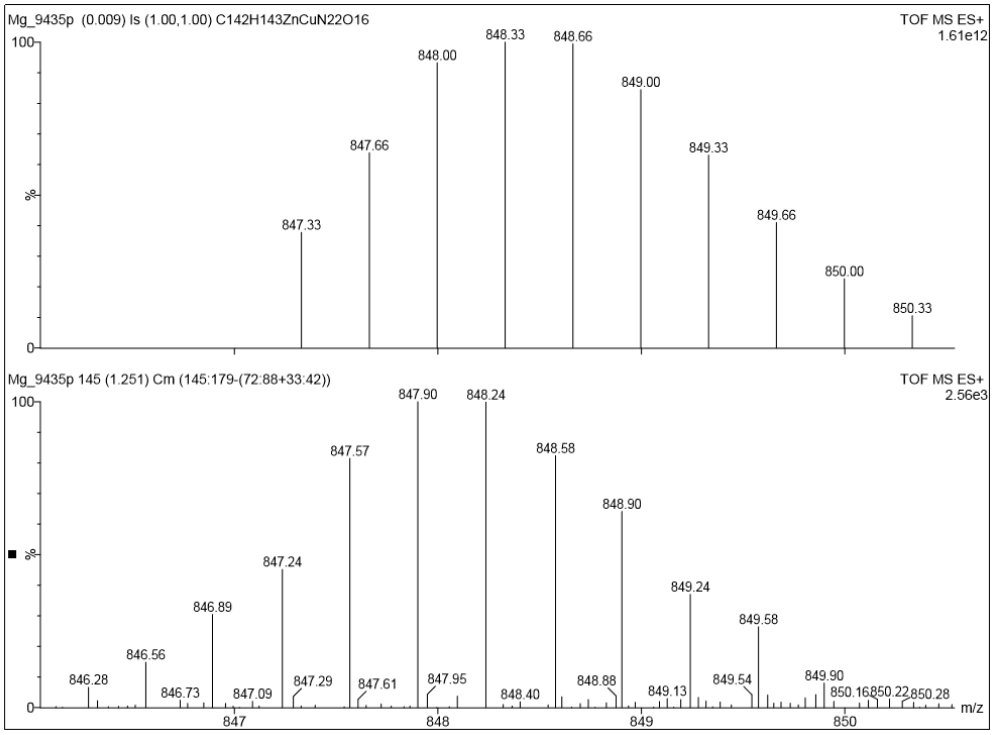

Figure S88. ESI-MS m/3z traces of (**Helix HQT i+3**)$_2$ZnCu hetero bi-metallic peptoid duplex synthesized by mix approach (bottom) and calculated ESI-MS spectrum (top).

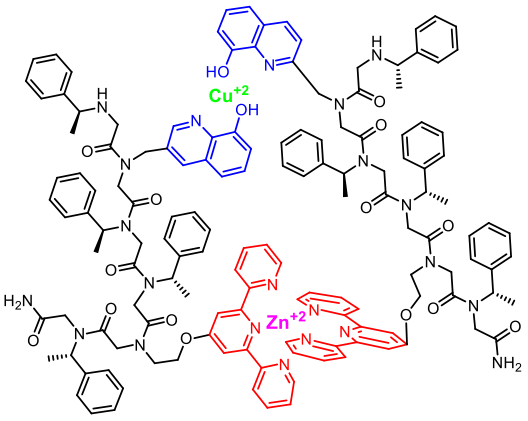

Chemical Formula: $C_{142}H_{146}CuN_{22}O_{16}Zn^{4+}$
Exact Mass: 2541.99
Molecular Weight: 2545.74

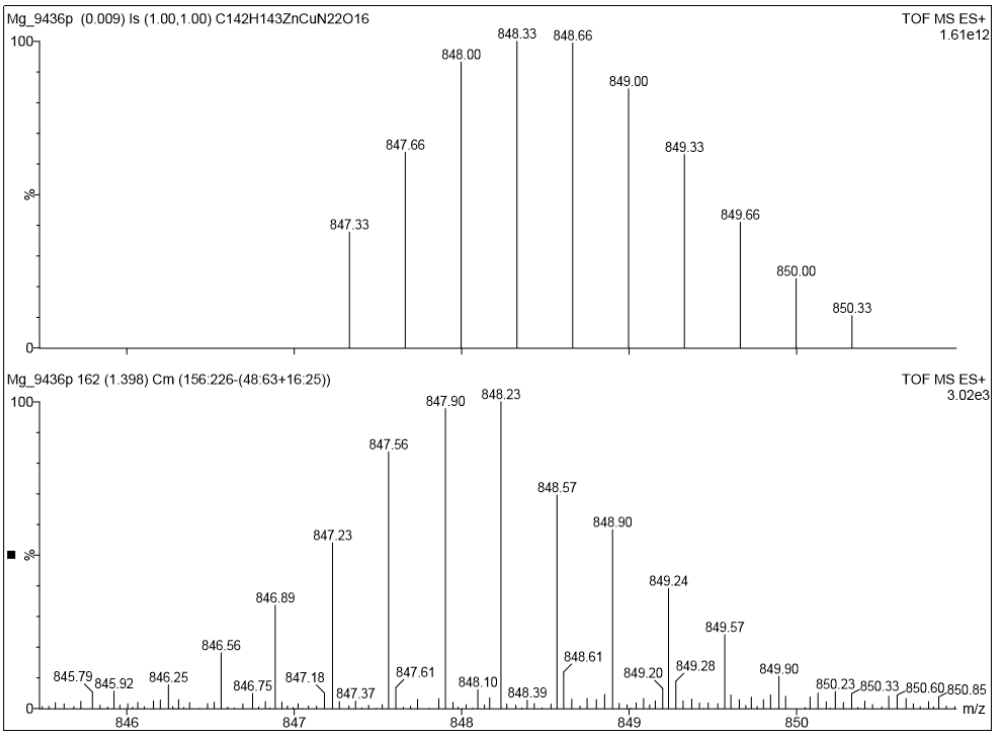

Figure S89. Experimental isotopic analysis by ESI-MS m/3z traces of (**Helix HQT i+3**)$_2$ZnCu hetero bi-metallic peptoid duplex synthesized by step approach for EPR analysis (bottom) and calculated ESI-MS spectrum (top).

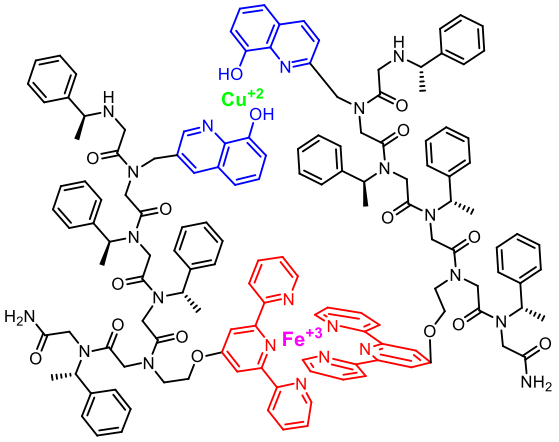

Chemical Formula: $C_{142}H_{146}CuFeN_{22}O_{16}^{5+}$
Exact Mass: 2533.99
Molecular Weight: 2536.20

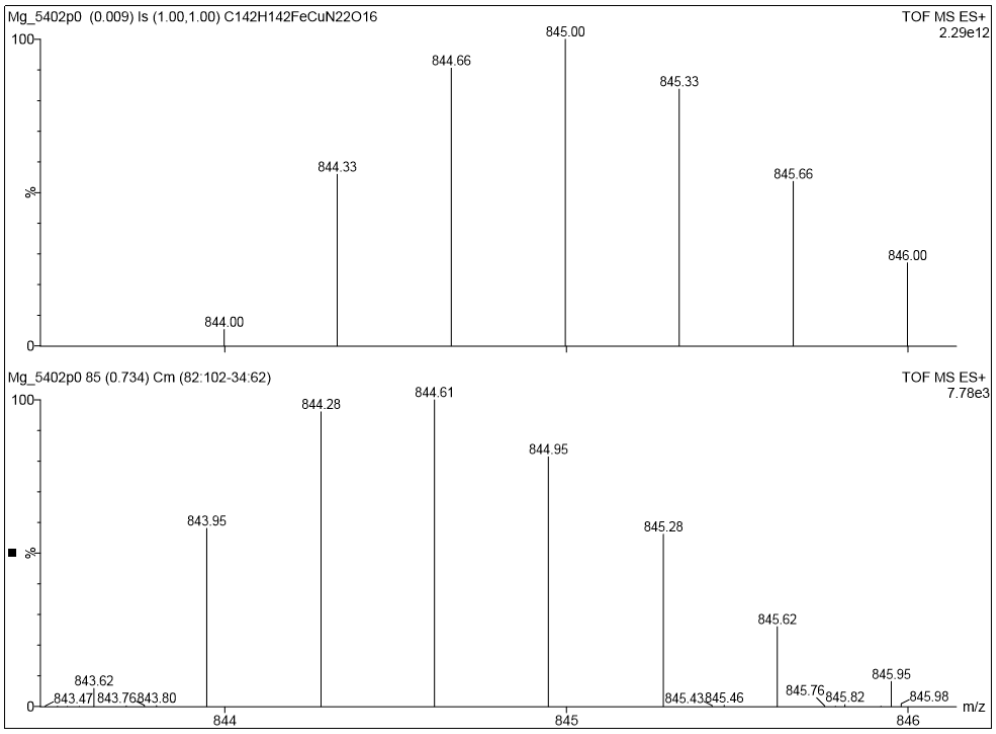

Figure S90. Experimental isotopic analysis by ESI-MS m/3z traces of (**Helix HQT i**+3)$_2$FeCu hetero bi-metallic peptoid duplex synthesized by mix approach at 50 ^{0}C for 2 hours (bottom) and calculated ESI-MS spectrum (top).

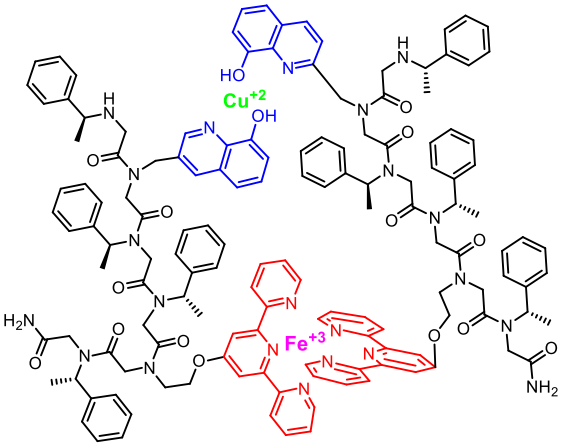

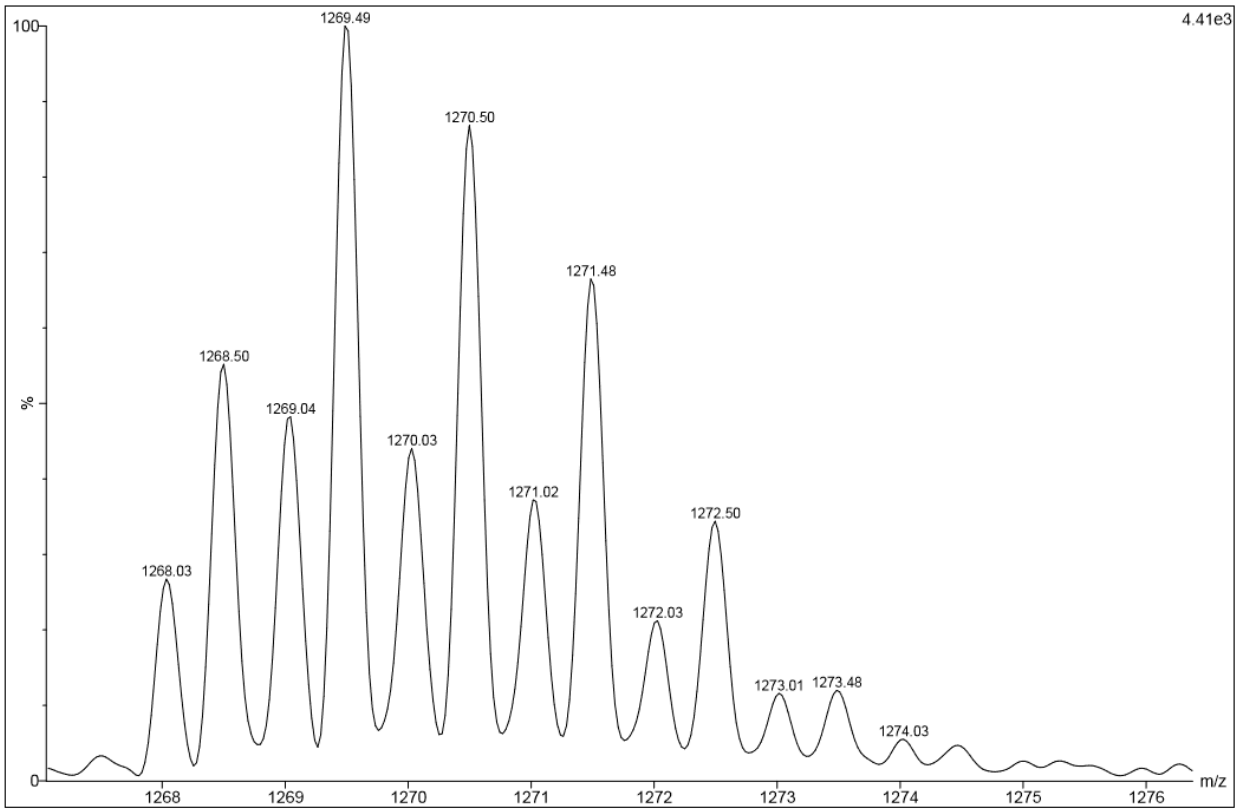

Figure S91. MALDI m/2z spectrum of (**Helix HQT i+3**)$_2$FeCu hetero bi-metallic peptoid duplex synthesized by step approach.